creative commons
COMMONS DEED

저작자표시-비영리-변경금지 2.0 대한민국

이용자는 아래의 조건을 따르는 경우에 한하여 자유롭게

- 이 저작물을 복제, 배포, 전송, 전시, 공연 및 방송할 수 있습니다.

다음과 같은 조건을 따라야 합니다:

저작자표시. 귀하는 원저작자를 표시하여야 합니다.

비영리. 귀하는 이 저작물을 영리 목적으로 이용할 수 없습니다.

변경금지. 귀하는 이 저작물을 개작, 변형 또는 가공할 수 없습니다.

- 귀하는, 이 저작물의 재이용이나 배포의 경우, 이 저작물에 적용된 이용허락조건을 명확하게 나타내어야 합니다.
- 저작권자로부터 별도의 허가를 받으면 이러한 조건들은 적용되지 않습니다.

저작권법에 따른 이용자의 권리는 위의 내용에 의하여 영향을 받지 않습니다.

이것은 이용허락규약(Legal Code)을 이해하기 쉽게 요약한 것입니다.

Disclaimer

dCollection

이학박사 학위논문

Donor-specific FoxP3^{+} regulatory T cell-mediated immune tolerance in an intrahepatic murine allogeneic islet transplantation model by short-term blockade of CD40-CD154 interaction

간 내 동종이형 췌도 이식 생쥐모델에서 단기간 CD40-CD154 상호작용 차단에 의한 공여자 특이 FoxP3^{+} 조절 T 세포 매개 면역관용

2020년 8월

서울대학교 대학원

치의과학과 면역 및 분자 미생물 치의학 전공

이석주

이학박사 학위논문

Donor-specific FoxP3$^+$ regulatory T cell-mediated immune tolerance in an intrahepatic murine allogeneic islet transplantation model by short-term blockade of CD40-CD154 interaction

간 내 동종이형 췌도 이식 생쥐모델에서 단기간 CD40-CD154 상호작용 차단에 의한 공여자 특이 FoxP3$^+$ 조절 T 세포 매개 면역관용

2020년 8월

서울대학교 대학원

치의과학과 면역 및 분자 미생물 치의학 전공

이석주

Donor-specific FoxP3^{+} regulatory T cell-mediated immune tolerance in an intrahepatic murine allogeneic islet transplantation model by short-term blockade of CD40-CD154 interaction

by

Seok-Joo Lee

Under the supervision of

Professor Chung-Gyu Park, MD., Ph.D.

A Thesis Submitted in Partial Fulfillment of

the Requirement for the Degree of

Doctor of Philosophy

August 2020

School of Dentistry

The Graduate School

Seoul National University

Donor-specific FoxP3^{+} regulatory T cell-mediated immune tolerance in an intrahepatic murine allogeneic islet transplantation model by short-term blockade of CD40-CD154 interaction

지도교수 박정규

이 논문을 이학박사 학위논문으로 제출함

2020 년 5 월

서울대학교 대학원

치의과학과 면역 및 분자미생물 치의학 전공

이석주

이석주의 이학박사 학위논문을 인준함

2020 년 7 월

위 원 장 _____ (인)

부위원장 _____ (인)

위 원 _____ (인)

위 원 _____ (인)

위 원 _____ (인)

Abstract

Donor-specific FoxP3^{+} regulatory T cell-mediated immune tolerance in an intrahepatic murine allogeneic islet transplantation model by short-term blockade of CD40-CD154 interaction

Seok-Joo Lee
Program in Immunology and Molecular Microbiology
Department of Dental Science
The Graduate School
Seoul National University

Objectives

Anti-CD154 blockade-based regimens remain unequaled in prolonging graft survival in various organ transplantation models. Several studies have focused on transplantation tolerance with the anti-CD154 blockade, but none of these studies has investigated the mechanisms associated with its use as the sole treatment in animal models, delaying our understanding of anti-CD154 blockade-mediated immune tolerance. The purpose of this study was to investigate the mechanism underlying the anti-CD154 monoclonal antibody (mAb) blockade in inducing immune tolerance using an intrahepatic murine allogeneic islet transplantation model.

Methods

B6 mice were intraperitoneally administered with streptozotocin to induce diabetes. Allogeneic BALB/c islets were infused into the liver of diabetic B6 mice via a cecal vein route. Anti-CD154 mAb (MR1) was administered on -1, 0, 1, 3, 5, and 7 days post-transplantation at 0.5 mg per mouse. To elucidate if immune tolerance was induced, second BALB/c islets were transplanted under the kidney capsule of B6 mice engrafted formerly with BALB/c islet in the liver. BALB/c skin grafts were transplanted to the flank of B6 mice to investigate if immune tolerance to BALB/c islets could be extended to other BALB/c organs. IFN-γ ELISpot assay and depletion of regulatory T (Treg) cells in intrahepatic islet transplanted DEREG mouse model were conducted in order to reveal the mechanism of immune tolerance. Suppressive capacity of $FoxP3^+$ Treg cells isolated from tolerant and naïve B6 mice was analyzed by conducting mixed lymphocyte reaction assays.

Results

I showed that short-term MR1 monotherapy could prolong the allogeneic islet grafts to more than 250 days in the murine intrahepatic islet transplantation model. The second islet grafts transplanted under the kidney capsule of the recipients were protected from rejection. I also found that rejection of same-donor skin grafts transplanted to the tolerant mice was modestly delayed. Using a DEREG mouse model, $FoxP3^+$ Treg cells were shown to play important roles in transplantation tolerance. In mixed lymphocyte reactions, Treg cells from the tolerant mice showed more potency in suppressing BALB/c splenocyte stimulated Teff cell proliferation than those from naïve mice.

Conclusion

In this study, I demonstrated for the first time that a short-term blockade of CD40-CD154 interaction could induce FoxP3^{+} Treg cell-mediated immune tolerance in the intrahepatic murine allogeneic islet transplantation model. My model provided the foundation to elucidate the molecular mechanism of in vivo CD154 blockade-mediated FoxP3^{+} Treg cell induction. I expect that my animal model will contribute to the accomplishment of immune tolerance in pre-clinical and clinical studies.

Keywords: Anti-CD154 mAb (MR1), Immune tolerance, Regulatory T cell, Islet transplantation, Liver

Student number: 2014-22041

Contents

List of figures

List of abbreviations

AEC: 3-Amino-9-EthylCarbazole

APC: Antigen Presenting Cell

B6: C57BL/6

BALB/c: BALB/c AnHsd

BGL: Blood Glucose Level

BSA: Bovine Albumin Serum

C3H: C3H/HeJ

CD: Cluster of Differentiation

DC: Dendritic Cell

DEREG: Depletion of REGulatory T

DST: Day Post Transplantation

DT: Diphtheria Toxin

DTR: Diphtheria Toxin Receptor

EDTA: EthyleneDiamineTetraAcetic acid

eGFP: enhanced Green Fluorescence Protein

ELISpot: Enzyme-Linked Immunospot

FBS: Fetal Bovine Serum

FoxP3: Forkhead box P3

HBSS: Hank’s Balanced Salt Solution

HEPES: Hydroxyethyl Piperazine Ethane Sulfonic acid

IBMIR: Instant Blood Mediated Inflammatory Reaction

ICOS: Inducible T cell COStimulator

IEQ: Islet EQuivalent

IFN-γ: Interferon-gamma

IS: Immuno-Suppressive

iTreg: inducible Treg

KLRG-1: Killer cell Lectin-like Receptor subfamily G member 1

LFA-1: Lymphocyte associated Function Antigen 1

mAb: monoclonal antibody

MEM: Minimum Essential Medium

MEM-NEAA: MEM-Non Essential Amino Acid

MHC: Major Histocompatibility Complex

MLR: Mixed Lymphocyte Reaction

NHP: Non-Human Primate

NPI: Neonatal Porcine Islet

nTreg: natural Treg

PBS: Phosphate-Buffered Solution

PBST: PBS with Tween20

PFA: ParaFormAldehyde

PD-1: Programmed cell death protein 1

RPMI 1640: Rowewell Park Memorial Institute 1640

SRS: .Subcapsular Renal Space

STZ: Streptozotocin

T1D: Type 1 Diabetes

TBST: Tris-Buffered Saline with Tween 20

TCR: T Cell Receptor

TPX: Transplantation

Treg: Regulatory T cell

I. Introduction

1. Type 1 diabetes and pancreatic islet transplantation

Diabetes mellitus is a general term for heterogeneous metabolic disruptions for which the main symptom is a loss of glucose homeostasis, resulting in chronic hyperglycemia[1]. The cause of diabetes mellitus is either impaired insulin secretion, impaired insulin action or both. Type 1 diabetes (T1D) is classified as a chronic autoimmune disease which leads to absolute insulin deficiency[2,3]. Autoreactive T cells are the main mediators of β-cell destruction[3]. Although patients are given exogenous insulin for normal glycemic control, this treatment often increases the risk of severe hypoglycemia[4]. As an alternative strategy, allogeneic islet transplantation is a promising therapy for patients with T1D[5-7]. To date, more than 1,500 patients have undergone β-cell replacement therapy at 40 different international centers, and 50-70% of them have shown insulin independence at 5 years[8]. However, patients receiving life-long immunosuppressive (IS) drugs to minimize donor-specific immune responses are susceptible to several adverse effects, such as infections, malignancies, and organ toxicities[9,10] as IS drugs themselves are toxic and can suppress autoreactive as well as protective T cell responses.

IS drugs for graft maintenance are mainly based on a combination of six mechanistically different agents: calcineurin inhibitor, mycophenolic acid, azathioprine, mTOR inhibitor, belatacept, and corticosteroid (CS)[11]. In particular, CS has been used since the early days of organ transplantation and remains a basic component of many IS protocols[12]. This drug blocks T cell-derived and APC-derived cytokine and cytokine expression via various mechanisms[13-17]. However, chronic administration of CS has been reported to induce pancreatic β-cell damage with

deteriorative effects on insulin production and peripheral action in healthy people[18]. Thus, to avoid the risk of toxicity with transplanted islets, the Edmonton protocol with CS-sparing regimens has been developed for better treatment of T1D[19]. Although this protocol can successfully restore endogenous insulin production and glycemic control, long-term graft survival of islets is not still satisfactory. Issues of IS regimen-related toxicity, immune response, and unsuitable implantations site are yet to be overcome.

2. Immune tolerance

2.1. Definition and significance

Immune tolerance is subdivided into two major types: central tolerance and peripheral tolerance. In central tolerance, many immature lymphocytes in generative lymphoid organs die as they recognize autoantigens with high avidity[20]. Some of the surviving lymphocytes develop into $CD4^+FoxP3^+$ regulatory T (Treg) cells[20] or undergo receptor editing in order to rescue themselves from apoptosis[21]. In peripheral tolerance, some autoreactive lymphocytes are inactivated or deleted as a result of encountering antigens in the absence of co-stimulation or innate immunity[22]. They are also inactivated or deleted by the suppression of $FoxP3^+$ Treg cells[22]. In autoimmunity or transplantation, immune tolerance is more specifically defined as a lack of immunological reactivity to autoantigens or foreign tissue antigens (second-party) in an organ graft, achieved without the need for IS drugs while retaining immune cells that are still reactive to all other foreign antigens (third-party)[23]. IS drug-mediated immunosuppression is distinguished from immune tolerance as it downregulates the whole immune system including the resistance to third-party antigens. Immune tolerance induction is therefore attractive as a strategy for enabling

the acceptance of major histocompatibility complex (MHC)-mismatched allo- and xenografts without compromising the host's resistance to infections or risking other complications. Several attempts have been made to induce immune tolerance in various rodent models of transplantation using co-stimulatory signal blockades, induction and expansion of Treg cells, peripheral T cell deletion, and mixed hematopoietic chimerism[24,25]. Also, the role of novel immunomodulatory cell groups, such as mesenchymal stromal cells (MSCs) and regulatory macrophages, in response to tolerogenic therapies is currently under investigation[26,27].

2.2. Discrepancies between rodent models and human trials

Transplantation tolerance induction in a rodent model has been reported[28,29]. For example, Lin and his colleagues demonstrated that the survival of secondary transplanted BALB/c skin grafts without the use of IS therapies was achieved in the B6 recipient, which accepted vascularized osteomyocutaneous BALB/c allografts. In contrast, the C3H (third-party) skin was acutely rejected in the same recipient upon re-challenge[30]. Unfortunately, five decades of pre-clinical and clinical research outcomes in solid organ transplantation have demonstrated that, unlike in the studies conducted using rodent models, immune tolerance induction in non-human primates (NHPs) and humans is extremely difficult to achieve[31,32] and may only be applicable in a limited subset of patients[33-35]. The only strategy that has so far achieved relatively consistent organ transplantation tolerance in human clinical trials is mixed chimerism, but that is extremely short-lived[36]. The current protocols for mixed chimerism with bone marrow transplantation are still accompanied by several risks, including graft rejection, graft versus host disease, and regimen toxicity. Another side effect is T cell depletion, through infection and loss of memory T cells from the

emergence of new T cells[36]. These issues show that achieving clinically translatable immune tolerance is very challenging. This concern is in line with our previous work, in which we found that porcine xeno-islets transplanted into the liver of NHPs survived only when the recipients were under regular administration of IS therapies, implying a failure of immune tolerance induction in our pre-clinical studies[37]. Although there are several possible explanations for these inconsistent outcomes between rodents and NHPs, a lack of definite therapies demonstrating the clear success of immune tolerance in the rodent model has delayed our understanding of in vivo tolerance, hampering the progress of research to the next level.

3. Anti-CD154 blockade

3.1. CD154-CD40 interaction and CD154 antagonism

CD154 (CD40L) is a type II transmembrane protein belonging to the tumor necrosis factor subfamily[38]. CD154 is a co-stimulatory molecule mainly expressed on the surface of activated T cells; its expression is tightly regulated to maintain the activation of T cells[38]. CD40 is constitutively expressed on the surface of antigen-presenting cells (APCs), including dendritic cells (DCs), macrophages, and B cells[38,39]. On CD154-CD40 co-stimulation, APCs upregulate the expression of MHCs and co-stimulatory molecules including CD80 and CD86[38], priming the cellular immune system. In humoral immunity, CD154-CD40 co-stimulation is also important for the function of B cells by way of promoting isotype switching and antibody affinity maturation[38].

Blockade of the CD154-CD40 interaction is believed to be the most powerful strategy to achieve long-term graft survival in experimental transplantation models[40].

Most of the studies achieving long-term graft survival, including one of our reports[37], adopted anti-CD154 blockade based regimens to suppress donor-specific immune responses against allografts[41-43] and xenografts[44-48]. The anti-CD154 blockade has been reported to have several immune-regulatory mechanisms, including depleting CD154-expressing activated T cells[49], promoting the conversion of conventional $CD4^+$ T cells into peripheral $FoxP3^+$ Treg cells[50], suppressing allo-specific $CD4^+$ T cells by natural $FoxP3^+$ Treg cells[51], preventing the maturation of alloantigen-presenting DCs[52], promoting the generation of tolerance-inducing plasmacytoid DCs[52], and preventing antibody-mediated rejection[53,54].

Despite the promising effect of CD154 blockade in organ transplantation, clinical interest in this strategy is strongly limited by thrombotic complications[55,56]. The undesirable thrombotic effects of anti-CD154 blockade are due to binding to CD154 expressed either on activated platelets or in released soluble form[57]. This preformed anti-CD154 mAb immune complex has been demonstrated to cause thrombocytopenia, leading to thrombosis in a rodent model[58]. However, the use of clinically applicable heparin has been shown to diminish the thrombotic events during anti-CD154 mAb treatment in pre-clinical trials[59]. The Fc domain of anti-CD154 mAbs binding to platelet Fc receptors has been reported as contributing to platelet activation and aggregation[58,60]; this suggests that anti-CD154 Ab without the Fc domain may avoid the platelet aggregation and subsequent thromboembolism that are triggered by anti-CD154 mAbs. For example, use of a clinical translatable Fc-silent anti-CD154 domain antibody has provided promising results in mouse transplant models[61], indicating its potential clinical usage in human trials. Also, a non-crosslinking monovalent antibody specific to CD154, including a monovalent PEGylated anti-CD154 Fab antibody fragment (CDP7657)[62], could be a promising

strategy to circumvent adverse thromboembolic events.

3.2. Islet transplantation in experimental animal models

The superiority of adopting the anti-CD154 blockade in combination therapy regimens has been demonstrated in islet transplantation since the long-term survival of allo- and xenografts has been achieved in various rodent models[63-67]. In murine islet allotransplantation models, various therapy regimens combined with anti-CD154 blockade enabled long-term graft survival of allogeneic islets in recipients[68-70]. Among these studies, one has shown that the administration of anti-CD154 mAb with anti-ICOS mAb achieved transplantation tolerance in a murine islet allo-transplantation model where re-transplantation of donor islets was accepted by the same recipients, without the need to administer IS drugs[70]. Similar results have been reported in porcine islet xenotransplantation models[71-73] that the combined blockade of CD154 and LFA-1 achieved long-term graft survival with a possible explanation of a molecular mechanism via PD-1. Transplantation tolerance has also been reported in their models; mice treated with anti-CD154 mAb and anti-LFA-1 mAb showed long-term survival of xeno-islets with selective immunomodulatory activities over donor islets, but not over third-party antigens[73].

These studies have emphasized the role of FoxP3$^+$ Treg cells in achieving long-term graft survival and transplantation tolerance in islet transplantation models. However, the combined regimens used make it difficult to establish whether the anti-CD154 blockade truly induces immune tolerance. There have been reports on the effect of anti-CD154 monotherapy in islet transplantation in rodent and NHP models[74-76]; however, none of these studies investigated the mechanisms associated with Treg cells, which are known to play a critical role in tolerance induction. This

omission makes it difficult to determine the efficacy of anti-CD154 mAb therapy for tolerance induction.

3.3. FoxP3$^+$ Treg cells

Sakaguchi, Rudensky, Ramsdell, and their colleagues first identified the Forkhead box P3 (FoxP3), a master regulator of Treg development[77-80]. Sakaguchi and his team found that neonatal thymectomy in mice resulted in an autoimmune oophoritis[81], confirming the evident necessity of T cells to prevent organ-specific autoimmune disease[82,83]. They further identified distinct subsets of suppressive T cells expressing CD4 and CD25 on their surface. They demonstrated that transferring CD4$^+$CD25$^-$ cells into athymic nude mice provoked autoimmune disease. However, co-transferring these cells with CD4$^+$CD25$^+$ Treg cells was shown to prevent autoimmune disease onset[84]. Although the regulatory role of Treg cells in lymphoid tissues has been well characterized, the function of activated Treg cells in non-lymphoid regions remains unknown. In various transplantation models, Treg cells have been found to play a critical role in tolerant grafts because of their suppressive activity[85]. However, the relative importance of Treg cells in grafts versus those in the lymphoid tissues has not been clarified. It is not yet known whether they are of the same origin or are a different type of cells.

Anti-CD154 blockade based regimens have been reported to induce the expansion of antigen-specific Treg cells in several transplant models[86-89]. In addition, immune tolerance induced by CD154 blockade is transferable, as it can be delivered to naïve recipients by the adoptive transfer of CD4$^+$FoxP3$^+$ Treg cells of tolerant recipients, demonstrating the potency of CD154 antagonism in inducing infectious tolerance[90,91]. More recent data from another group showed that anti-CD154

blockade based regimens could also increase the ratio of intragraft Treg cells to effector $CD4^+$ and $CD8^+$ T cells in allogeneic corneal and orthotopic lung transplantation models[92,93], implicating the efficacy of CD154 blockade in shifting the balance from an alloreactive response to a regulatory one.

CD154 antagonism has been proven capable of inducing peripheral $FoxP3^+$ Treg cells in a rodent model where adoptively transferred OT-I & OT-II T cells protected transplanted skin grafts expressing ovalbumins[89]. However, practical difficulties in attempting to generate genetically engineered NHPs is making it challenging to determine whether the regulatory cell groups observed in pre-clinical studies following CD154 antagonism are induced by the peripheral induction of de novo inducible Treg (iTreg) cells or the expansion of pre-existing natural Treg (nTreg) cells or both. Anti-CD154 blockade can contribute to Treg-mediated immune regulation in different forms or by any means with the aid of other IS drugs in several rodent and NHP models. However, it remains unknown whether anti-CD154 blockade alone is truly capable of inducing Treg cell-mediated immune tolerance in a transplantation rodent model. Therefore, it is suggested that the MHC-mismatched transplantation mouse model should be treated only with anti-CD154 blockade in order to elucidate whether anti-CD154 mAb does in fact induce immune tolerance by generating graft-protective Treg cells. This information would add a further layer of knowledge to enable fine-tuning of CD154 blockade-mediated transplantation tolerance at both pre-clinical and clinical levels.

4. Transplantation sites for human and murine islets

The kidney subcapsule has been adopted as a site for islet transplantation in an experimental rodent model due to the advantage of graft retrieval for histological

and functional analysis of the islet grafts[94]. However, since the success of the Edmonton protocol[19], hepatic infusion via the portal vein is currently accepted as a clinical site for islet transplantation[8] despite the potential risks, including thrombosis, hepatic ischemia, and an instant blood-mediated inflammatory reaction (IBMIR)[95,96].

Although bone marrow cavities and brachioradialis muscles have been suggested as alternative sites for clinical islet transplantation[97,98], recent improvements in islet purification and IS therapies with their minimal invasive approach in surgery make intrahepatic islet transplantation a feasible option for most patients[6,7]. The liver also offers anatomical advantages as a result of its first-pass exposure to both nutrients and insulin, sensing the blood glucose level to regulate it immediately without the delay of insulin secretion[99].

Hence, in order to minimize the interspecies variation, a rodent model of intrahepatic islet transplantation, which mimics the clinical islet transplantation, seemed more appropriate to expand current understanding of immune tolerance across species. In addition, we previously established a novel technique of transplanting islets via the cecal vein, which can lead to more effective control of bleeding-related death, compared to portal vein infusion[100]. Using newly developed techniques, I chose to transplant MHC-mismatched islet allografts into the liver of rodents, aiming to investigate the mechanism behind anti-CD154 mAb on its own in inducing immune tolerance.

5. Aim of this study

The aims of the study were as follows:

1. To investigate whether anti-CD154 blockade alone can achieve long-term graft

survival in an intrahepatic murine allogeneic islet transplantation model

2. To evaluate whether immune tolerance is achieved in intrahepatic islet transplanted diabetic mice

3. To elucidate the mechanism of immune tolerance

6. Summary

In this study, I demonstrated that, following CD154 blockade, augmented graft-protective $FoxP3^+$ Treg cells play a critical role in the induction of transplantation tolerance, preventing allograft rejection in the intrahepatic murine islet transplantation model.

II. Material and Methods

1. Animals

All experimental procedures were approved by the Seoul National University (SNU) Institutional Animal Care and Use Committee and were conducted according to international guidelines concerning the care and treatment of experimental animals and the SNU animal experiment ethical guidelines and regulations. All animals were aged 8 weeks. Female C57BL/6 (B6, H-2^b), BALB/c AnHsd (BALB/c, H-2^d), and C3H/HeJ (C3H, H-2^K) inbred mice were purchased from the Jackson Laboratory (Bar Harbor, ME, USA). Female knock-in B6 (DEREG) mice expressing Forkhead box P3 (FoxP3) together with diphtheria receptor (DTR) and enhanced Green Fluorescent Protein (eGFP) were also purchased from the Jackson Laboratory. FoxP3 tagged with eGFP reporter mice were kindly provided by Alexander Y. Rudensky (Memorial Sloan Kettering Cancer Center, New York, NY, USA).

2. Monoclonal antibodies and diphtheria toxin treatment protocols

Anti-CD154 mAb (MR1; Bio X Cell, West Lebanon, NH, USA) diluted in phosphate-buffered saline (PBS) solution were intraperitoneally administered at 0.5 mg per mouse on days -1, 0, 1, 3, 5, and 7 post-transplantation. Diphtheria toxin (DT) diluted in PBS solution was intraperitoneally injected on days 28, 29, 31, and 32 post-transplantation at 1.5 μg per mouse. The concentration of DT was carefully titrated for every experiment to obtain the optimized in vivo activity with as little toxicity as possible[101]. A working concentration of DT (1 μg DT/ 100 μl PBS) for depleting $FoxP3^+$ Treg cells has been recommended in DEREG mouse models[101].

Administration of 1.5 μg of DT intraperitoneally for 4 days was chosen in this study; at this concentration, Treg cells were completely ablated and no pathological signs (including gradual weight loss, hypothermia, or slow or labored breathing) were observed in the mice.

3. Diabetic induction

For diabetic induction, mice were fasted for 5 hours before streptozotocin (STZ; Sigma-Aldrich, St. Louis, MO, USA) administration; 120 mg/kg of STZ in citrate buffer solution (Sigma-Aldrich) was intraperitoneally injected twice (one time a day). Mice injected with STZ had free access to standard laboratory food and water. Only the mice with more than 16.8mmol/L (=302.67mg/dL) blood glucose level (BGL) for three consecutive days were considered to have diabetic status[102,103]. The mouse tail was snipped to obtain blood, and the BGL was measured with a OneTouch Ultra device kit (Lifescan, Inc., Chesterbrook, PA, USA). After diabetic induction, mice were caged for the next 5-6 days to excrete the remaining STZ from the body before islet transplantation.

4. Islet isolation

Collagenase P (Roche, Basel, Switzerland) was dissolved in Hanks' balanced salt solution (HBSS; Mediatech, Herndon, VA, USA) at a concentration of 0.3mg/ml. The solution was infused through the bile duct where the right and left hepatic ducts converge. The inflated pancreas was then precisely excised from adjacent organs and transferred into a sterile glass vial for subsequent incubation at 36°C for 20 minutes. Digested islets were sieved and purified using discontinuous ficoll density gradients (GE Healthcare Life Sciences, Chicago, IL, USA). Isolated islets located between

1.069 and 1.096 density gradients were handpicked and transferred into warmed complete RPMI1640 media (Hyclone Laboratories, Inc., Logan, UT, USA) supplemented with 10% fetal bovine serum (FBS) (Sigma-Aldrich) and 1% antibiotic-antimycotic (Gibco, Carlsbad, CA, USA). The complete media was additionally supplemented with 1% L-glutamine (Gibco), 0.1% 2-mercaptoethanol (Gibco), 1% HEPES (Gibco), and 1% MEM NEAA (Gibco). Purified islets were cultured overnight to enhance viability before transplantation. Pancreatic islet transplantation into the liver and kidney is described below:

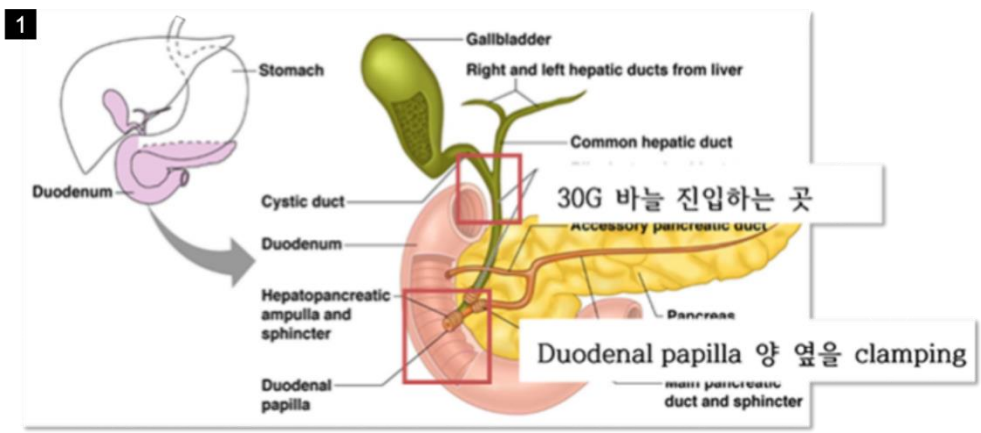

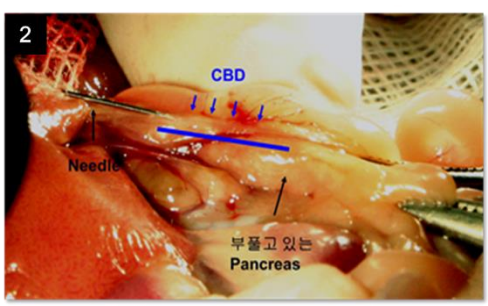

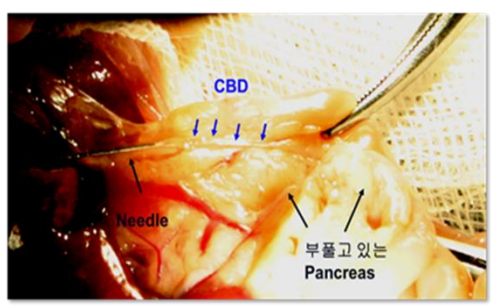

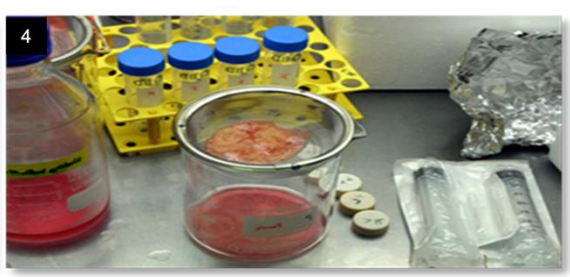

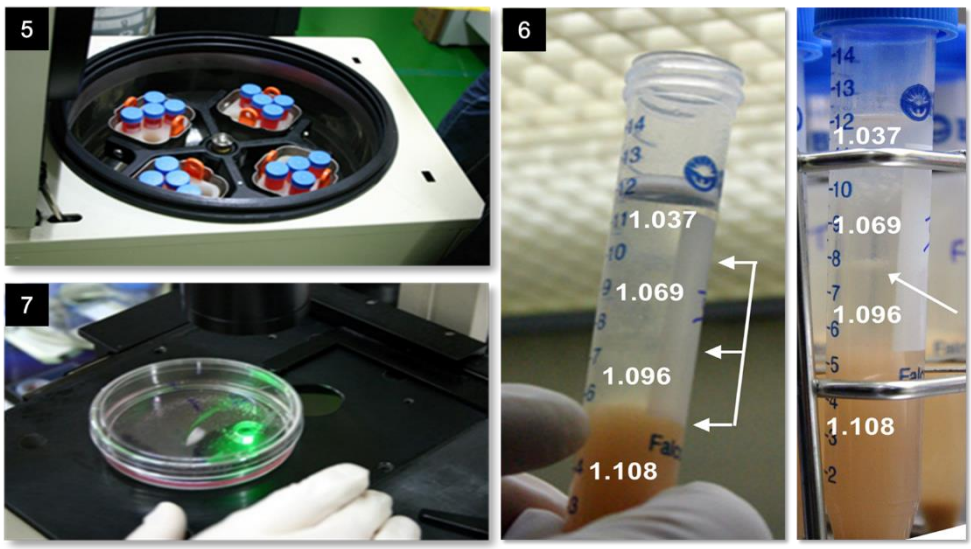

Figure 1. Procedure for islet isolation

1. Schematic diagram for intraductal injection. 2. Intraductal injection and inflating pancreas. 3. Digested pancreas 4. Sieving. 5. Washing. 6. Ficoll gradient for islet isolation. Isolated islets located between 1.069 and 1.096 density gradients are denoted by the white arrow. 7. In vitro islet culture.

5. Intrahepatic islet transplantation

All surgical procedures were carried out with isoflurane anesthesia. The lower midline abdomen of the anesthetized mouse was incised, and the cecum was exposed on the aseptic drape. Under an operating microscope (SZ2-STU3; Olympus, Tokyo, Japan), using round forceps, the cecal vein was gently stretched and subsequently penetrated by a 26-G needle (Korea Vaccine, Gyeonggi-do, Korea). Using a Hamilton syringe (Hamilton, Reno, NV, USA), 700 islet equivalents (IEQs) uniformly dispersed in a polyethylene (PE) tube (Becton Dickinson, Franklin Lakes, NJ, USA) were precisely infused into the cecal vein. For bleeding control, absorbable

hemostats (Johnson & Johnson, New Brunswick, NJ, USA) and aseptic gauze (DaeHan FM, Gyeonggi-do, Korea) were immediately placed on the punctured vein before retrieving the needle from the vein. The punctured area was covered with absorbable hemostats and aseptic gauze and softly compressed by round forceps for at least 3 min as the needle was agilely and reliably removed from the vein. The opened peritoneum and skin were then sutured with a surgical thread (Ethicon Inc., Bridgewater, NJ, USA), and antibiotics and painkiller cocktail drugs (cefazolin 90mg/kg, Metacam 1mg/kg, Maritrol 30mg/kg) were administered via a subcutaneous route.

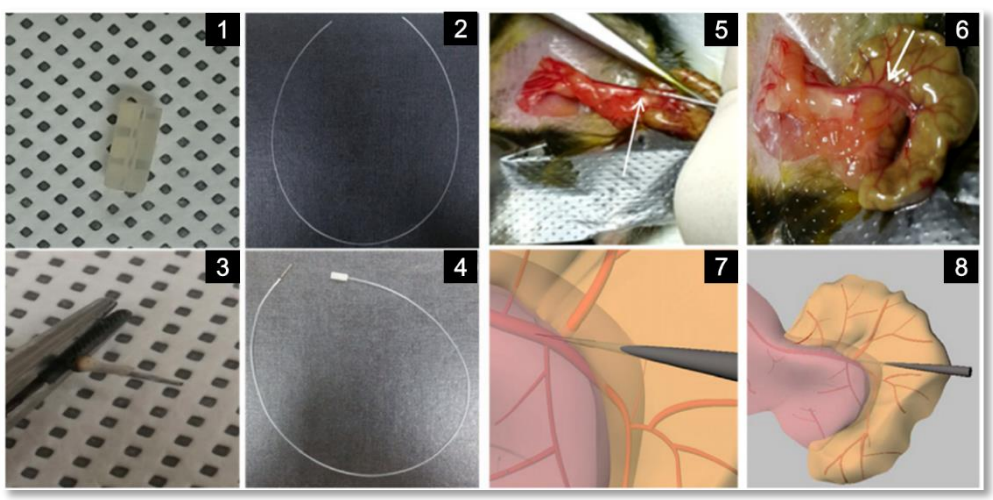

Re-organized diagram adopted from: N. Byun et al. / Journal of Immunological Methods 427 (2015) 122–125

Figure 2. Procedure for intrahepatic islet transplantation via a cecal vein

1. 1 cm long silicon tube. 2. 40 cm long polyethylene tube. 3. 26-gauge needle shaft with its needle hub separated from the needle adaptor. 4. Needle shaft assembled with PE tube and silicon tube. 5. Inserted needle via a cecal vein; penetrated cecal

vein is denoted by the white arrow. 6. Punctured area covered with absorbable hemostats and aseptic gauze. The site of needle insertion is denoted by the white arrow. 7-8. Schematic illustration of needle insertion.

6. Renal subcapsular islet transplantation

All surgical procedures were carried out with isoflurane anesthesia. The left flank of the anesthetized mouse was incised and the kidney was gently pulled out of the abdominal cavity. To advance the islets into the subcapsular renal space (SRS), the capsule was carefully scratched (typically less than 1 mm in length) using a 30-G needle (Korea Vaccine) and the PE tube loaded with aggregated 400 or 500 IEQs was inserted into the SRS. Using a Hamilton syringe, islets were agilely advanced into the SRS. After retrieving the PE tube from the SRS, the punctured capsule was sealed using a cautery kit (Bovie Medical Corporation, Clearwater, FL, USA). The islet-bearing kidney was relocated into the abdominal cavity, and the opened peritoneum and skin were sutured with a surgical thread.

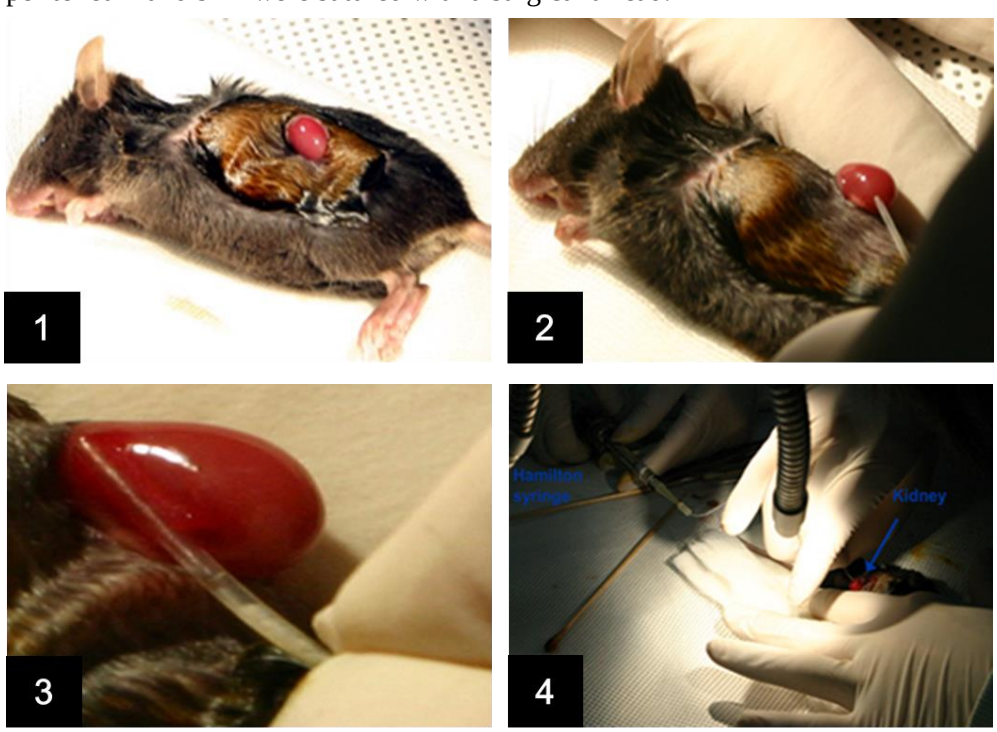

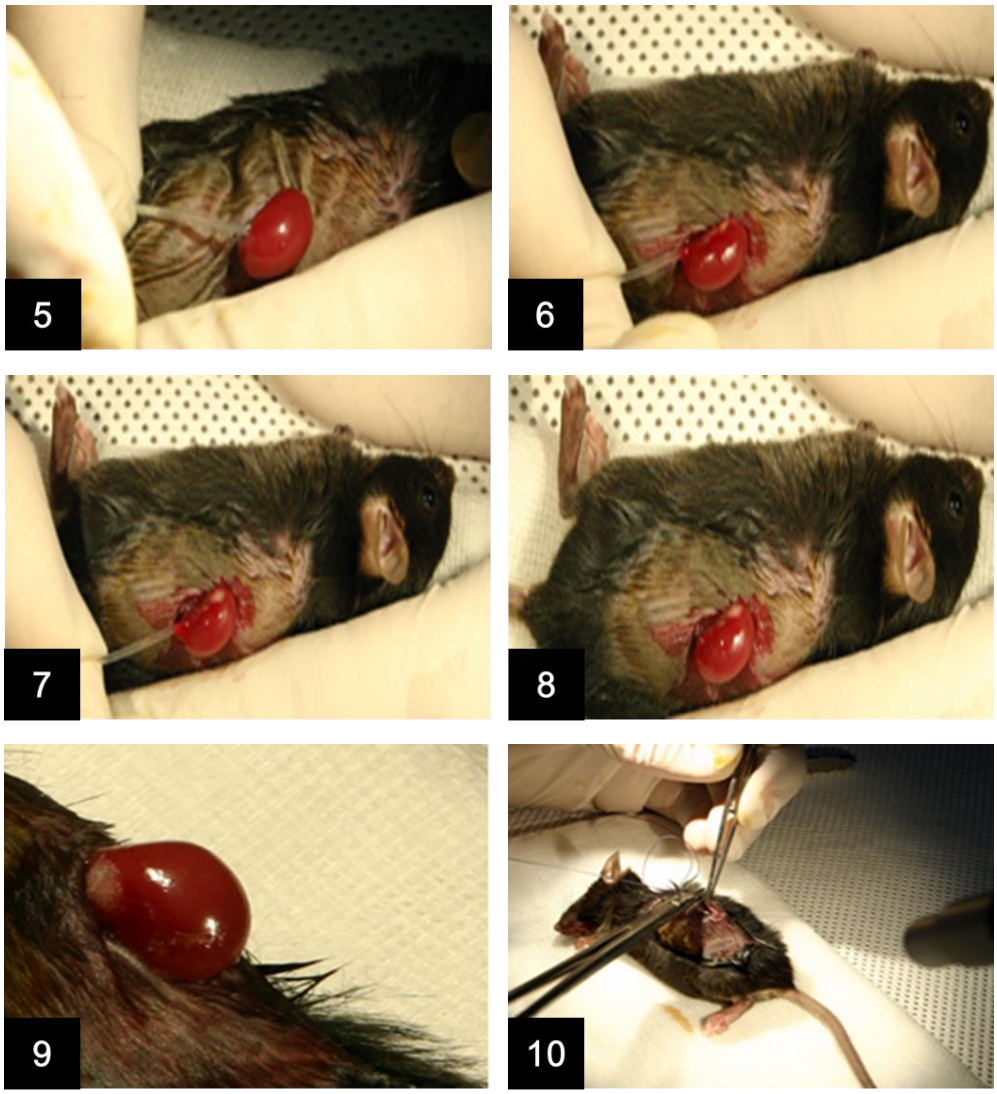

Figure 3. Procedure for renal subcapsular islet transplantation

1. Kidney exposed on the incised skin. 2. Scratched renal capsule before PE tube entry. 3. Entry of PE tube under the capsule. 4. Islet advancement by Hamilton syringe. 5-7. Advancing islets from PE tube to SRS. 8. Retrieval of PE tube. 9. Sealing the entry site using a cautery kit. 10. Kidney relocation and closure of peritoneum and skin.

7. Skin transplantation

All surgical procedures were carried out with isoflurane anesthesia. Allogeneic BALB/c and syngeneic B6 skin grafts were adopted as donors and the tail skins were removed using a surgical blade (Feather, Osaka, Japan). Truncated BALB/c and B6 skin grafts were attached on the bottom of a sterile petri dish. After anesthetizing the B6 recipient, skin of 1.5 x 1.5 cm size on the left flank was carefully removed without damaging the peritoneum. Adequate size BALB/c and B6 skin grafts were cut and placed onto the exposed peritoneum. Skin grafts on the peritoneum were secured with non-adhering dressings (Johnson & Johnson) and sheer bandages (Johnson & Johnson) for 7 days. On day 7 post-transplantation, the bandages were carefully removed and the skin grafts were observed daily.

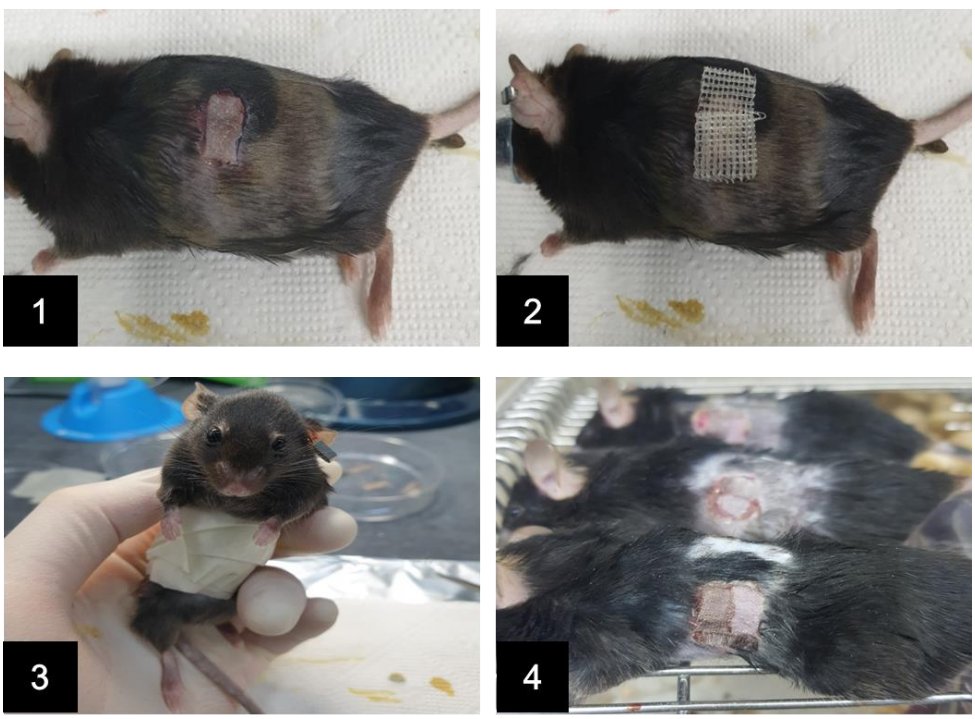

Figure 4. Procedure for skin transplantation

1. BALB/c skin graft placed on the left flank of a B6 mouse. 2. Non-adhering dressings covering the graft. 3. Sheer bandage wrapped around the body. 4. Removal

of bandage after 7 days.

8. Nephrectomy (kidney removal)

All surgical procedures were carried out with isoflurane anesthesia. The left flank of the anesthetized mouse was incised, and the kidney was gently pulled out of the abdominal cavity. After separating the kidney from adjacent organs and fat tissues, the renal artery and vein were tightly clamped using hemostatic clamp forceps. The renal artery and vein were ligated with an aseptic silk thread under the jaw of clamping forceps. Using a surgical blade (Feather), the kidney on the jaw of clamping forceps was delicately removed. The extracted kidney was then transferred into the 4% paraformaldehyde (4% PFA; Santa Cruz Biotechnology, Dallas, TX, USA), and the opened peritoneum and skin were securely closed with a surgical thread.

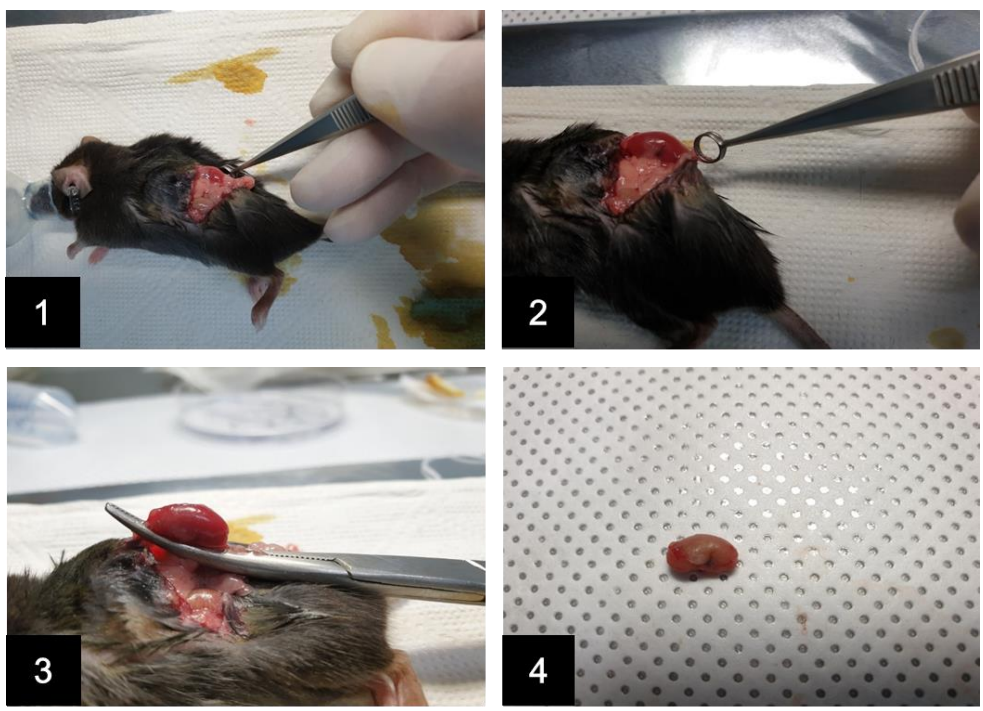

Figure 5. Procedure for nephrectomy

1. Incised skin and peritoneum before kidney exposure. 2. Islet-bearing kidney exposed on the skin. 3. Clamped renal artery and vein using hemostatic clamp forceps. 4. Extracted islet-bearing kidney.

9. Immunohistochemistry

Immunohistochemistry (IHC) staining was carried out as described previously[37]. Excised liver, kidney, and pancreas were fixed in 4% PFA for overnight. Using a microtome, paraffin embedded tissues were sectioned at 4 μm-thickness, and were attached onto the glass slides. For deparaffination, the slides were incubated in xylene (Thermo Fisher Scientific, Waltham, MA) for overnight, and subsequently rehydrated in a graded alcohol series. The target antigens were retrieved by microwaving the slides in Tris-EDTA buffer (Zytomed Systems GmbH, Berlin, Germany) for 20 minutes. After washing in TBST buffer 3 times, blocking solution (Thermo Fisher Scientific) was added for 10 minutes in a wet chamber. Paraffin-embedded tissue sections were triple stained. For primary antibody staining, anti-insulin guinea pig IgG (Genetex, Irvine, CA, USA), anti-CD3 rabbit IgG (Dako Laboratories, Santa Clara, CA, USA), and anti-FoxP3 rat IgG (eBioscience, San Diego, CA, USA) antibodies were used. For secondary antibody staining, goat anti-guinea pig IgG-AP (Abcam, Cambridge, UK), goat anti-rabbit IgG-HRP (Abcam), and goat anti-rat IgG-AP (Abcam) were used. The precipitates, Fast Red (Zytomed System GmbH, Berlin, Germany), DAB (GBI Labs, Bothell, WA, USA), and LV Blue (Vector Laboratories, Burlingame, CA, USA) were applied for color development. The sections were visualized with imaging microscopy (Axio Imager A1; Carl Zeiss, Heidenheim, Germany).

10. Mixed lymphocyte reaction

For stimulators, a BALB/c mouse was sacrificed to obtain the spleen, and isolated splenocytes were irradiated with 25 Gy of γ-ray. For responders, a naïve FoxP3-eGFP transgenic B6 mouse was sacrificed to obtain the splenocytes, which were further purified into Thy1.2$^+$ T cells using a Thy1.2 magnetic bead separation (Magnetic-Activated Cell Sorting; Miltenyi, Bergisch Gladbach, Germany). Using a FACS Aria sorter III (BD Bioscience, Franklin Lakes, NJ, USA), Thy1.2$^+$ T cells were divided into the GFP$^+$ Treg cells and GFP$^-$ Teff cells. 5x10^5 GFP$^-$ Teff cells were labeled with 1μM of CFSE (Thermo Fisher Scientific) and co-cultured with irradiated 5x10^5 BALB/c splenocytes in 96-well round-bottom plate for 5 days. In this co-culture, GFP$^+$ Treg cells isolated from tolerant and naïve FoxP3-eGFP transgenic mice were added at a ratio of 2:1 (2.5x10^5), 8:1 (6.25x10^4), and 32:1 (1.56x10^4), respectively. GFP$^-$ Teff cells stimulated with anti-CD3 (eBioscience) & CD28 Abs (eBioscience) were used as a positive control. After 5 days of incubation, the cells were harvested and stained with PerCP-Cy5.5-anti-mouse H2-K^b Ab (Biolegend, San Diego, CA, USA), fixable viability dye eFluor660 (Invitrogen, Carlsbad, CA, USA), and PE-anti-mouse FoxP3 (eBioscience) to analyze only the proliferation of viable B6 Teff cells. The analysis was conducted using a FACS Canto II flow cytometer (BD Biosciences).

11. IFN-γ ELISpot assay

Splenocytes of tolerant recipients were stained with APC-Cy7-anti-mouse CD8 Ab (eBioscience), and CD8$^+$ T cells were subsequently isolated using a FACS Aria sorter III (BD Bioscience). Microtitre plates (EMD Millipore Corporation, Billerica, MA, USA) were coated overnight at 4°C with anti-mouse IFN-γ mAb (15 μg/ml; eBioscience) and then blocked for 2 hours with 10% FBS-supplemented RPMI1640

media (Hyclone Laboratories, Inc.) at 37°C in a 5% CO_2 incubator. After removing the media, $7x10^4$ $CD8^+$ T cells were seeded with $5x10^5$ of 20 Gy irradiated BALB/c splenocytes in 10% FBS-supplemented RPMI1640 media for 24 hours at 37°C in a 5% CO_2 incubator. After incubation, cells were washed off, and the plates were then washed three times with PBST (0.1% TWEEN20). After washing the plates a further three times with sterile PBS, biotinylated anti-mouse IFN-γ detection antibodies diluted (3 μg/ml, eBioscience) in PBS (1% bovine serum albumin (BSA)) were added and incubated overnight at 4°C. After washing, 1 μg of streptavidin-alkaline phosphatase (eBioscience) diluted at a ratio of 1:100 in ELISA diluent buffer (eBioscience) was added in 100 μl for 2 hours at room temperature. Then, color was developed by adding 100 μl of AEC substrates (BD Bioscience) and stopped by washing off using tap water. The spots were analyzed using an ELISpot reader system (AID, Strassberg, Germany).

12. FoxP3 analysis

For histologic FoxP3 analysis, $FoxP3^+$ cells and $CD3^+$ cells were counted in three independent assays using a cell counter-ImageJ (NIH, Bethesda, MD, USA). The $FoxP3^+/CD3^+$ ratio was calculated. For intracellular $FoxP3^+$ analysis, peripheral blood was obtained from the retro-orbital plexus of mice. Red blood cells were lysed by Red Blood Cell Lysing Buffer Hybri-Max™ (Sigma-Aldrich). To block non-specific binding, the samples were incubated with 2.4G2, which was purified from hybridoma supernatant with protein G columns, for 10 minutes at room temperature. After FACS buffer washing, the cells were stained with PerCP-Cy5.5-anti-mouse CD4 Ab (eBioscience) and PE-anti-mouse CD25 Ab (BD Bioscience) for 1 hour at 4°C. After fixation and permeabilization, the cells were stained with APC-anti-

mouse FoxP3 (eBioscience) or IgG2a isotype control (clone:eBR2a; eBioscience) for 1 hour at 4°C. The analysis was conducted using a FACS Canto II flow cytometer (BD Biosciences).

13. Statistical analysis

All statistical analyses were performed using GraphPad Prism 5 (GraphPad Software, La Jolla, CA, USA). Statistical significance was determined by paired or unpaired two-tailed Student's t-test. All *p*-values were defined as: * level of significance, $p<0.05$.

III. Results

1. Anti-CD154 blockade single treatment in intrahepatic islet transplantation model

1.1. Short-term anti-CD154 mAb treatment alone significantly prolonged the survival of BALB/c islets transplanted into the liver of diabetic B6 mice

To determine the effect of the CD154 blockade alone, I administered MR1 for a short time to diabetic B6 mice transplanted with BALB/c islets via a cecal vein route (Fig 1A). STZ-treated mice were caged for the next 5-6 days prior to islet transplantation to excrete the remaining STZ from the body and 700 IEQs were transplanted to the recipients on day 0 (Fig 1A). It was of note that all mice injected with MR1 maintained normoglycemia for more than 100 days (less than 250 mg/dL), whereas the untreated mice rejected the islet allografts within 20 days (Fig 1B-C). MR1 treatment alone showed statistically significant (p=0.0002) prolongation of the allogeneic islet survival compared to the non-treated group (Figure 1C). All mice treated with MR1 were normoglycemic until they were euthanized. Altogether, these results indicate that MR1 treatment alone results in indefinite islet allograft survival in the liver.

A

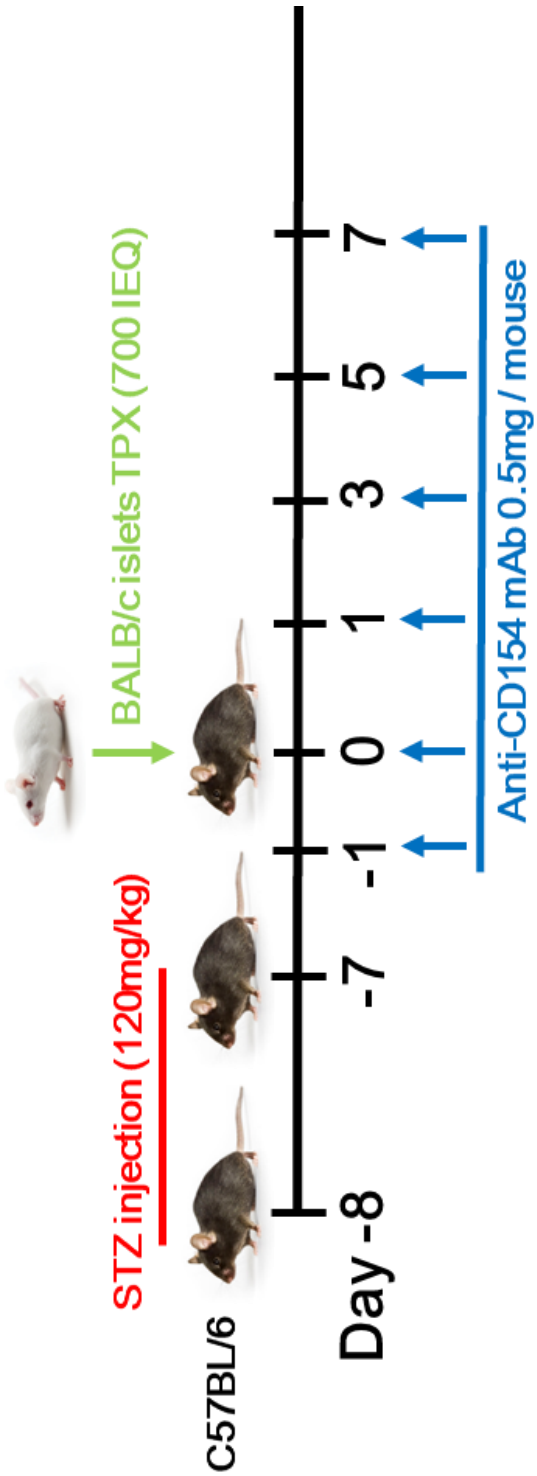
C57BL/6
STZ injection (120mg/kg)
BALB/c islets TPX (700 IEQ)
Anti-CD154 mAb 0.5mg / mouse
Day -8
-7
-1
0
1
3
5
7

B

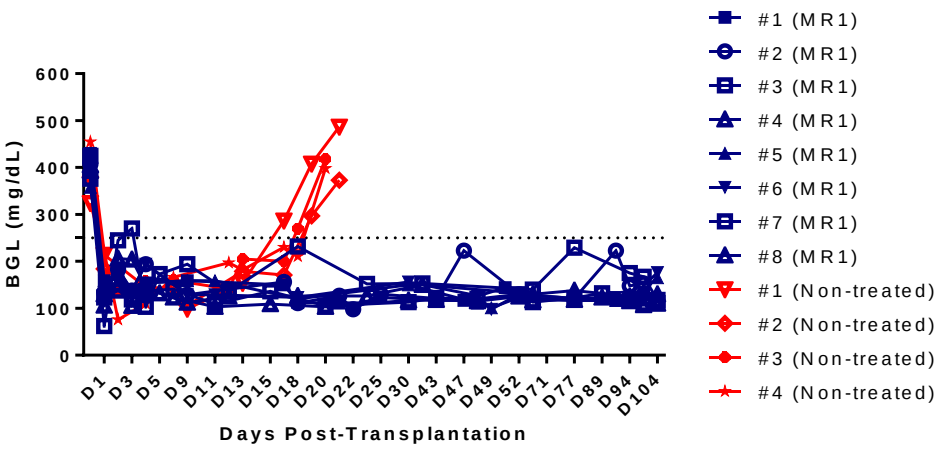
BGL (mg/dL)
600
500
400
300
200
100
0
D1
D3
D5
D9
D11
D13
D15
D18
D20
D22
D25
D30
D43
D47
D49
D52
D71
D77
D89
D94
D104
Days Post-Transplantation
#1 (MR1)
#2 (MR1)
#3 (MR1)
#4 (MR1)
#5 (MR1)
#6 (MR1)
#7 (MR1)
#8 (MR1)
#1 (Non-treated)
#2 (Non-treated)
#3 (Non-treated)
#4 (Non-treated)

C

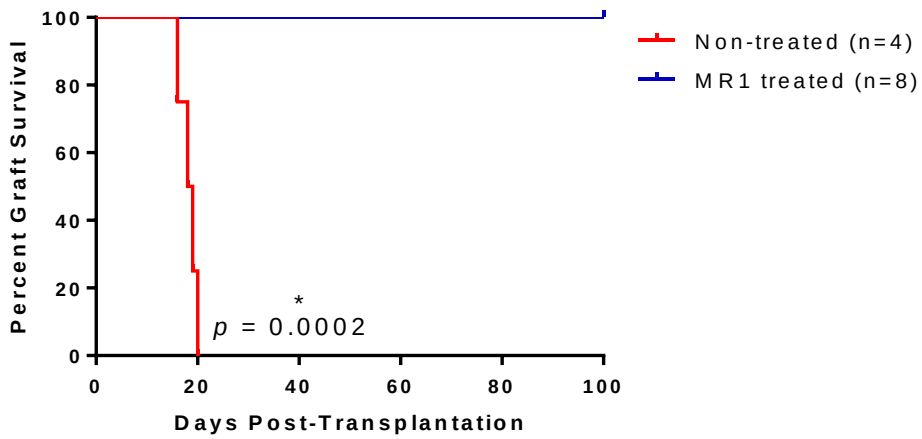
Percent Graft Survival
100
80
60
40
20
0
0
20
40
60
80
100
Days Post-Transplantation
*
p = 0.0002
Non-treated (n=4)
MR1 treated (n=8)

Figure 1. Effect of short-term MR1 single treatment on intrahepatic islet survival in vivo. A. Schematic illustration of the experimental setup. Diabetic C57BL/6 mice were transplanted with BALB/c allogenic islets (700 IEQ) through the cecal vein route. Anti-CD154 mAb (MR1) were intraperitoneally administered on days -1, 0, 1, 3, 5, and 7 (n=8). Non-treated mice were used as controls (n=4). B. BGL was measured with a OneTouch Ultra device from day 0. The blood was obtained from snipped tail. C. The survival graph was plotted from B. Statistical significance was determined by the Mantel-Cox (log-rank) test. Asterisk (*) indicates statistical significance ($p<0.05$). All normoglycemic mice were sacrificed at DPT 257 (#1-4) or DPT 105 (#5-8) for histologic analysis.

1.2. Engraftment of allogeneic islets by short-term anti-CD154 mAb treatment

The immunostaining of the liver showed that islets located near the liver sinusoids were positive for insulin and remained intact for more than 250 days in MR1-treated mice only and not in untreated mice (Fig 2A-B). $FoxP3^+$ Treg cells were not found in the grafts where only a few $CD3^+$ T cells were infiltrated (Fig 2A). However, the number of $FoxP3^+$ Treg cells were relatively increased near the grafts where infiltrating $CD3^+$ T cells were abundantly detected (Fig 2A). Untreated mice showed $CD3^+$ lymphoid aggregates in the liver sinusoids but failed to stain for β-cells in whole liver (Fig 2B). Also, the MR1-treated mice still showed a complete lack of β-cells in the pancreas, whereas these cells were present in wild type mice (Fig 2C). These findings proved that the recovered normoglycemia was solely controlled by the engrafted allo-islets in the liver, and not by pancreatic regeneration. Overall, these results indicate that MR1 treatment alone results in successful engraftment of islet allograft in the liver.

A

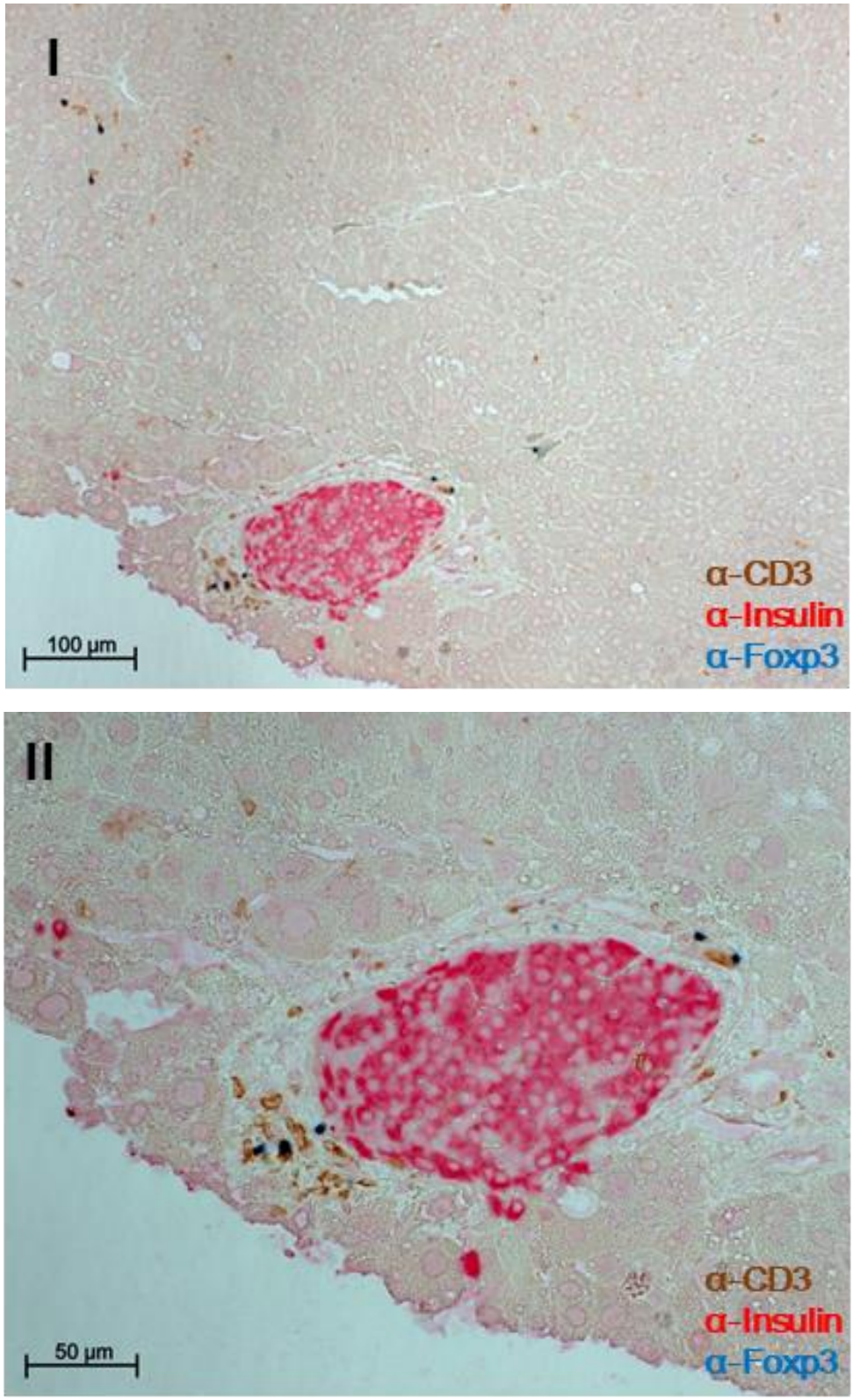

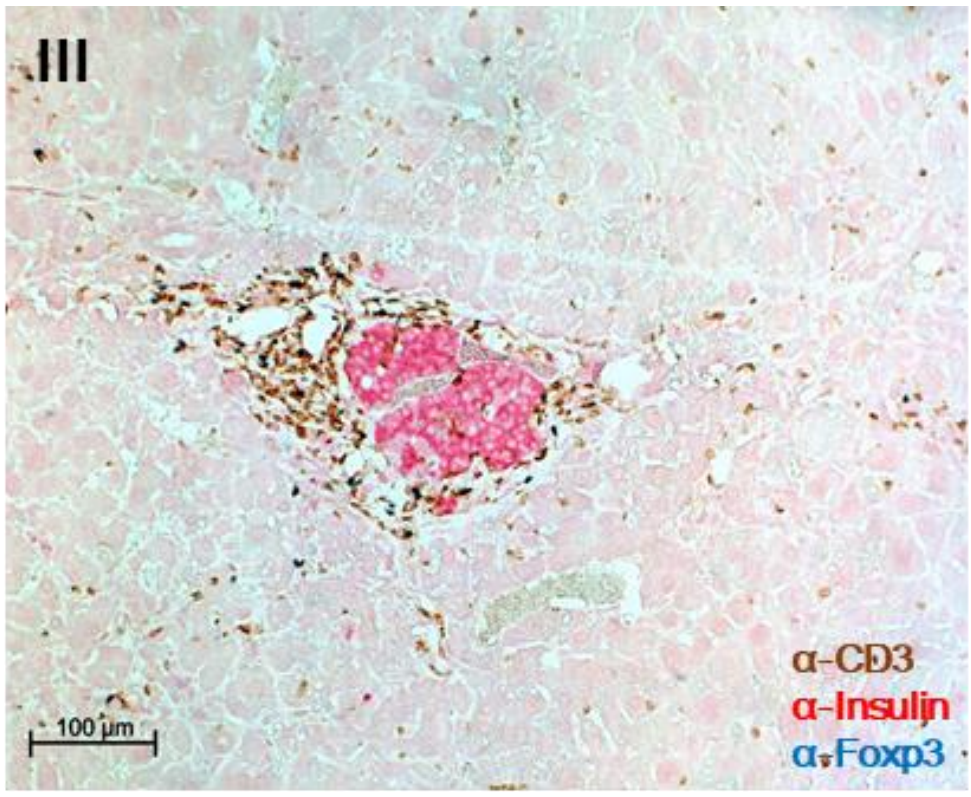
III
α-CD3
α-Insulin
α-Foxp3
100 µm


IV
α-CD3
α-Insulin
α-Foxp3
50 µm

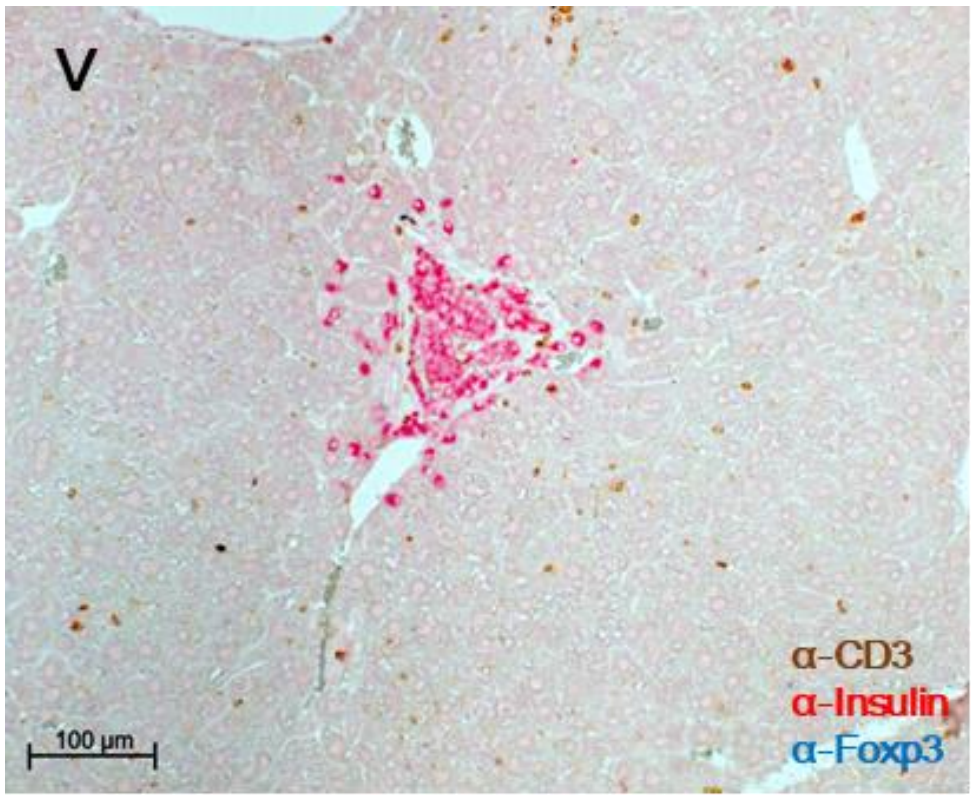
V
α-CD3
α-Insulin
α-Foxp3
100 µm

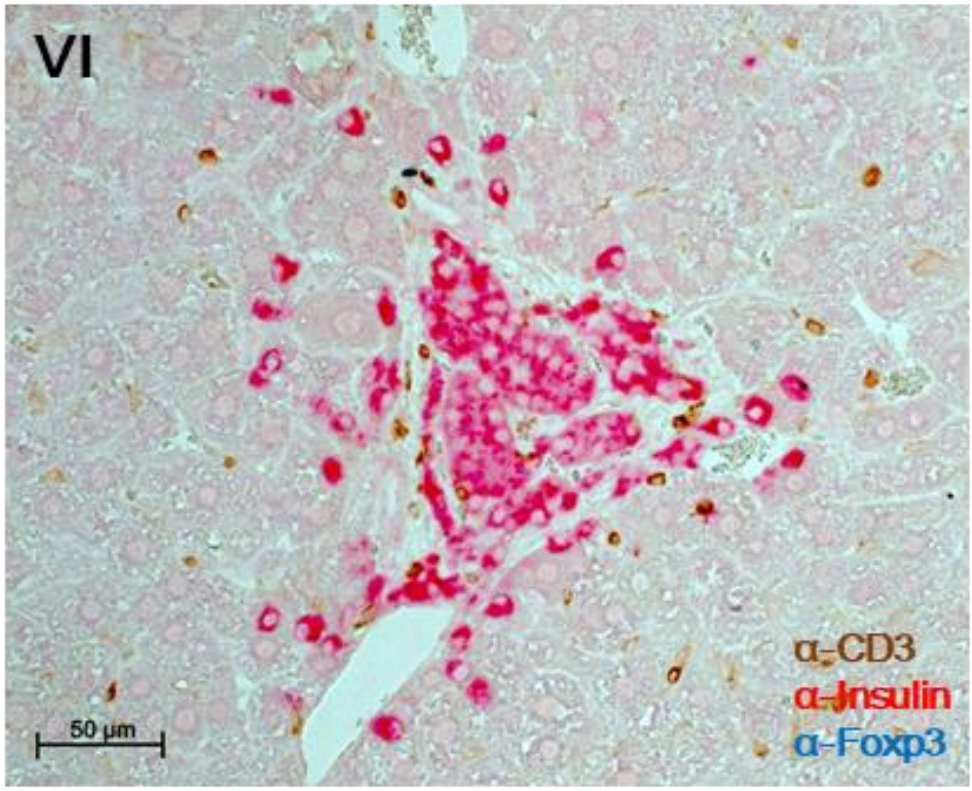
VI
α-CD3
α-Insulin
α-Foxp3
50 µm

B

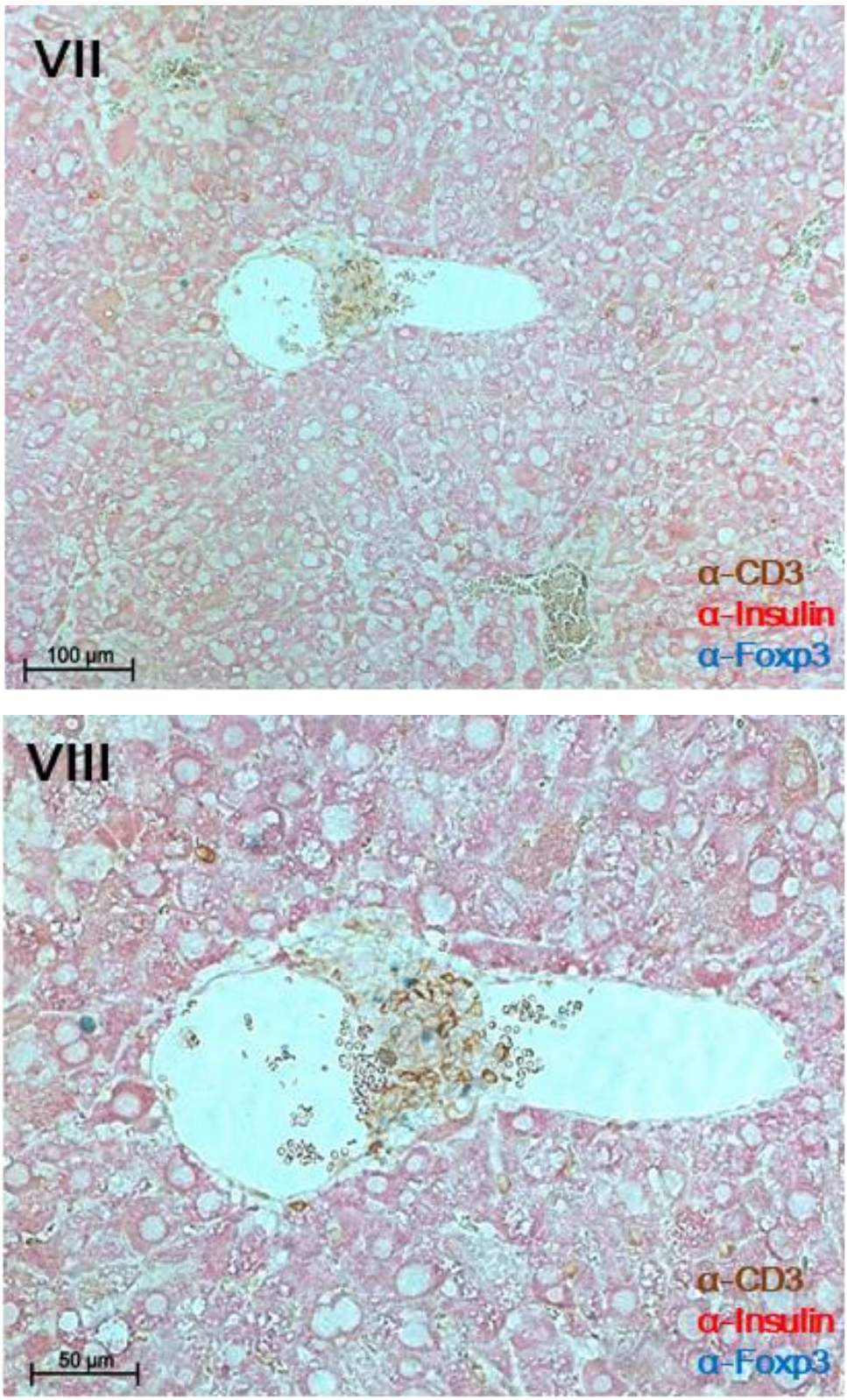
VII
α-CD3
α-Insulin
α-Foxp3
100 µm
VIII
α-CD3
α-Insulin
α-Foxp3
50 µm

C

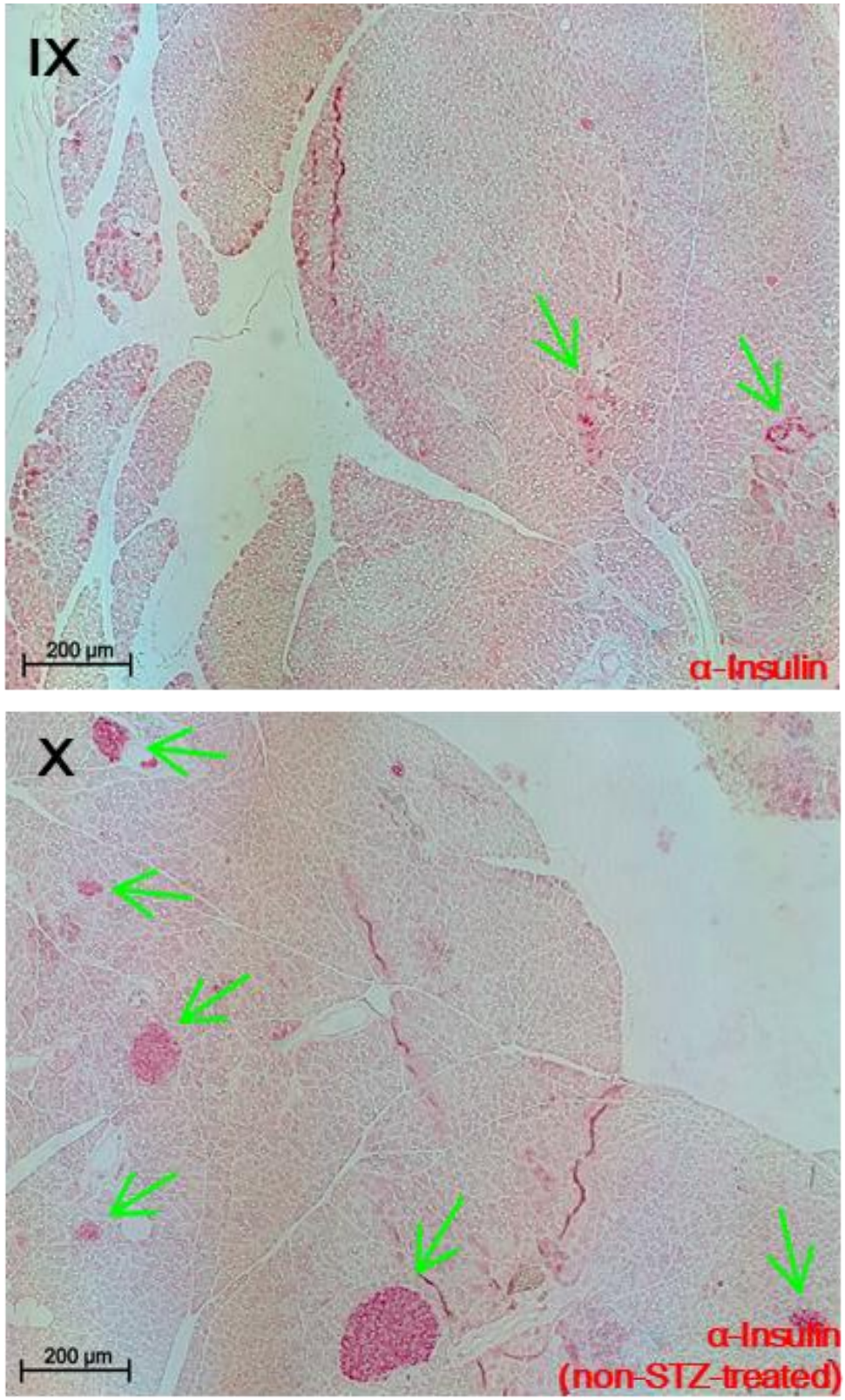

Figure 2. Successful engraftment of islet grafts in liver. Immunohistochemistry (IHC) stain of paraffin-embedded islet transplanted liver and pancreatic tissues. Section slides were triple-stained with anti-CD3 (brown), anti-insulin (red), and anti-FoxP3 (blue) or mono-stained with anti-insulin (red). A. I-II (DPT 105), III-VI (DPT 257): liver section of islet transplanted mouse. Original magnification 100μm, and 50μm. B. VII-VIII: liver section of graft rejected mouse. Original magnification 100μm, and 50μm. C. IX: pancreatic section of islet transplanted mouse. X: pancreatic section of non-STZ-treated mouse. Original magnification 200μm. Stained islets in pancreatic section were denoted by green arrows.

2. Survival of allogeneic islets by immune tolerance

2.1. Secondly transplanted BALB/c islets under the kidney capsule of the B6 mice engrafted formerly with BALB/c islet in the liver were permanently accepted

I investigated whether MR1 alone could induce immune tolerance in my model. Thus, without administering additional IS therapy, I transplanted second allo-islets under the kidney capsule of B6 recipients that had formerly been transplanted with BALB/c islets into the liver. Among those mice which were maintaining normoglycemia for more than 100 days, one group was transplanted with second-party (donor-specific) BALB/c islets, and the other group was transplanted with both BALB/c and C3H islets (third-party) beneath the left kidney capsule (Fig 3A). On day 14 or 34 post-transplantation, islet-bearing kidneys were removed by nephrectomy. Surprisingly, I found that second-party (donor-specific) BALB/c islets survived for periods up to kidney removal in all mice, whereas third-party C3H islets were completely rejected at 14 days post-transplantation (DPT) (Fig 3B). Immunostaining analysis of the surviving graft-bearing kidneys revealed that donor islets transplanted under the kidney capsule remained almost intact in all mice, while heavy infiltration of $CD3^{+}FoxP3^{+}$ Treg cells was mostly observed in the peri-graft sites (Fig 3C). Subsequent immunostaining showed that allo-islets remained intact in the liver even after the removal of islet-bearing kidney (Fig 3D). Considering the fact that $CD3^{+}FoxP3^{+}$ Treg cells were consistently found around the surviving allo-islets, these immune-regulatory cells might contribute to immune tolerance in my model. Overall, these results may indicate that long-term graft survival is due to the

immune tolerance induced by MR1 in the intrahepatic islet allo-transplantation model.

A

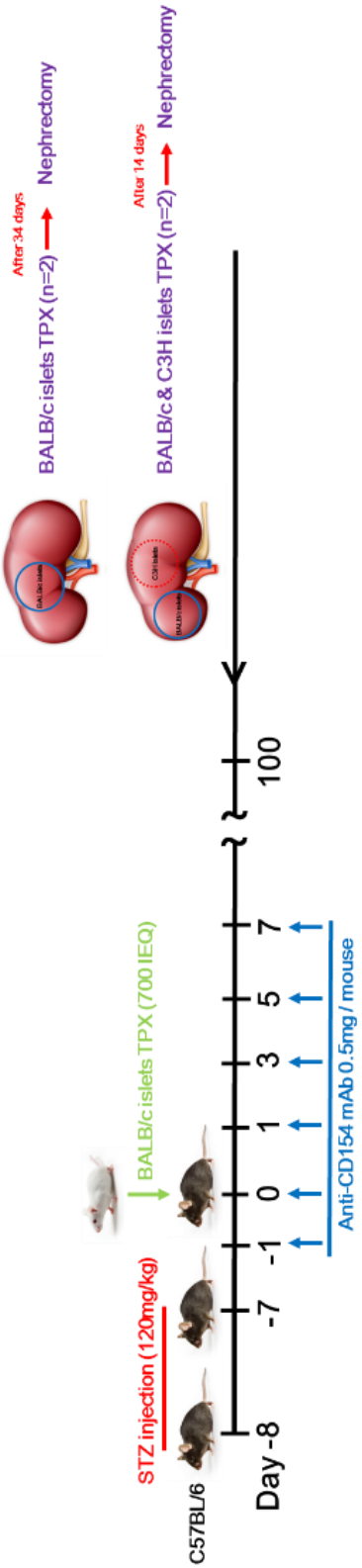
After 34 days
BALB/c islets TPX (n=2)
Nephrectomy
After 14 days
BALB/c & C3H islets TPX (n=2)
Nephrectomy
BALB/c islets TPX (700 IEQ)
STZ injection (120mg/kg)
C57BL/6
Day -8
-7
-1
0
1
3
5
7
100
Anti-CD154 mAb 0.5mg / mouse

B

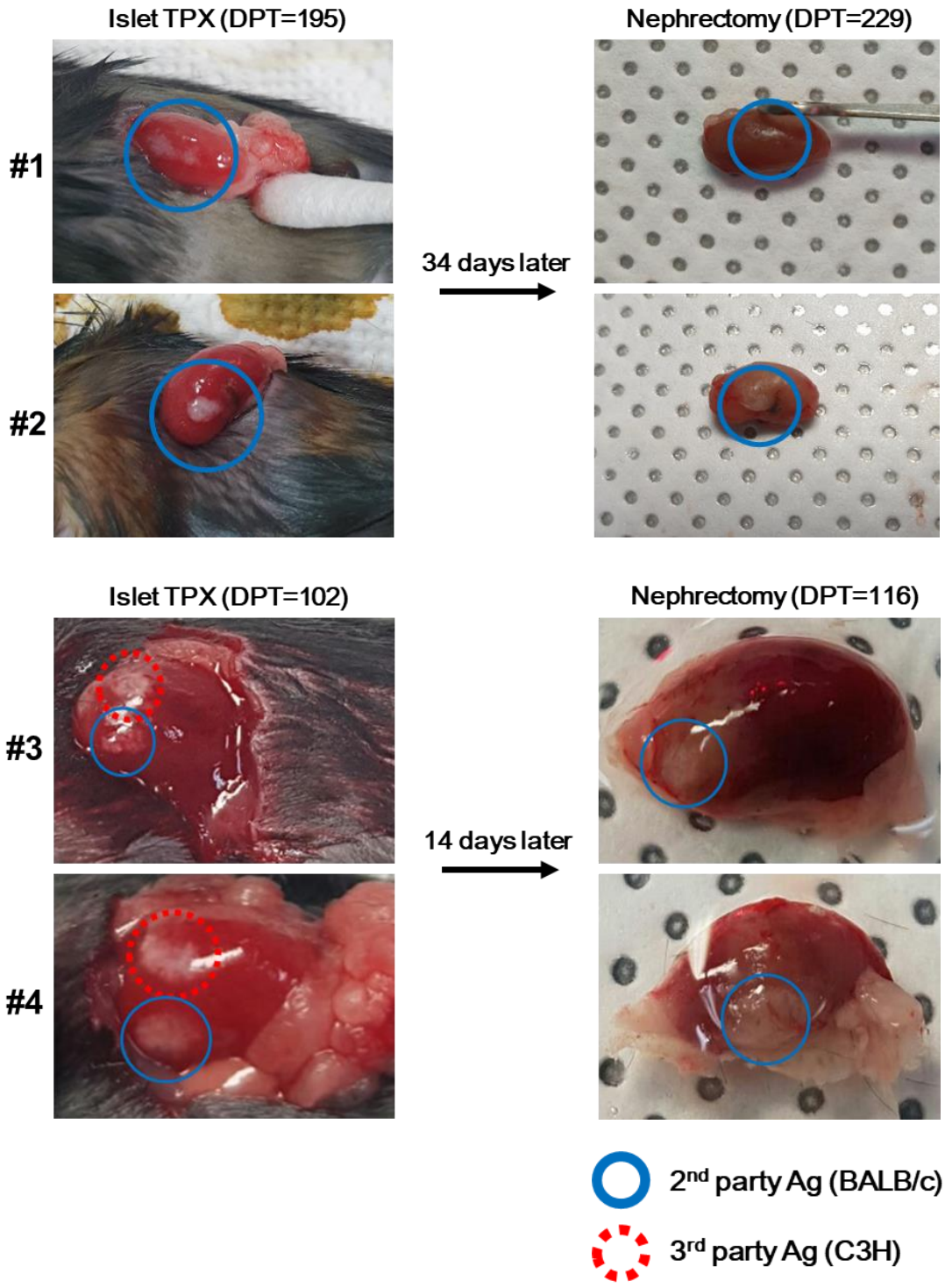
Islet TPX (DPT=195)
Nephrectomy (DPT=229)
#1
34 days later
#2
Islet TPX (DPT=102)
Nephrectomy (DPT=116)
#3
14 days later
#4
2nd party Ag (BALB/c)
3rd party Ag (C3H)

C

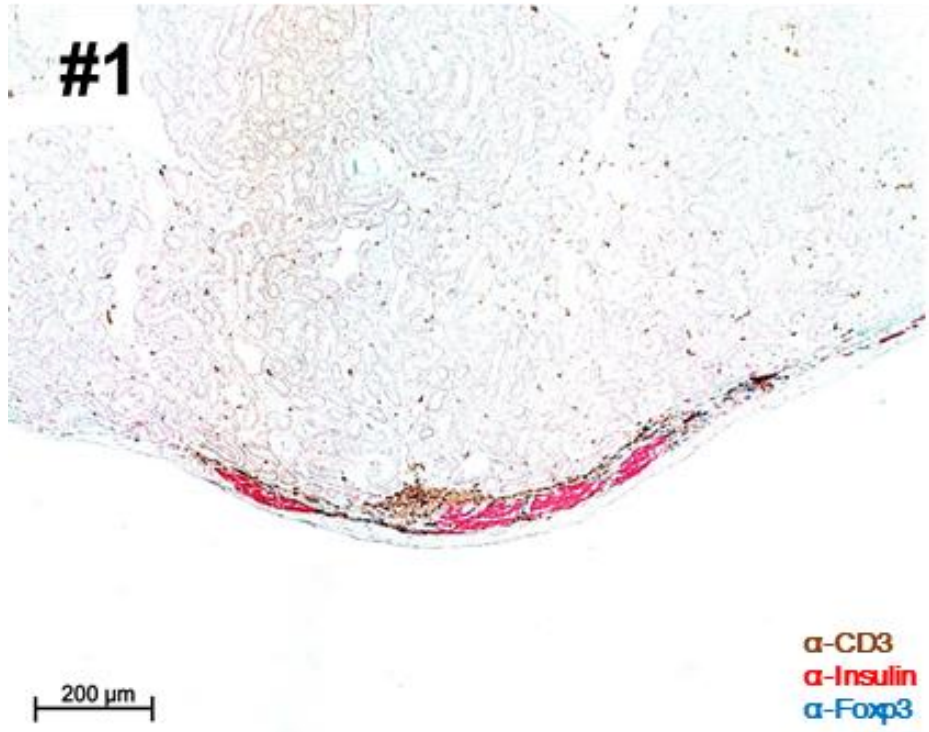

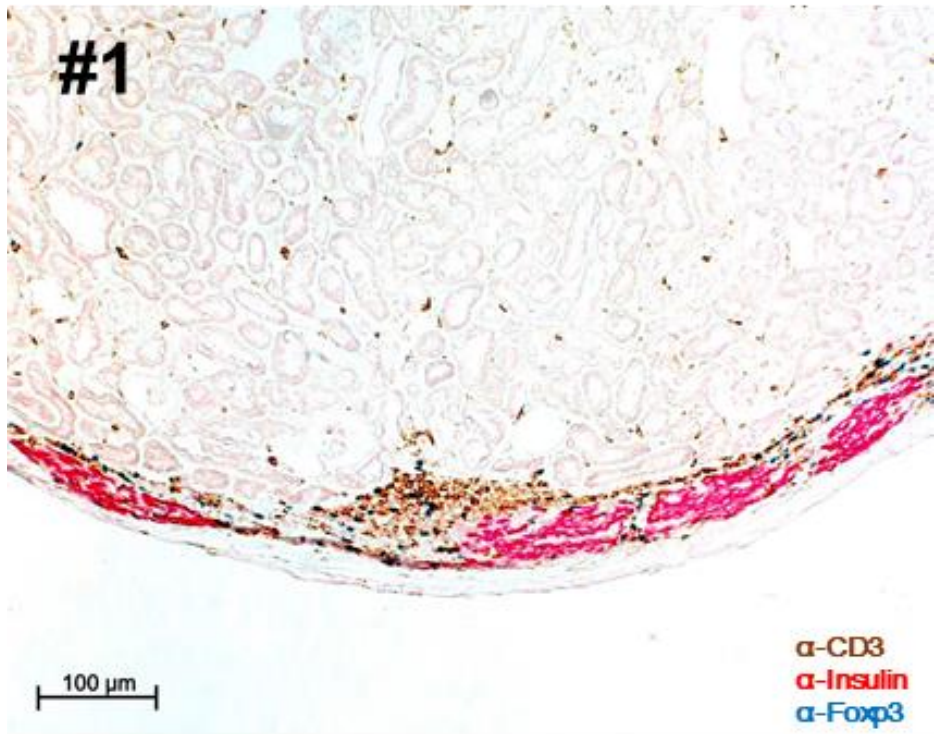

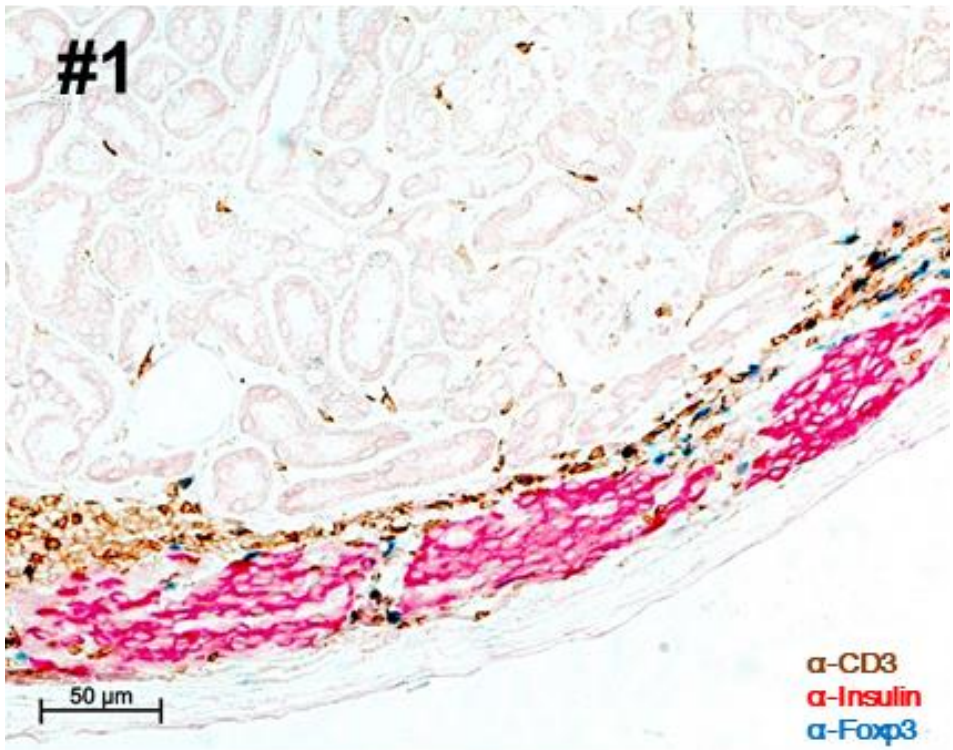
#1
50 µm
α-CD3
α-Insulin
α-Foxp3

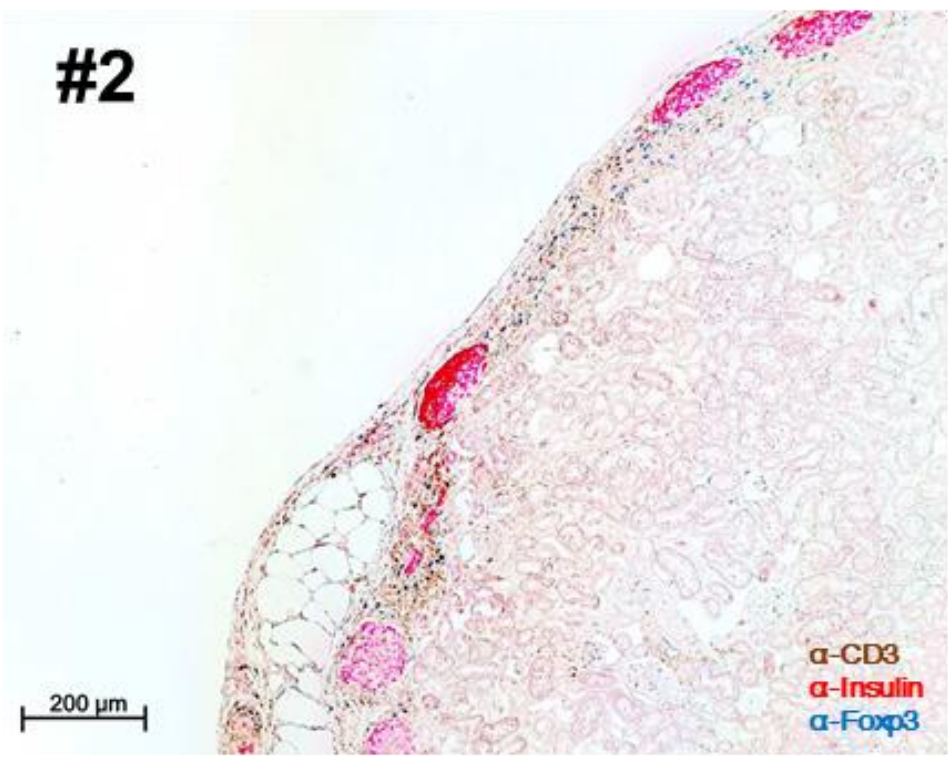
#2
200 µm
α-CD3
α-Insulin
α-Foxp3

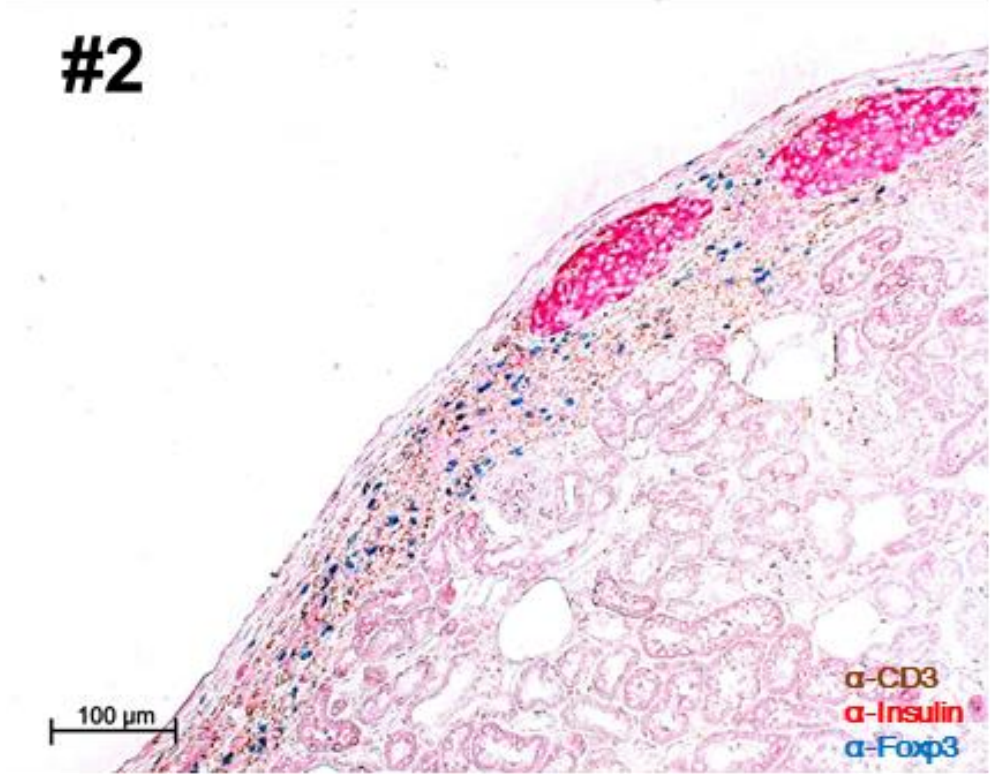
#2
100 µm
α-CD3
α-Insulin
α-Foxp3

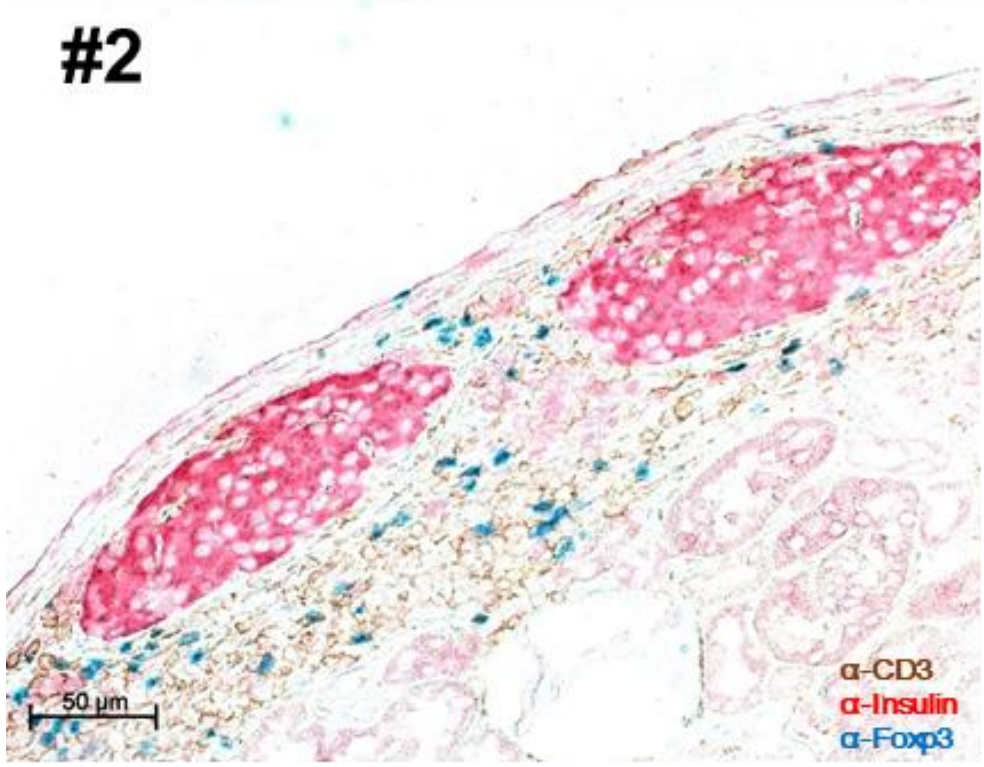
#2
50 µm
α-CD3
α-Insulin
α-Foxp3

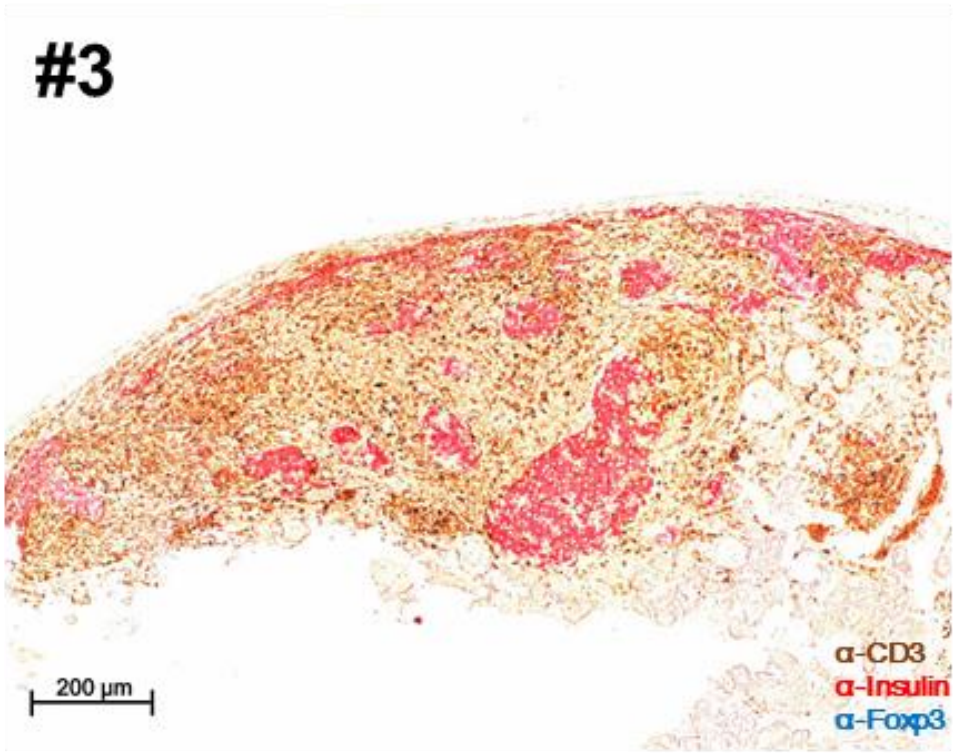
#3
200 µm
α-CD3
α-Insulin
α-Foxp3

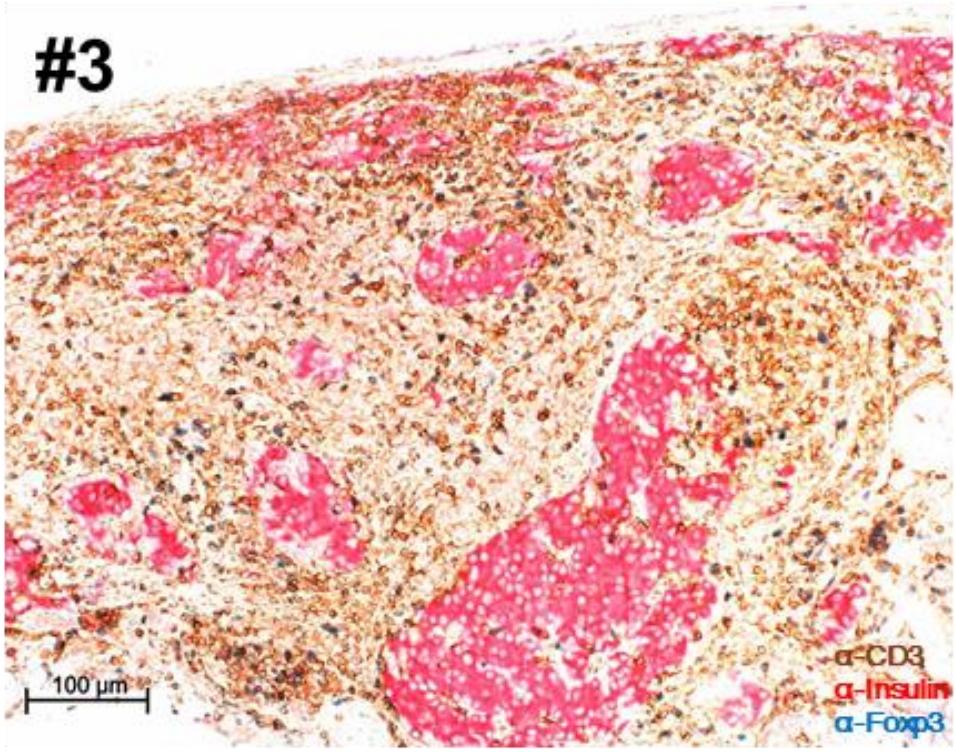
#3
100 µm
α-CD3
α-Insulin
α-Foxp3

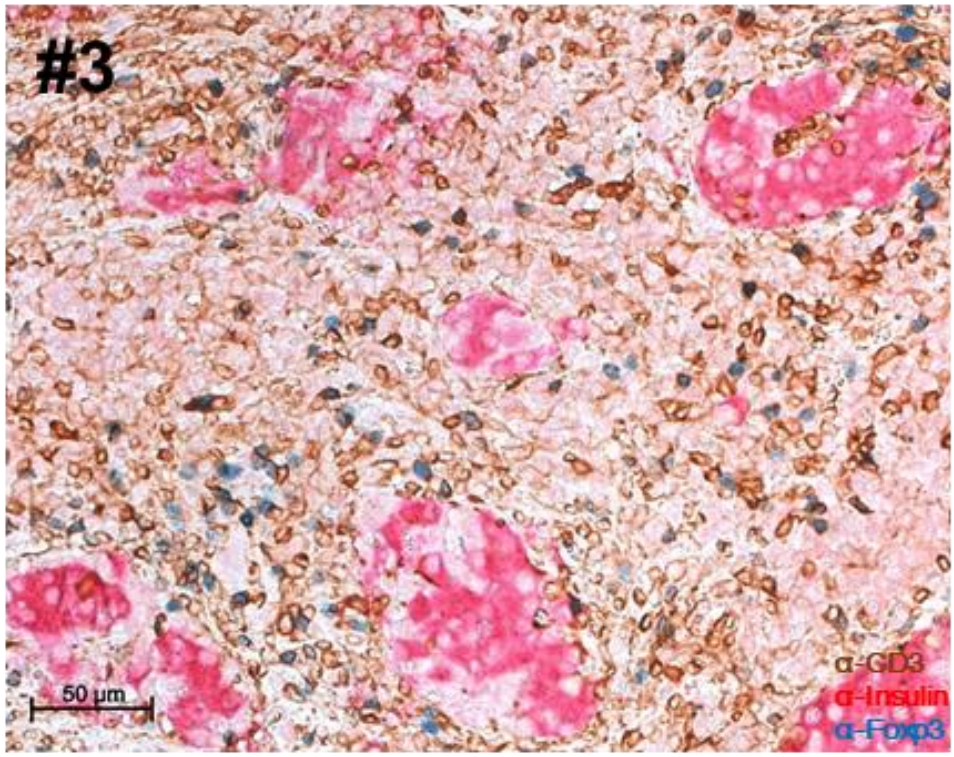
#3
50 µm
α-CD3
α-Insulin
α-Foxp3

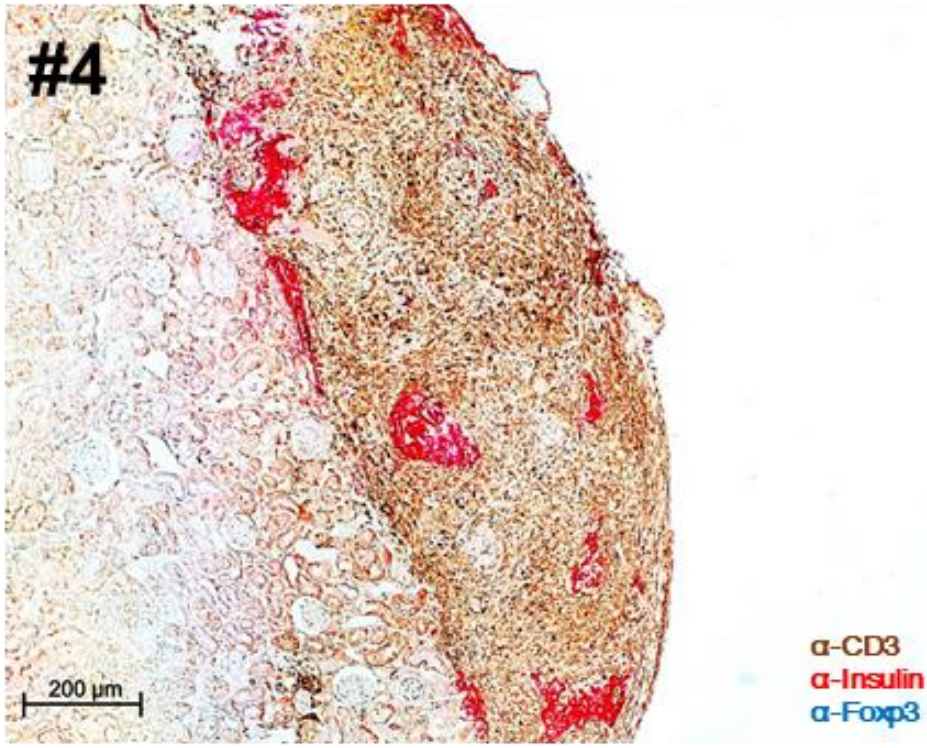
#4
200 µm
α-CD3
α-Insulin
α-Foxp3

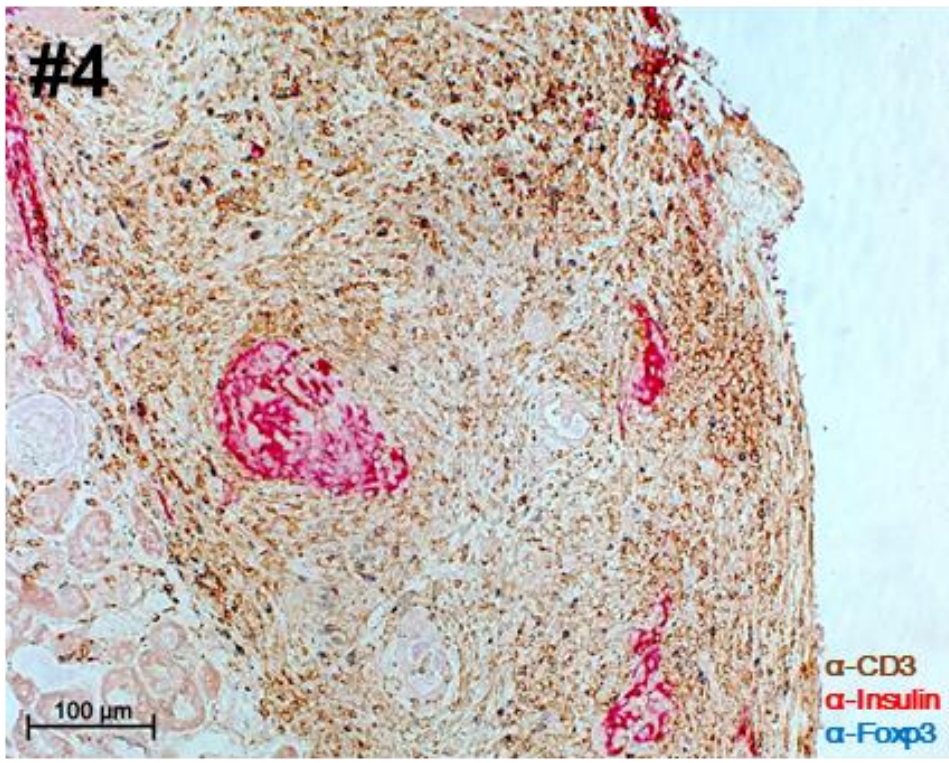
#4
100 µm
α-CD3
α-Insulin
α-Foxp3

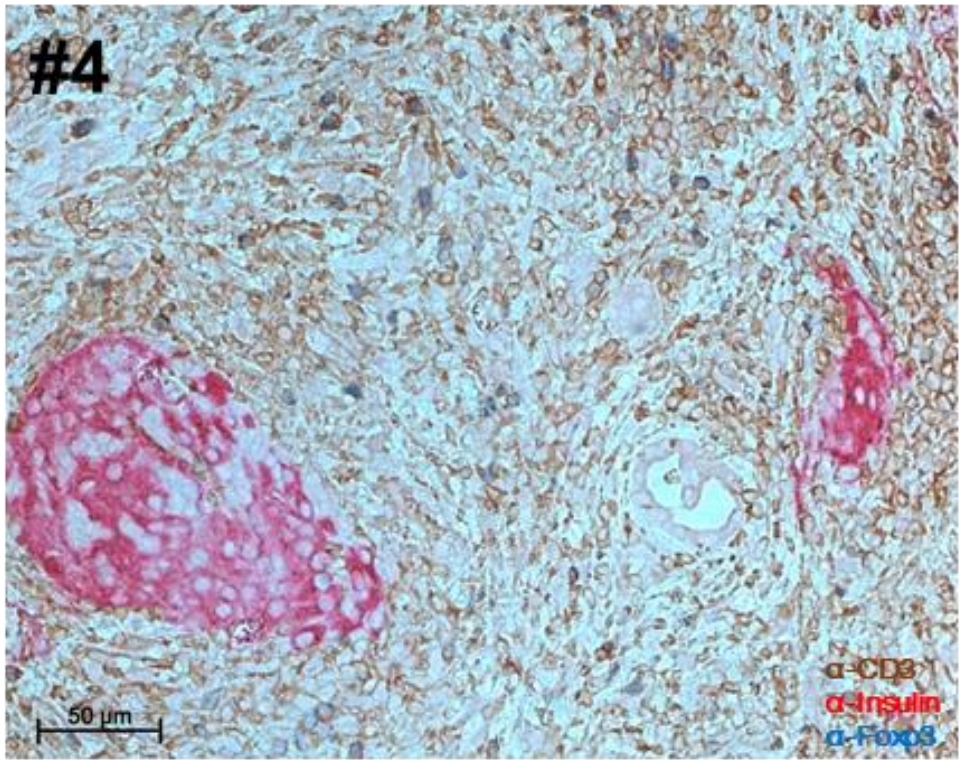
#4
50 µm
α-CD3
α-Insulin
α-Foxp3

D

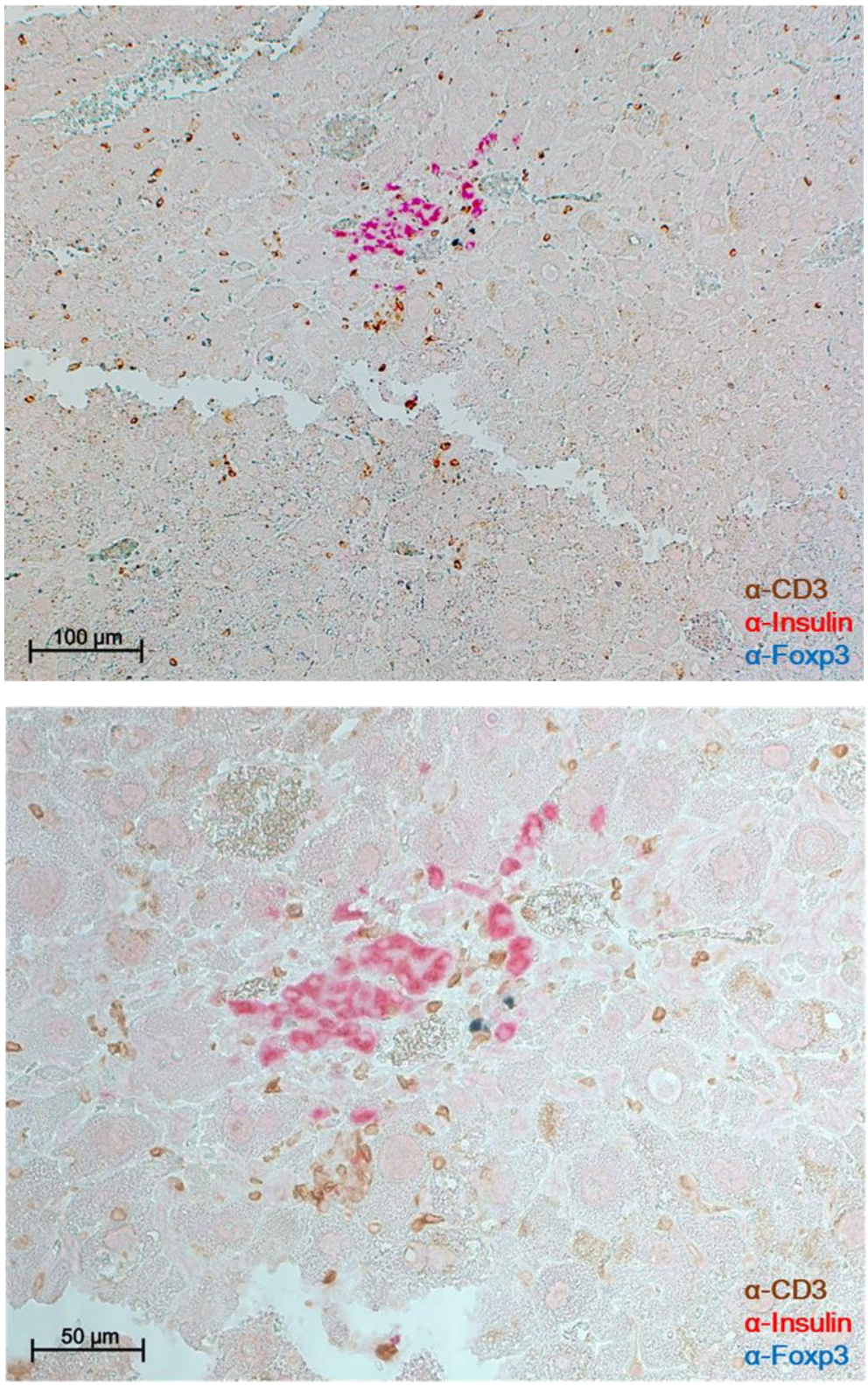

Figure 3. Second transplantation of BALB/c and C3H islets under the kidney capsule to confirm tolerance. A. Schematic illustration of the experimental setup. After recovery to normoglycemia, second allo-islets were transplanted under the left kidney capsule of the recipients without administration of immunosuppressive drugs. BALB/c islets (blue line circle) with or without C3H islets (red dot circle) were re-transplanted under the left kidney capsule without any immunosuppressive drugs. 400 IEQ (#1, #2) or 500 IEQ (#3, #4) were handpicked and implanted. After 34 or 14 days, nephrectomy was performed to remove islet-bearing kidneys. B. #1-2 mice were transplanted with single BALB/c islets (blue line circle), and #3-4 mice were transplanted with BALB/c islets (blue line circle) and C3H islets (red dot circle) at different sites of the same kidney. After 34 or 14 days later, the islet-bearing kidneys were removed (nephrectomy) and fixed with 4% PFA for subsequent immunostaining. C. IHC stain of the surviving islets under the kidney capsule. Section slides were triple-stained with anti-CD3 (brown), anti-insulin (red), and anti-FoxP3 (blue). Original magnification 200μm, 100μm, and 50μm. D. IHC stain of the islets in remaining liver. Section slides were triple-stained with anti-CD3 (brown), anti-insulin (red), and anti-FoxP3 (blue). Original magnification 100μm, and 50μm.

2.2. Modest delay in BALB/c skin graft rejection in tolerant B6 mice

Next, in order to investigate whether transplantation tolerance to islet allografts could be extended to allogeneic skin grafts in my model, I prepared three groups: tolerant B6 mice with engrafted intrahepatic BALB/c islets by MR1 monotherapy, naïve B6 mice, and pre-sensitized B6 mice previously injected intraperitoneally with irradiated BALB/c splenocytes (Fig 4A). BALB/c splenocytes were irradiated with 25 Gy of γ-ray and pre-sensitized B6 mice were caged for next 20 days to fully develop BALB/c antigen specific immune system (Fig 4A). All groups were then transplanted with syngeneic (B6) and allogeneic (BALB/c) skin grafts on the left flank of the body, and the skin grafts were inspected daily until they were fully engrafted (Fig 4B-C). I found that both tolerant and naïve B6 mice accepted syngeneic skin grafts at DPT 10 (Fig 4C). It is of note that, unlike naïve B6 mice, which rejected BALB/c skin allografts at DPT 14, tolerant B6 mice showed a modest prolongation of skin allograft survival for up to DPT 16-17 (Fig 4B-C). Meanwhile, pre-sensitized B6 mice rejected the BALB/c skin graft at DPT 9-10 (Fig 4B-C). Altogether, tolerant B6 mice showed a regulated immune response against skin allografts.

A

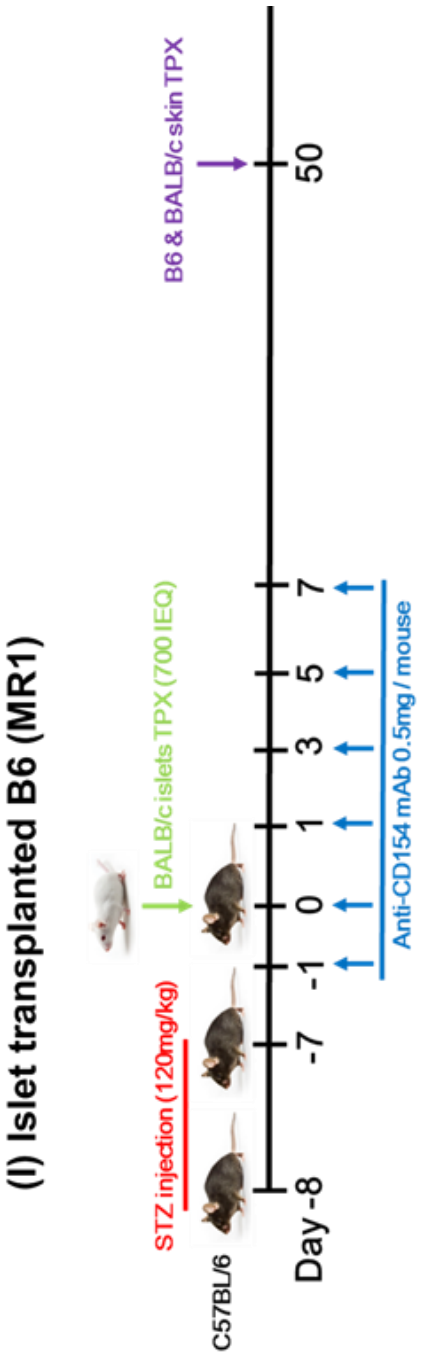
(I) Islet transplanted B6 (MR1)
C57BL/6
STZ injection (120mg/kg)
BALB/c islets TPX (700 IEQ)
B6 & BALB/c skin TPX
Day -8
-7
-1
0
1
3
5
7
50
Anti-CD154 mAb 0.5mg / mouse

(II) Naïve B6

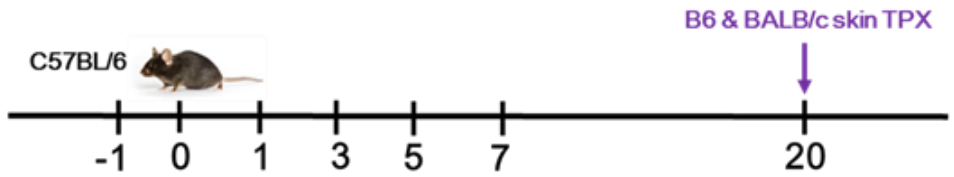

(III) Presensitized B6

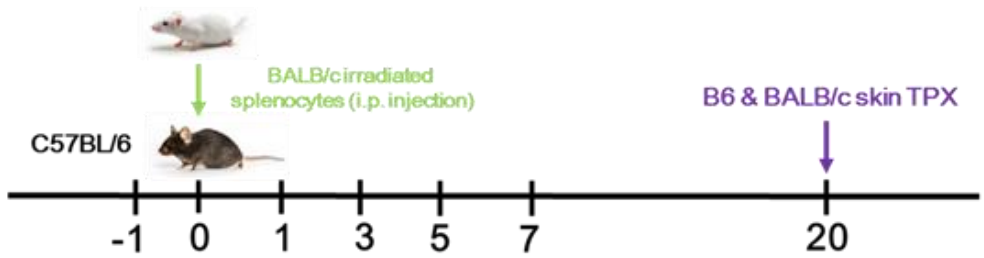

B

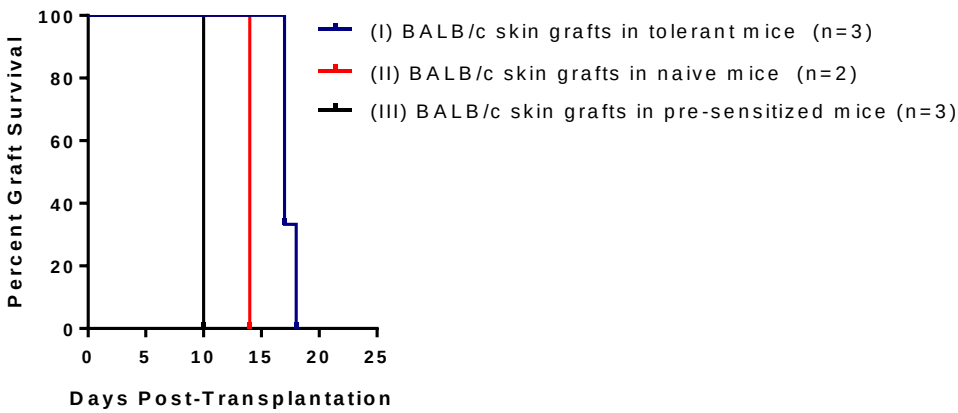
Percent Graft Survival
100
80
60
40
20
0
0
5
10
15
20
25
Days Post-Transplantation
(I) BALB/c skin grafts in tolerant mice (n=3)
(II) BALB/c skin grafts in naive mice (n=2)
(III) BALB/c skin grafts in pre-sensitized mice (n=3)

C

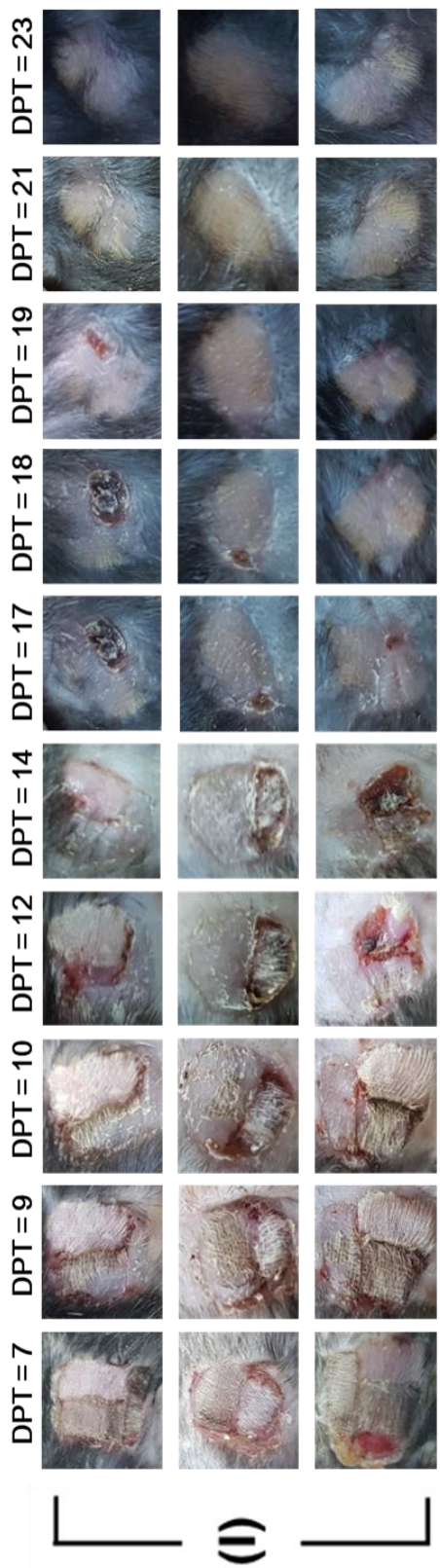

DPT = 7
DPT = 9
DPT = 10
DPT = 12
DPT = 14
DPT = 17
DPT = 18
DPT = 19
DPT = 21
DPT = 23

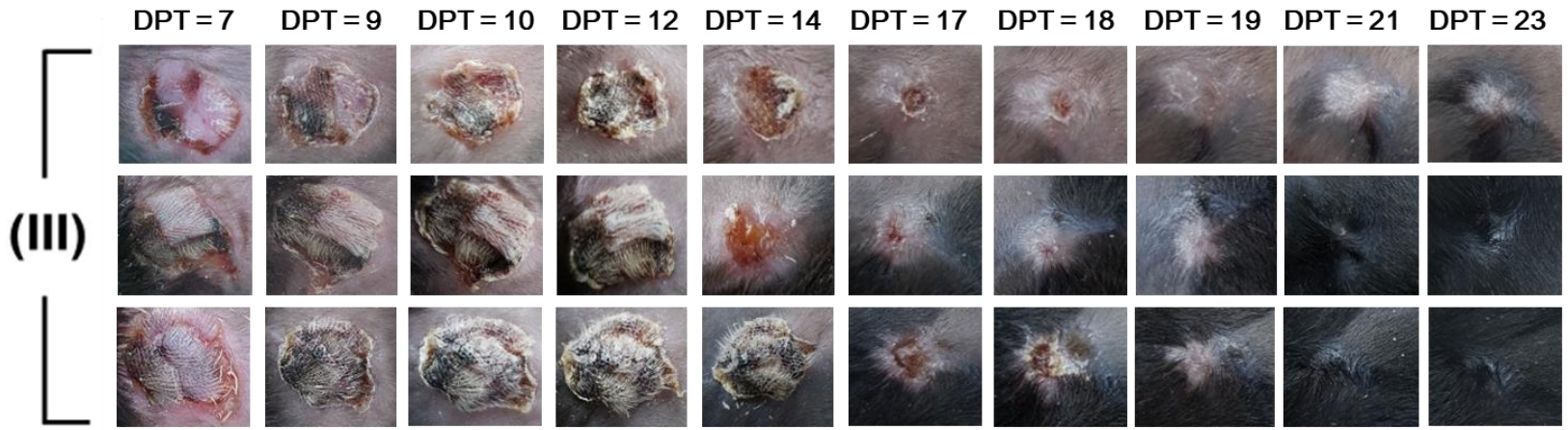
DPT = 7
DPT = 9
DPT = 10
DPT = 12
DPT = 14
DPT = 17
DPT = 18
DPT = 19
DPT = 21
DPT = 23
(III)

Figure 4. Second transplantation of skin grafts to confirm tolerance.

A. Schematic illustration of the experimental setup. Tail skin grafts were obtained from naïve B6 and BALB/c mice and transplanted into the left flank of (I) tolerant, (II) naïve, and (III) pre-sensitized B6 mice. Pre-sensitized B6 mice were prepared by intraperitoneally injecting irradiated BALB/c splenocytes ($7x10^5$ cells/mouse). B. Survival graph of BALB/c skin grafts was plotted from C. C. On day 7 post-transplantation, the bandages were carefully removed and skin grafts were observed daily. Representative photographs of skin grafts at days 7, 9, 10, 12, 14, 17, 18, 19, 21 and 23 after transplantation are shown.

2.3. Engrafted intrahepatic BALB/c islets was not affected by the rejection of same donor skin grafts

Interestingly, tolerant B6 mice still maintained normoglycemia (Fig 5A) throughout the observation period even after the rejection of BALB/c skin, implicating that the immune response of skin allograft rejection does not induce the rejection of engrafted intrahepatic allo-islets. All tolerant mice were normoglycemic until they were euthanized (Fig 5A). Subsequent immunostaining of the liver showed undamaged allo-islets, with infiltration of $CD3^{+}FoxP3^{+}$ T cells in the peri-graft sites (Fig 5B). Overall, BALB/c skin graft rejection did not affect the survival of intrahepatic BALB/c islets in tolerant B6 mice.

A

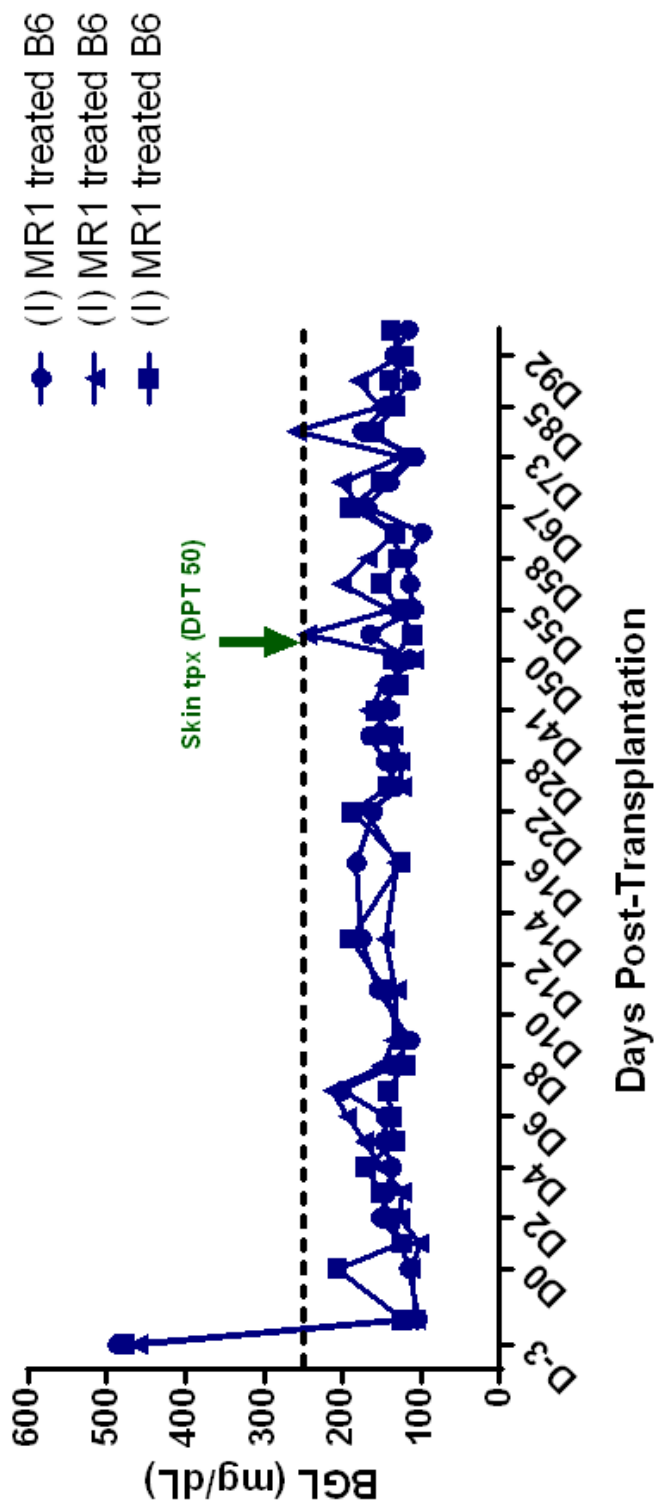
(I) MR1 treated B6
(I) MR1 treated B6
(I) MR1 treated B6
Skin tpx (DPT 50)
BGL (mg/dL)
600
500
400
300
200
100
0
D-3
D0
D2
D4
D6
D8
D10
D12
D14
D16
D22
D28
D41
D50
D55
D58
D67
D73
D85
D92
Days Post-Transplantation

B

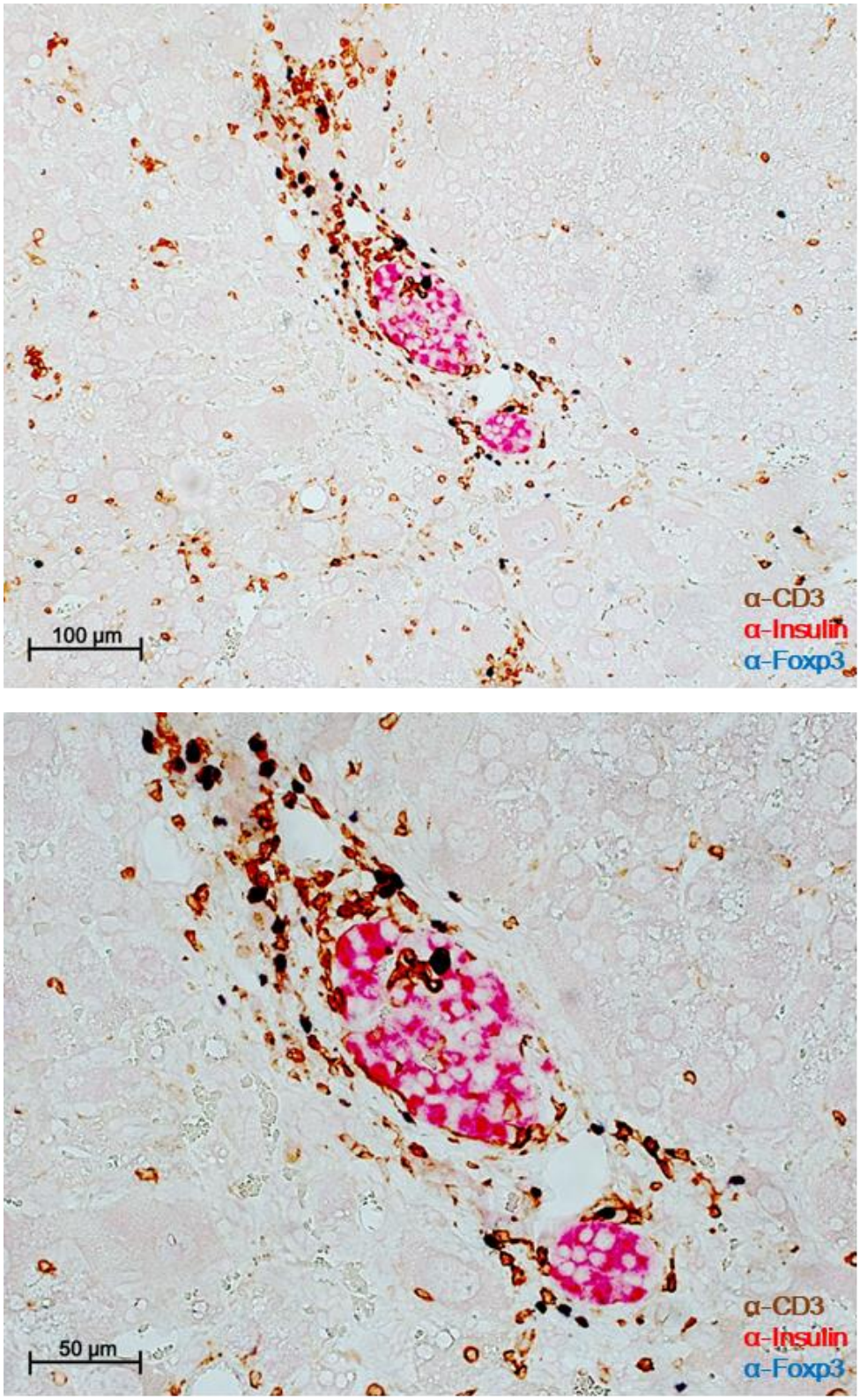

Figure 5. Protection of intrahepatic allogeneic islets after same donor skin graft rejection.

A. BGL was measured with a OneTouch Ultra device from day 0. The blood was obtained from snipped tail. B. IHC stain of liver tissues of tolerant B6 mice. Section slides were triple stained with anti-CD3 (brown), anti-insulin (red), and anti-FoxP3 (blue). Original magnification 100μm, and 50μm.

3. Mechanism of immune tolerance

3.1. Alloreactive $CD8^+$ T cells were neither anergized nor deleted in tolerant B6 mice

In order to examine the underlying mechanisms of immune tolerance exerted by MR1, I first performed an IFN-γ ELISpot assay using $CD8^+$ T cells isolated from tolerant B6 mice. Only $CD8^+$ T cells were isolated from the recipients, which were maintaining the normoglycemia for more than 100 days. $CD8^+$ T cells stimulated with irradiated BALB/c splenocytes secreted comparable amounts of IFN-γ compared to the control (Fig 6A), as they showed no significant difference in the number and activity of IFN-γ secreting $CD8^+$ T cells between tolerant and control mice (Fig 6B), indicating that alloantigen recognizing $CD8^+$ T cells were neither anergized nor deleted.

A

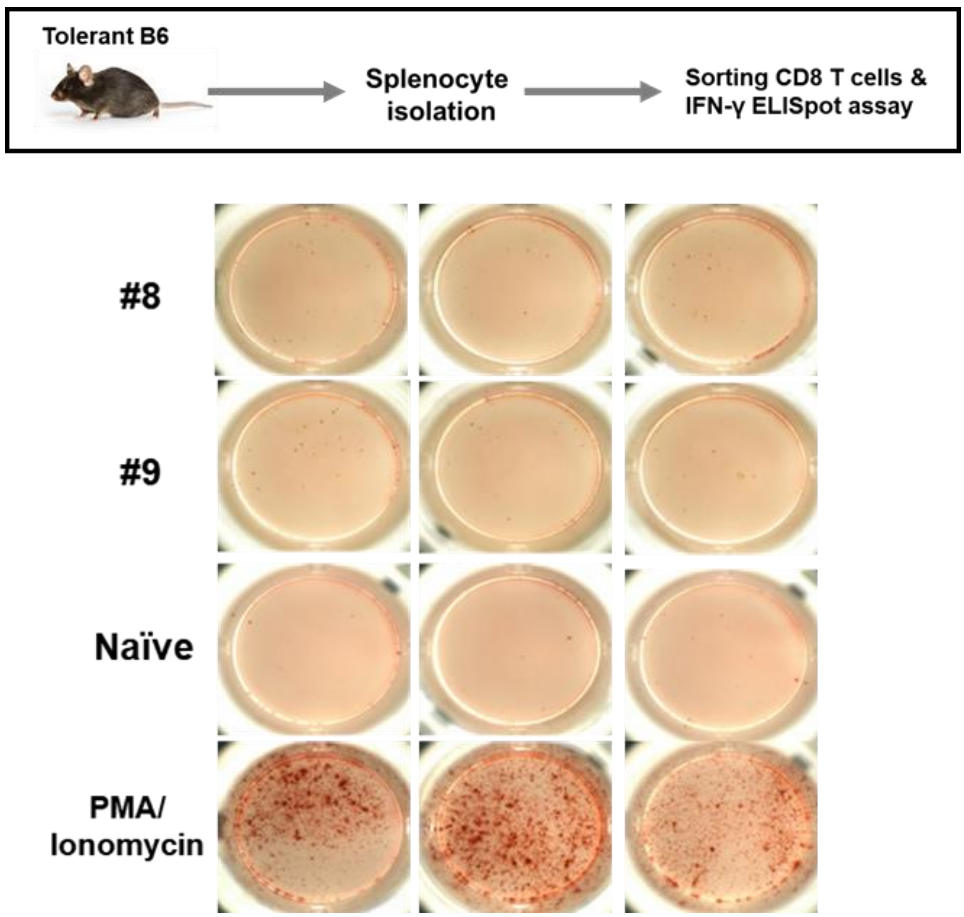
Tolerant B6
Splenocyte isolation
Sorting CD8 T cells & IFN-γ ELISpot assay
#8
#9
Naïve
PMA/ Ionomycin

B

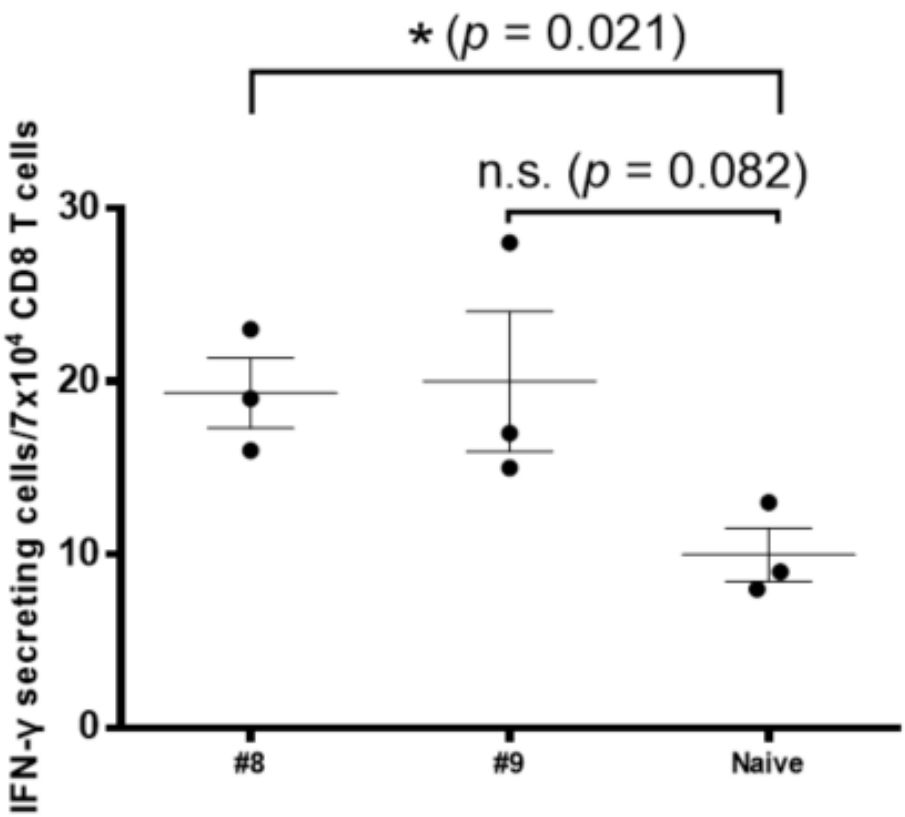
* (p = 0.021)
n.s. (p = 0.082)
IFN-γ secreting cells/7x10⁴ CD8 T cells
30
20
10
0
#8
#9
Naive

Figure 6. Alloreactive $CD8^+$ T cells were neither anergized nor deleted.

A. Analysis of IFN-γ secreting $CD8^+$ T cells in tolerant mice using an ELISpot assay. $CD8^+$ T cells stimulated with PMA (50ng/ml) and Ionomycin (1μg/ml) were used as a positive control. The number and activity of IFN-γ secreting $CD8^+$ T cells among whole cells in the ELISpot wells were automatically analyzed using an ELISpot Reader system. B. The number of IFN-γ secreting $CD8^+$ T cells was calculated from A. Statistical significance was determined by unpaired Student's t test.

3.2. $CD4^+FoxP3^+$ Treg cells in tolerant B6 mice play a key role in protecting islet allografts from rejection

In order to evaluate the role of Treg cells, I exploited B6 DEREG mice in which $FoxP3^+$ Treg cells can be selectively depleted in vivo upon administration of DT. Diabetic B6 DEREG mice were transplanted with BALB/c islets via a cecal vein route under short-term MR1 monotherapy (Fig 7A). When normoglycemia was achieved, DT was intraperitoneally injected at DPT 28, 29, 31, and 32 (Fig 7A). The complete ablation of $CD4^+CD25^+FoxP3^+$ Treg cells was confirmed in peripheral blood by FACS analysis (Fig 7B). Within 2 weeks of DT administration, hyperglycemia (≥600mg/dL) recurred, indicating that the islet allograft was being rejected in the liver (Fig 7C). Immunostaining analysis of the whole liver of these mice showed the total absence of islets, with heavy infiltration of $CD3^+$ T cells near the sinusoids, confirming the complete rejection of engrafted intrahepatic allo-islets (Fig 7D). Collectively, these data suggest that $FoxP3^+$ Treg cells play a critical role in protecting the allo-islets from rejection.

A

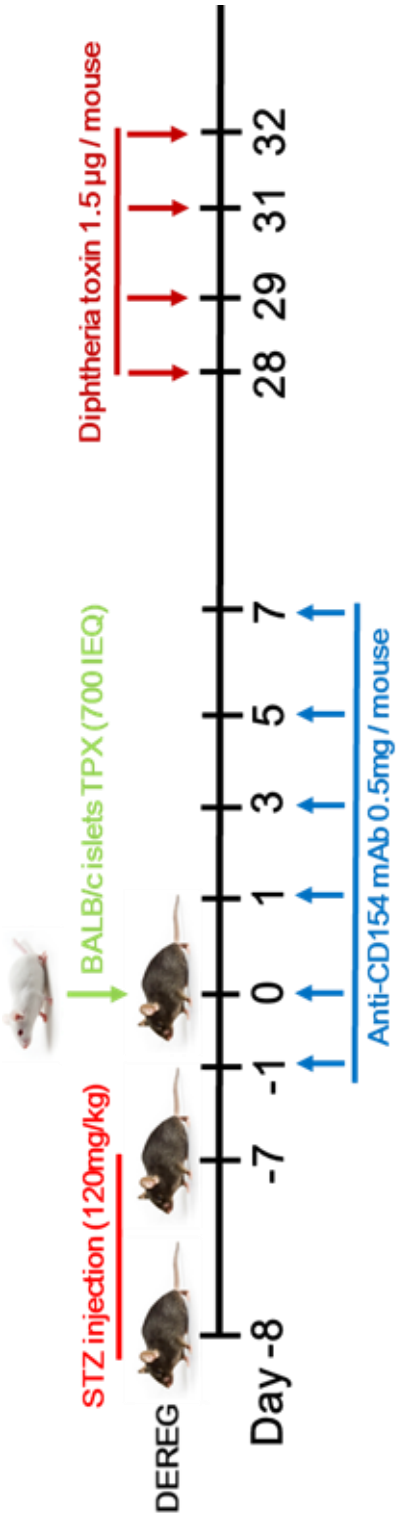
Diphtheria toxin 1.5 µg / mouse
BALB/c islets TPX (700 IEQ)
STZ injection (120mg/kg)
DEREG
Anti-CD154 mAb 0.5mg / mouse
Day -8
-7
-1
0
1
3
5
7
28
29
31
32

B

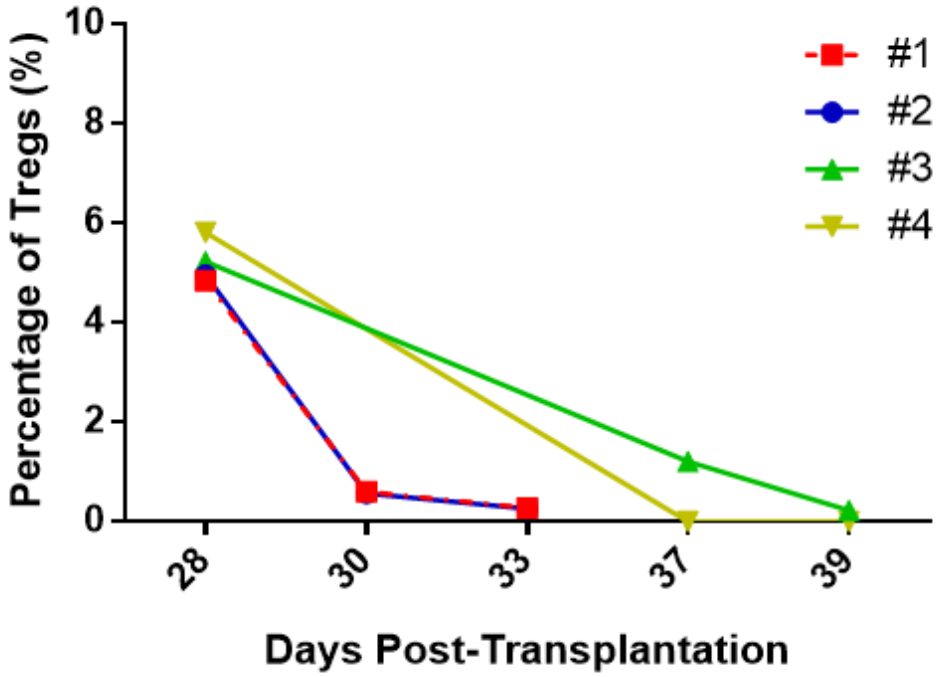
Percentage of Tregs (%)
10
8
6
4
2
0
28
30
33
37
39
Days Post-Transplantation
#1
#2
#3
#4

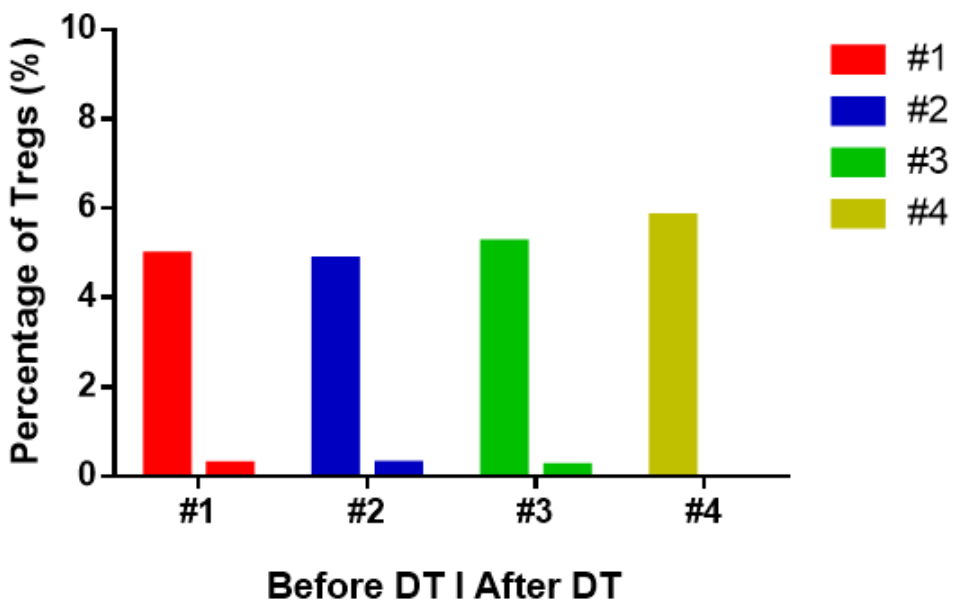
Percentage of Tregs (%)
10
8
6
4
2
0
#1
#2
#3
#4
Before DT I After DT
#1
#2
#3
#4

C

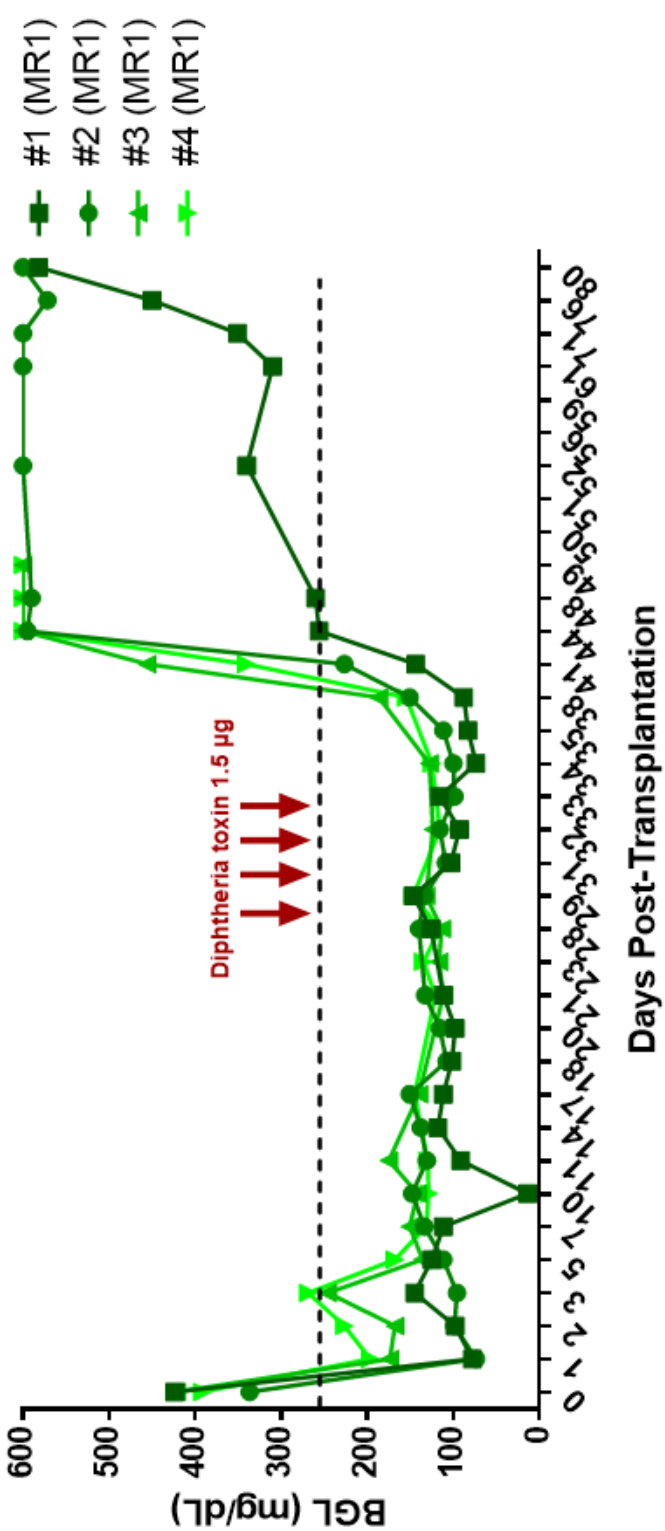
#1 (MR1)
#2 (MR1)
#3 (MR1)
#4 (MR1)
Diphtheria toxin 1.5 µg
BGL (mg/dL)
600
500
400
300
200
100
0
Days Post-Transplantation

D

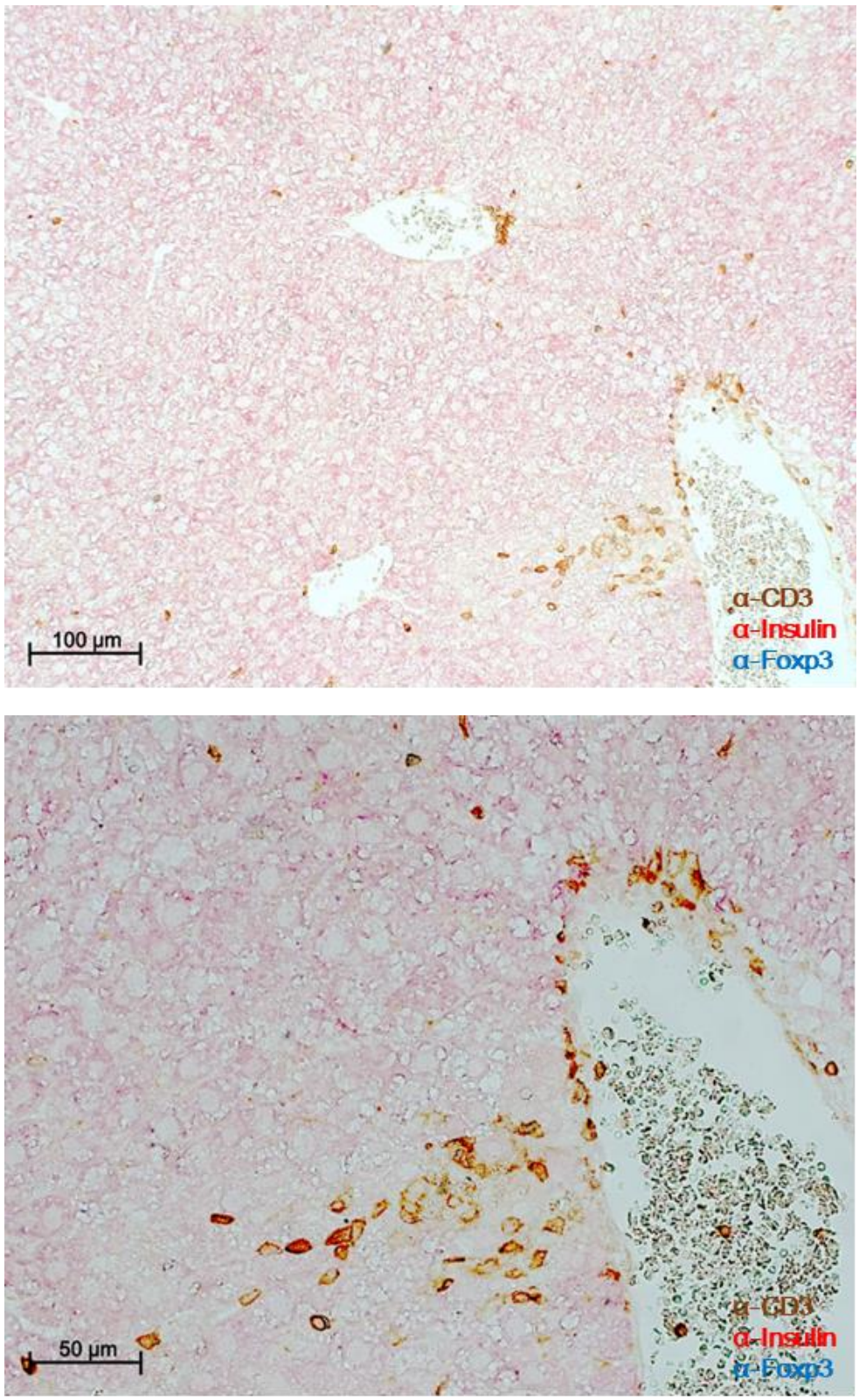

Figure 7. Analyzing the role of Treg cells in tolerant B6 mice.

A. Schematic illustration of the experimental setup. Diphtheria toxin was given on days 28, 29, 31, and 32 post-transplantation at 1.5 μg per dosage. B. Percentage of Treg cells in peripheral blood before and after diphtheria toxin treatment. C. BGL was measured with a OneTouch Ultra device from day 0. The blood was obtained from snipped tail. D. IHC stain of liver tissues of hyperglycemic B6 mice. Section slides were triple stained with anti-CD3 (brown), anti-insulin (red), and anti-FoxP3 (blue). Original magnification 100μm.

3.3. Ratio of FoxP3$^+$ T cell to CD3$^+$ T cell was not increased in tolerant B6 mice

Since anti-CD154 blockade based regimens could augment the ratio of FoxP3$^+$ Treg cells to effector T cells in transplantation models[92,93], I then assessed the ratio of FoxP3$^+$ Treg cells from the tissues to those from the recipients which rejected the allo-islets. The ratio of FoxP3$^+$ Treg cells to CD3$^+$ T cells has been obtained from three different islet engrafted areas (Fig 8A). However, I could not observe any significant difference between those two groups (Fig 8B). I also analyzed the ratio of FoxP3$^+$ Treg cells to CD4$^+$ T cells in peripheral blood obtained from tolerant and naïve mice. However, the ratio of FoxP3$^+$ Treg cells in peripheral blood was not significantly different between those two groups (Fig 8C). Taken together, anti-CD154 blockade alone failed to increase the ratio of FoxP3$^+$ Treg cells in my allogeneic islet transplantation model.

A

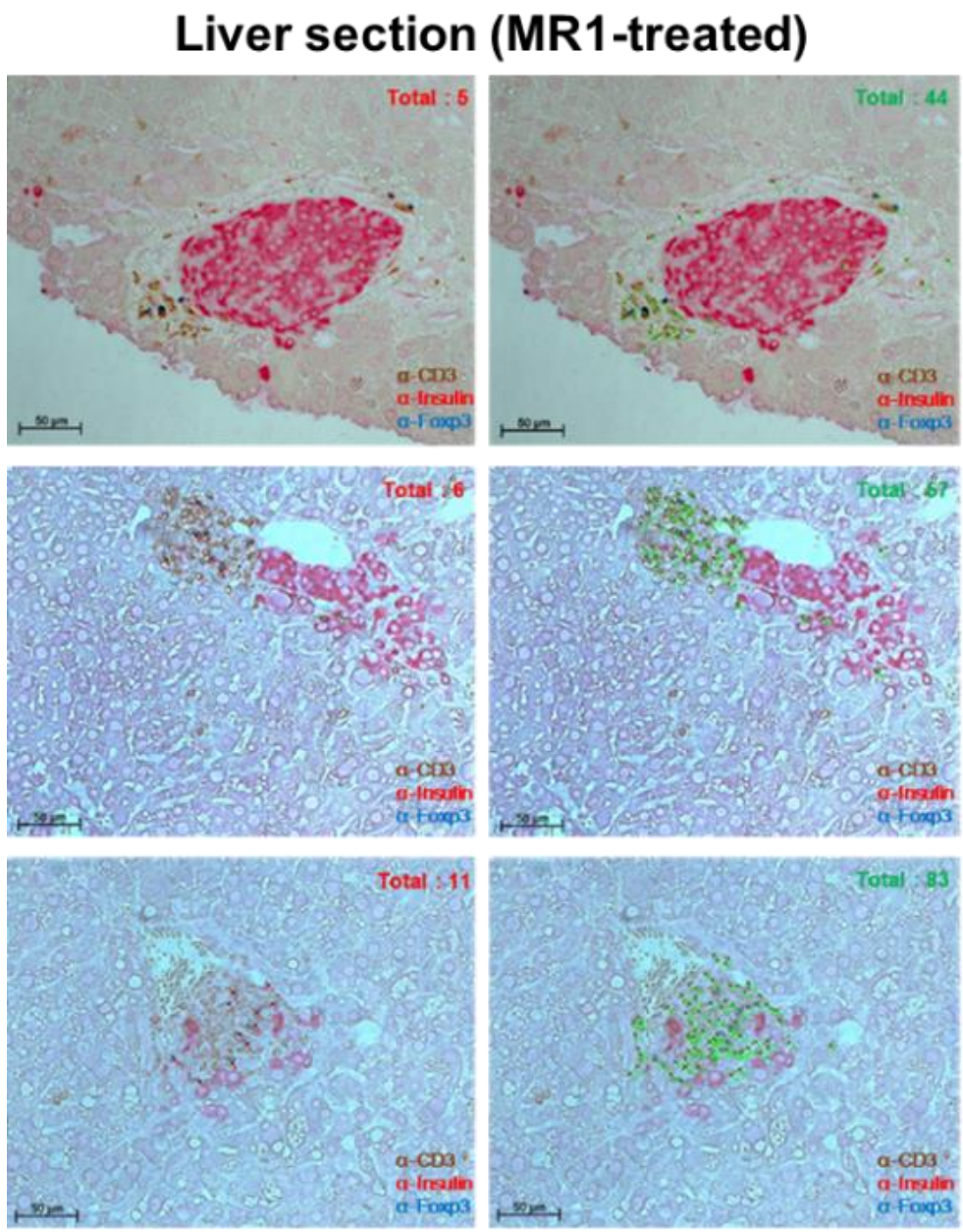
Liver section (MR1-treated)
Total : 5
α-CD3
α-Insulin
α-Foxp3
Total : 44
α-CD3
α-Insulin
α-Foxp3
Total : 6
α-CD3
α-Insulin
α-Foxp3
Total : 67
α-CD3
α-Insulin
α-Foxp3
Total : 11
α-CD3
α-Insulin
α-Foxp3
Total : 83
α-CD3
α-Insulin
α-Foxp3

Liver section (Rejected)

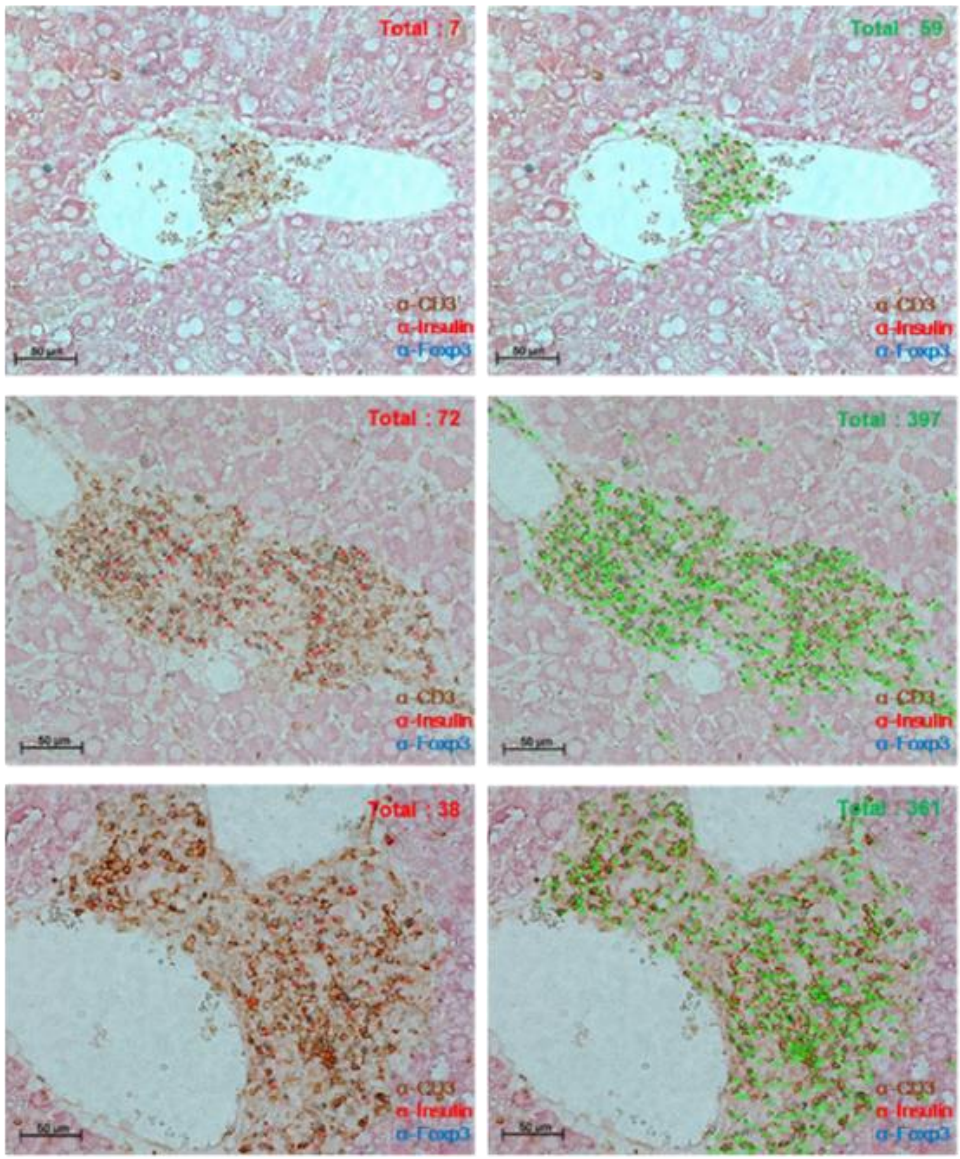

B

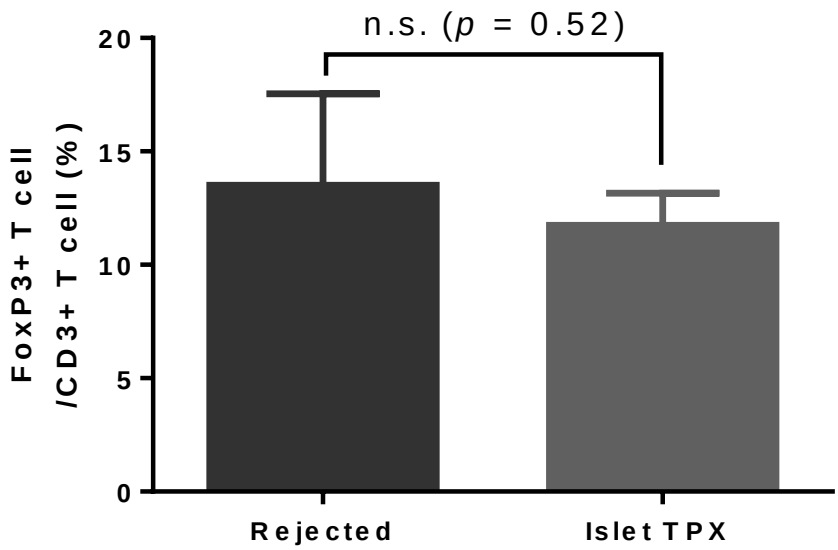
n.s. (p = 0.52)
FoxP3+ T cell /CD3+ T cell (%)
20
15
10
5
0
Rejected
Islet TPX

C

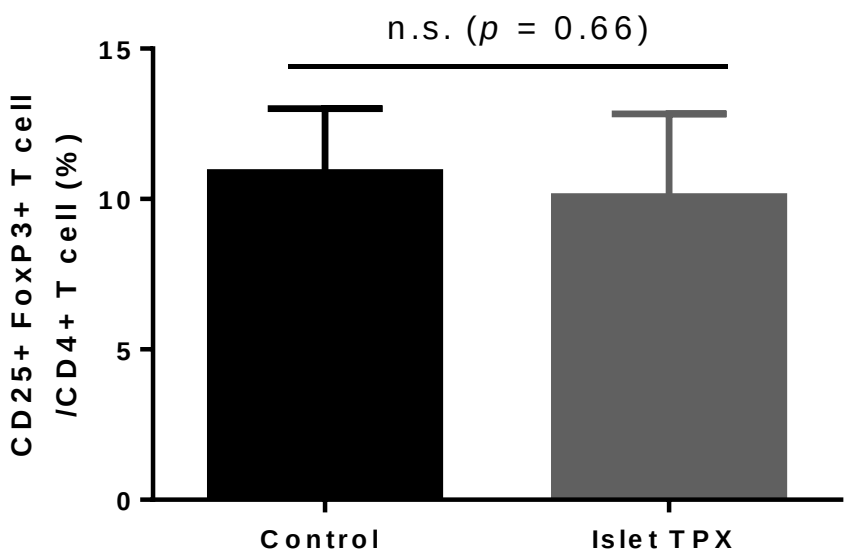
n.s. (p = 0.66)
CD25+ FoxP3+ T cell /CD4+ T cell (%)
15
10
5
0
Control
Islet TPX

Figure 8. Analysis of the ratio of FoxP3$^+$ Treg cells to CD3$^+$ T cells in tolerant & rejected B6 mice.

A. IHC stain of liver tissues of tolerant and rejected B6 mice. Section slides were triple stained with anti-CD3 (brown), anti-insulin (red), and anti-FoxP3 (blue). Original magnification 50μm. The ratio of FoxP3$^+$ Treg cells (red dot) to CD3$^+$ T cells (green dot) in the liver was analyzed using Cell Counter Image J software. The ratio was obtained from three different areas, and each group expressed as mean ± SD. B. The ratio of FoxP3$^+$ Treg cells to CD3$^+$ T cells near the graft sites was analyzed using Cell Counter Image J software. The ratio was obtained from three different areas, and each group expressed as mean ± SD.

3.4. Donor-specific FoxP3^{+} Treg cells were enriched in tolerant B6 mice

Thus, by conducting mixed lymphocyte reactions (MLR) analysis, I investigated whether Treg cells in tolerant mice would be qualitatively different compared with those from the naïve mice, with stronger suppressive capacity against alloantigens. The diabetic FoxP3-eGFP mice were infused with BALB/c islets via a cecal vein route with short-term MR1 monotherapy. When normoglycemia was achieved, FoxP3^{+} Treg cells and FoxP3^{-} Teff cells were separately obtained from the splenocytes of tolerant and naïve B6 mice (Fig 9A). CFSE-labeled FoxP3^{-} Teff cells from a naïve B6 mouse was adopted as a universal responder, and irradiated BALB/c or C3H APCs were co-cultured to stimulate the proliferation of responder cells (Fig 9A-B). FoxP3^{+} Treg cells isolated from tolerant and naïve B6 mice were added at ratios of 2:1, 8:1, and 32:1 respectively to the co-culture of stimulator and responder cells (Fig 9B). After 5 days incubation, cells were harvested and analyzed to examine the proliferation of viable B6 Teff cells. I found that almost one-half of the naïve Teff cells proliferated when co-cultured with irradiated BALB/c or C3H splenocytes (Fig 9C-F). Surprisingly, in the co-culture of Teff cells with BALB/c splenocytes, Treg cells from tolerant mice exhibited better suppressive capacity over Teff cell proliferation compared to the Treg cells obtained from the naïve mice (Fig 9C-D). However, in the co-culture with C3H splenocytes, Treg cells from both tolerant and naïve mice showed comparable suppressive capacity over Teff cell proliferation (Fig 9E-F). Taken together, MR1 monotherapy induced donor-specific Treg cells to protect allogeneic islet grafts in the liver.

A

Responder
Intrahepatically islet transplanted FoxP3-eGFP B6 (MR1-treated)
(200 DPT)
Splenocyte isolation
MACS
Thy1.2+ T cells isolation
FACS sorting
(I) Thy1.2+ GFP+ Treg cells
(II) Thy1.2+ GFP- Teff cells
Naïve FoxP3-eGFP B6
Splenocyte isolation
MACS
Thy1.2+ T cells isolation
FACS sorting
(III) Thy1.2+ GFP+ Treg cells
(IV)Thy1.2+ GFP- Teff cells
CFSE labelled (1μM)
Stimulator
BALB/c
or
C3H
Splenocyte isolation
γ-irradiation (25Gy)
(V) Irradiated splenocytes

B

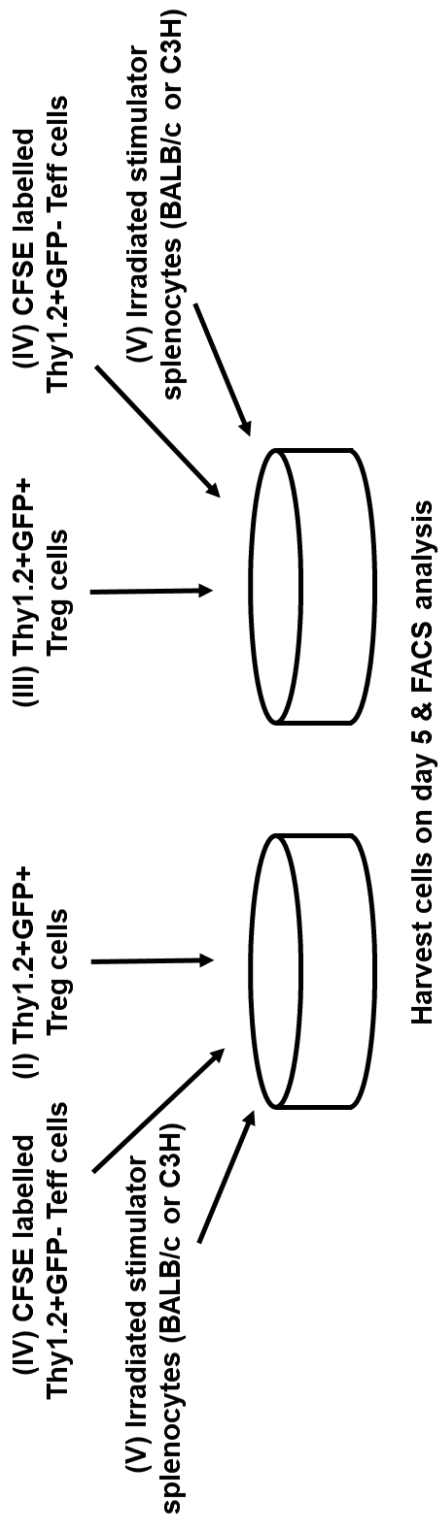
(IV) CFSE labelled
Thy1.2+GFP- Teff cells
(V) Irradiated stimulator
splenocytes (BALB/c or C3H)
(I) Thy1.2+GFP+
Treg cells
(III) Thy1.2+GFP+
Treg cells
(IV) CFSE labelled
Thy1.2+GFP- Teff cells
(V) Irradiated stimulator
splenocytes (BALB/c or C3H)
Harvest cells on day 5 & FACS analysis

C

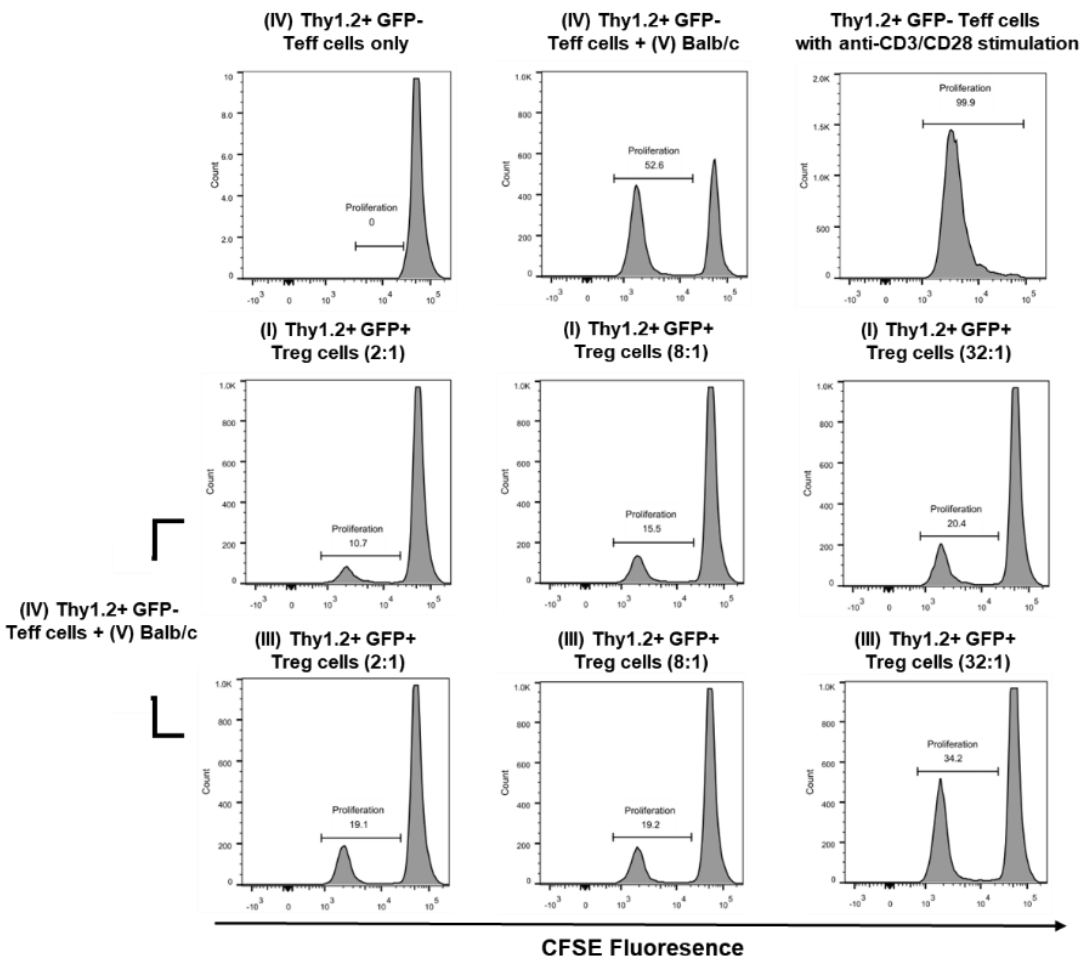
(IV) Thy1.2+ GFP- Teff cells only
(IV) Thy1.2+ GFP- Teff cells + (V) Balb/c
Thy1.2+ GFP- Teff cells with anti-CD3/CD28 stimulation
Proliferation 0
Proliferation 52.6
Proliferation 99.9
(I) Thy1.2+ GFP+ Treg cells (2:1)
(I) Thy1.2+ GFP+ Treg cells (8:1)
(I) Thy1.2+ GFP+ Treg cells (32:1)
Proliferation 10.7
Proliferation 15.5
Proliferation 20.4
(IV) Thy1.2+ GFP- Teff cells + (V) Balb/c
(III) Thy1.2+ GFP+ Treg cells (2:1)
(III) Thy1.2+ GFP+ Treg cells (8:1)
(III) Thy1.2+ GFP+ Treg cells (32:1)
Proliferation 19.1
Proliferation 19.2
Proliferation 34.2
Count
CFSE Fluoresence

D

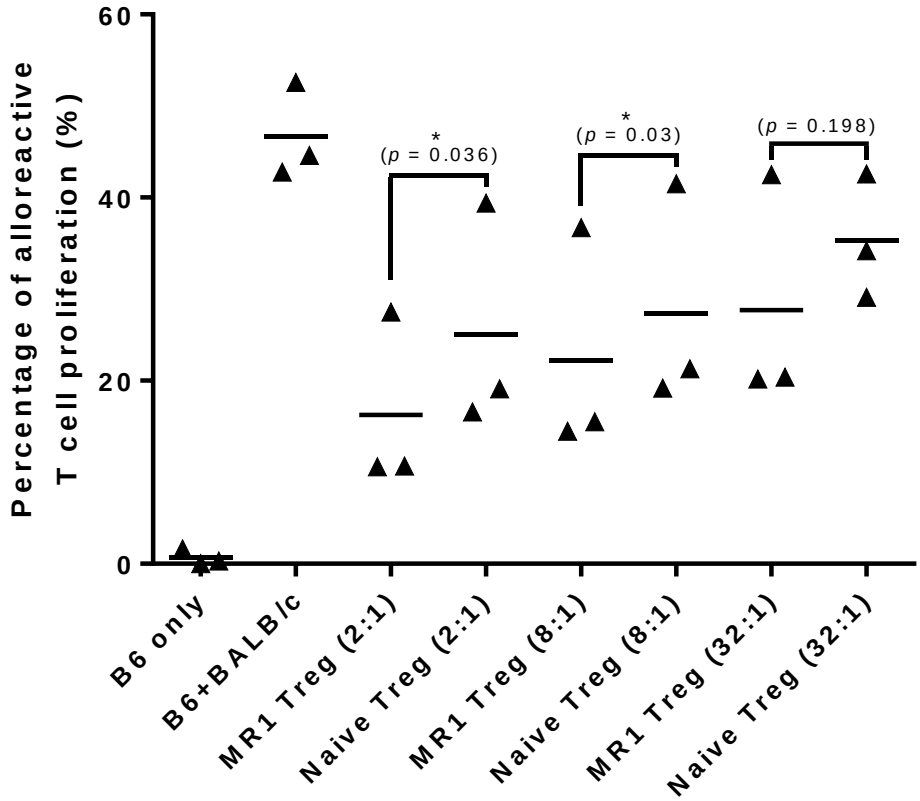
Percentage of alloreactive T cell proliferation (%)
60
40
20
0
*
(p = 0.036)
*
(p = 0.03)
(p = 0.198)
B6 only
B6+BALB/c
MR1 Treg (2:1)
Naive Treg (2:1)
MR1 Treg (8:1)
Naive Treg (8:1)
MR1 Treg (32:1)
Naive Treg (32:1)

E

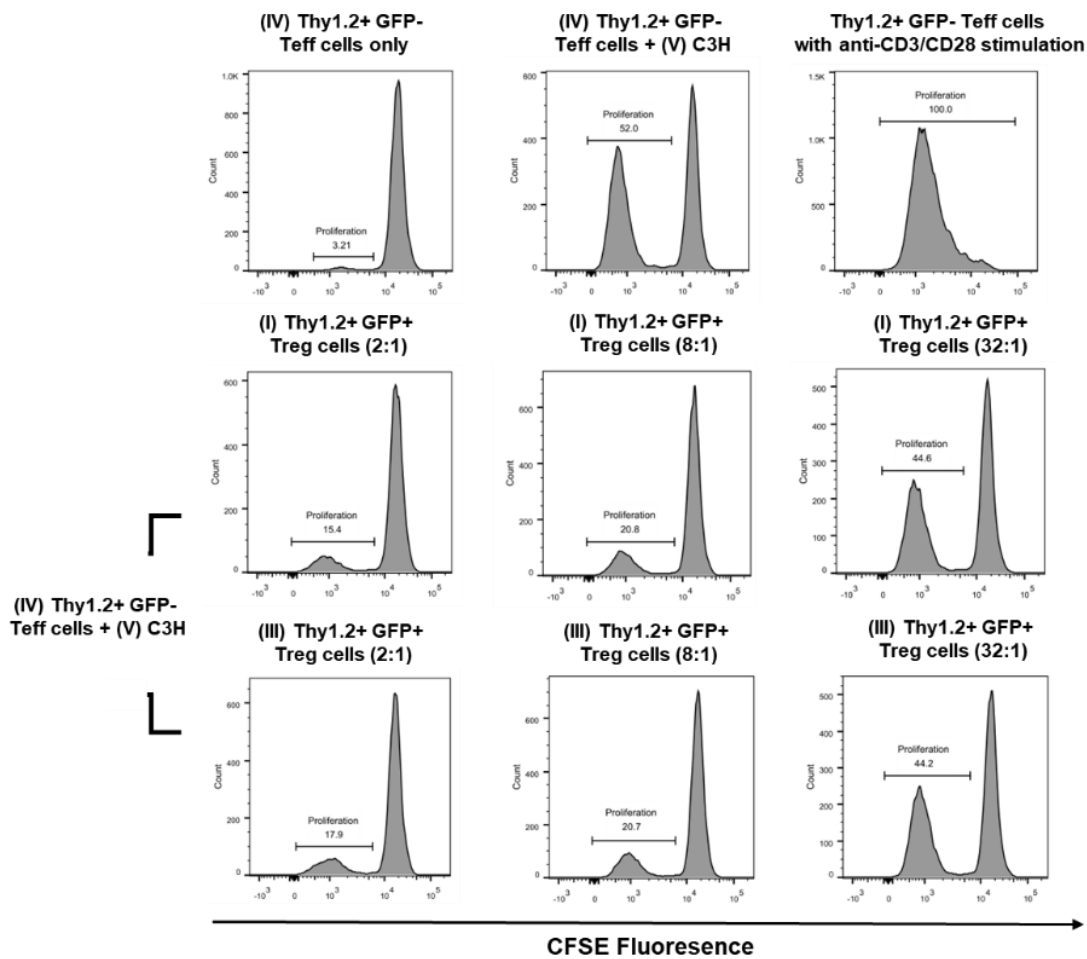
(IV) Thy1.2+ GFP-
Teff cells only
(IV) Thy1.2+ GFP-
Teff cells + (V) C3H
Thy1.2+ GFP- Teff cells
with anti-CD3/CD28 stimulation
Proliferation
3.21
Proliferation
52.0
Proliferation
100.0
(I) Thy1.2+ GFP+
Treg cells (2:1)
(I) Thy1.2+ GFP+
Treg cells (8:1)
(I) Thy1.2+ GFP+
Treg cells (32:1)
Proliferation
15.4
Proliferation
20.8
Proliferation
44.6
(IV) Thy1.2+ GFP-
Teff cells + (V) C3H
(III) Thy1.2+ GFP+
Treg cells (2:1)
(III) Thy1.2+ GFP+
Treg cells (8:1)
(III) Thy1.2+ GFP+
Treg cells (32:1)
Proliferation
17.9
Proliferation
20.7
Proliferation
44.2
Count
CFSE Fluoresence

F

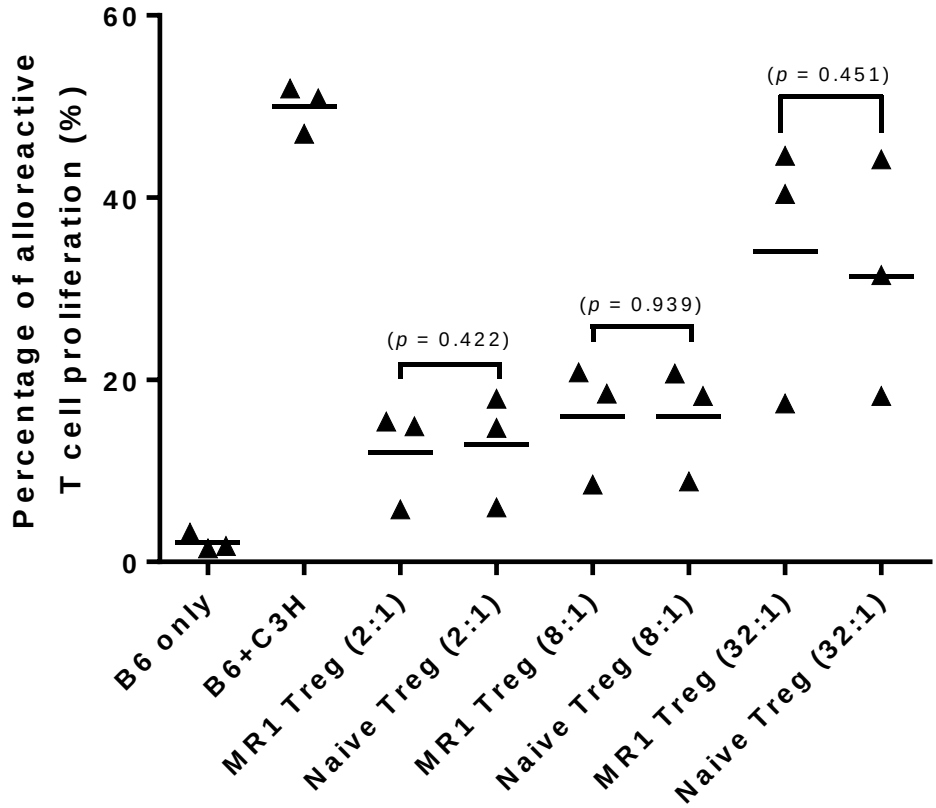
Percentage of alloreactive T cell proliferation (%)
60
40
20
0
(p = 0.422)
(p = 0.939)
(p = 0.451)
B6 only
B6+C3H
MR1 Treg (2:1)
Naive Treg (2:1)
MR1 Treg (8:1)
Naive Treg (8:1)
MR1 Treg (32:1)
Naive Treg (32:1)

Figure 9. Analysis of the suppressive capacity of FoxP3$^+$ Treg cells isolated from tolerant & naïve B6 mice.

A. Schematic illustration of MLR. Stimulator and responder cells were prepared as described Materials and Methods. B. Schematic illustration of cell co-culture. In a co-culture of CFSE-labeled naïve effector T cells with irradiated BALB/c or C3H splenocytes, Treg cells isolated from tolerant and naïve mice were added at a ratio of 2:1, 8:1, and 32:1, respectively. Cells were incubated in a 96-well round-bottom plate for 5 days. C & D. The suppressive ability of Treg cells against the proliferation of naïve effector T cells in the co-culture with irradiated BALB/c splenocytes was evaluated through FACS analysis. E & F. The suppressive ability of Treg cells against the proliferation of naïve effector T cells in the co-culture with irradiated C3H splenocytes was evaluated through FACS analysis. Naïve effector T cells stimulated with anti-CD3 and CD28 Abs were used as a positive control. The proliferation of each group was expressed as mean ± SD (n=3). Statistical significance was determined by paired Student's t-test. Asterisk (*) indicates statistical significance (p<0.05).

IV. Discussion

Immunostaining of whole liver sections showed successful engraftment of the allo-islets near the liver sinusoids. Although revascularization and remodeling of islet aggregates beneath the renal capsule have been well characterized,[104] islet grafts randomly located throughout the whole liver parenchyma are not easily accessed, making it relatively difficult to understand their structural changes during engraftment. Korsgren and colleagues proposed a model of intrahepatic islet revascularization where, unlike in the demarcation of the islet-thrombus mass in NHPs or humans, rodent islets generate large necrotic areas; this is probably because of acute ischemia that is induced by the sudden restriction of a portal branch and reflects the relatively large size of rodent islets compared to the diameter of the portal vein in these animals.[105] It follows that liver regeneration results in a cascade of growth factors that stimulate hepatocyte proliferation and re-modulation of the liver parenchyma,[106] allowing the incorporation of islets into the newly formed hepatic structure on re-vascularization.[107] Although this scenario may not be consistent with the engraftment in my model, it is worth taking into consideration since the process of incorporation and re-vascularization is inevitable for the long-term survival of islet grafts in the liver.

I confirmed that short-term MR1 monotherapy could achieve normoglycemia for more than 250 days in intrahepatic islet transplanted diabetic mice. The long-term survival of allogeneic islets by the short-term MR1 treatment implicates the modulation of immune responsiveness to the MHC-mismatched donor antigens in recipients. To evaluate whether immune tolerance was achieved in the mice, the second graft, along with third-party graft (islets from C3H mice), were transplanted

underneath the kidney capsule. Re-challenging allo-islets into the liver was not possible since re-administration of STZ could affect the established immune system of the recipients with its cytotoxicity[108]. Hepatic lobectomy was not available either because it is not a life-sustaining surgical method. By conducting nephrectomy, islet-bearing kidneys showed total acceptance of second-party islets but not of third-party islets. Successful acceptance of second allo-islets into the non-liver solid organ emphasized the apparent ability of MR1 to induce immune tolerance, regardless of the microenvironment of anatomic sites for the islet transplantation. Since I found the infiltration of Treg cells in the peri-graft sites (Fig 3C), it is conceivable that graft-protective Treg cells induced by MR1 treatment might have migrated into the kidney capsule, creating the immunologically privileged site where Treg cells may prevent immune-mediated graft damage, considering that Treg cells are key regulators of dominant tolerance for graft protection[109-111]. The mechanisms underpinning the inhibitory functions of Treg cells and their migration to peri-graft sites would be of interest for further investigation.

Next, I verified whether transplantation tolerance could be extended to organs other than islets by exploiting allogeneic skin transplantation. Among transplantation models, skin transplantation has been noted to be extremely challenging for achieving tolerance induction[112]. As expected, BALB/c skin transplanted to the tolerant B6 was all rejected, but graft survival was modestly prolonged compared to the same grafts in the control group. Most interestingly, tolerant B6 mice still maintained normoglycemia during and after the rejection phase of skin allografts. Similar results were reported in a recent study that in diabetic B6 mice treated with anti-LFA-1 and anti-CD154 mAb, intact neonatal porcine islets (NPI) were maintained beneath the kidney capsule with normoglycemic control, even after the

rejection of re-transplanted porcine skin xenografts[73]. These mice became diabetic when the NPI xenograft-bearing kidney was removed, and abundant FoxP3$^+$ Treg cells were observed near the peri-graft sites[73]. I also confirmed the existence of Treg cells near the peri-graft sites in the liver after the rejection of skin allografts, and the islets could be protected from potentially fatal immune responses during skin rejection by the Treg cells, as shown by Arefanian et al.[73]. The rejection of same-donor skin grafts in tolerant mice could be explained by two reasons. First, since the primary target of allogeneic immune responses is the MHC molecule[113], allogeneic MHC-specific tolerance mediated by Treg cells could, in some way, delay the rejection of skin allografts in tolerant mice. However, strong T cell-mediated immune responses mounted by abundant epidermal and dermal DCs[114-116] may exceed a threshold of Treg-mediated immuno-regulation, leading to the eventual failure of allogeneic skin grafts in all mice. Second, it is possible to consider the split tolerance[117-120], which corresponds to my observation that re-transplanted donor islets were accepted by a recipient while skin grafts from the same donor were rejected. Although the mechanism of split tolerance in accordance with anti-CD154 blockade has barely been studied, strong immunity against skin-specific antigens[121-123] could have been formed to break allogeneic MHC-specific tolerance, resulting in skin graft rejection.

Using the intrahepatic islet allo-transplantation DEREG mouse model, I showed that immune tolerance could be mediated by Treg cells. Whole liver sections showed complete destruction of the entire islets with the depletion of Treg cells. A limitation of this experiment was that upon DT treatment, all FoxP3$^+$ Treg cells were eradicated without selectively depleting the Treg cells responsible for graft protection. An in-depth study characterizing the distinctive markers of graft-

protective Treg cells should be conducted to target them selectively, which would lead to more precise interpretation of the role of the Treg cells among the FoxP3$^+$ heterogeneous population. Although CD154 blockade was reported as generating inducible Treg (iTreg) cells in OT-I & OT-II transgenic mouse transplanted with ovalbumin expressing skin grafts[89], it still remains controversial to define the lineage of Treg cells in the polyclonal T cell population in my model due to the lack of universal markers to distinguish natural Treg (nTreg) cells from iTreg cells[124].

Since the ratio of Treg to CD3$^+$ T cells in the peri-graft sites was not significantly different from that in the rejected control, further experiments were conducted to investigate whether these Treg cells contained qualitatively different characteristics. Indeed, the Treg cells in tolerant mice showed higher suppressive capacity on effector T cell proliferation after stimulation with the same allogeneic donor of BALB/c splenocytes, than with the third-party donor of C3H splenocytes. It is evident that MR1 enriched a lineage of donor-specific Treg cells in my model, but the underlying molecular mechanisms for the generation of the Treg cells have not yet been identified[89]. Previous work has implicated the tolerogenic plasmacytoid DCs in lymph nodes in generating donor-specific peripheral FoxP3$^+$ Treg cells in an allo-cardiac transplantation mouse model treated with anti-CD154 mAb and DST[52]. Moreover, immunogenic DCs, which are triggered by CD40 signaling, have been shown to convert into tolerogenic DCs when JAK3, a downstream molecule of CD40, is inhibited[125,126]. I assume that the production of co-stimulatory molecules and inflammatory cytokines for immunogenic DC activation may be hampered by inhibited CD40 signaling[127,128], thus driving them into tolerogenic DCs. Therefore, further analysis would be necessary if the treatment of anti-CD154 mAb can direct the tolerogenic programming of DCs in the co-culture with naïve T cells, thus leading

to the generation of Treg cells. The Notch ligand Jagged-1, which is expressed on the surface of DCs, has been shown to contribute to the induction and expansion of alloantigen-specific Treg cells[129-131]. Although the common signaling network between Jagged-1 and CD40 is yet fully understood, overexpression of Jagged-1 and blockade of CD40 signaling seems to be effective in prolonging allograft survival in transplantation models[132]. Therefore, JAK3 and Jagged-1 might be the key factors for further investigation of the specific molecular mechanism involved in the generation of donor-specific Treg cells by anti-CD154 mAb treatment.

The key points in my single-drug therapy enabling long-term control of blood glucose levels would be partially explained by the difference in MR1 dosage, which was higher and more frequently given than those in previous studies. Ferrer and colleagues revealed that MR1 monotherapy could decrease the frequency of $CD44^{high}$ $CD8^{+}$ T cells but elevate the frequency of KLRG-1^{high} $CD8^{+}$ T cells, leading to a delay in the expansion of antigen-specific $CD8^{+}$ T cells[89,133]. The differentiation into antigen-specific $CD8^{+}$ T cells was also delayed by depleted cytokine production at early stage[89]. Previous studies have also shown that the potent immunoregulatory function of anti-CD154 mAb is not simply restricted to blockade of the signal pathway of CD154-CD40; elimination of CD154 expressing immune cells by recruiting complement-mediated mechanisms is also important in avoiding islet allograft rejection[64]. Although the exact role of anti-CD154 mAb on CD154 expressing effector T cells was not the main focus of my study, antibody-based therapy for CD154-CD40 blockade could provide a beneficial effect in regulating immune responses with their additional unknown effects. Therefore, considering the effect of anti-CD154 mAb, increased dosage of MR1 administration could be effective by taking advantage of sparing time to develop donor-specific Treg cells in

weakened alloimmune responses at the early time point after transplantation.

A fundamental limitation of my study is that the clinical translation of immune tolerance by the use of CD154 blockade is currently unavailable due to the thromboembolism complications reported in previous clinical studies[55,56]. Although targeting the CD40 molecule expressed on APCs instead of CD154 has been attempted as an alternative avenue to obtain the comparable effect of anti-CD154 mAb without provoking thromboembolism[134], no CD40-targeting strategies have as yet proven to be satisfactory in organ transplantation. The pre-clinical use of anti-CD40 mAb is partially encouraging as it was effective in prolonging the survival of porcine organs, including the heart and kidney, in NHPs[135,136]. However, anti-CD40 mAb was not equally competent in preventing the early loss of porcine islets, as shown by our results, leading to a failure of long-term normoglycemic control in diabetic NHPs[137]. In vivo molecular silencing of CD40 by the use of small interfering RNA (siRNA) was reported to prolong the survival of renal allografts in rats to some extent[138]; however, several barriers, including the delivery of siRNA and the potential immunogenicity of RNA itself, need to be overcome to ensure efficacy and safety in translation to the clinic[139].

As anti-CD154 mAb was demonstrated to induce donor-specific FoxP3^{+} Treg cell-mediated immune tolerance in my animal model, there would be merit in investigating the role of anti-CD40 mAb in inducing immune tolerance in the same animal transplantation model. Interestingly, antagonistic anti-mouse CD40 mAb (201A3) has been developed at an opportune moment[140]; comparing the mechanism of transplantation tolerance by the use of either anti-CD154 mAb or anti-CD40 mAb in my rodent model advances the knowledge of anti-CD154 mAb mediated immune tolerance. I hope that cumulative research aiming to address the issues underlying

my animal model will lead to the achievement of CD154 blockade-mediated immune tolerance in humans; this will surely contribute to opening a new chapter in the field of clinical organ transplantation.

V. Conclusion

In conclusion, I demonstrated for the first time that short-term MR1 monotherapy could achieve transplantation tolerance, which is critical to protecting allo-islets in recipients. In addition, I found that transplantation tolerance is mediated by donor-specific FoxP3^{+} Treg cells. I expect that my model could provide concrete evidence for anti-CD154 mAb mediated immune tolerance, securing a beachhead to unveil the molecular mechanism of anti-CD154 mAb mediated Treg cell induction in the allo-islet transplantation.

VI. Schematic summary

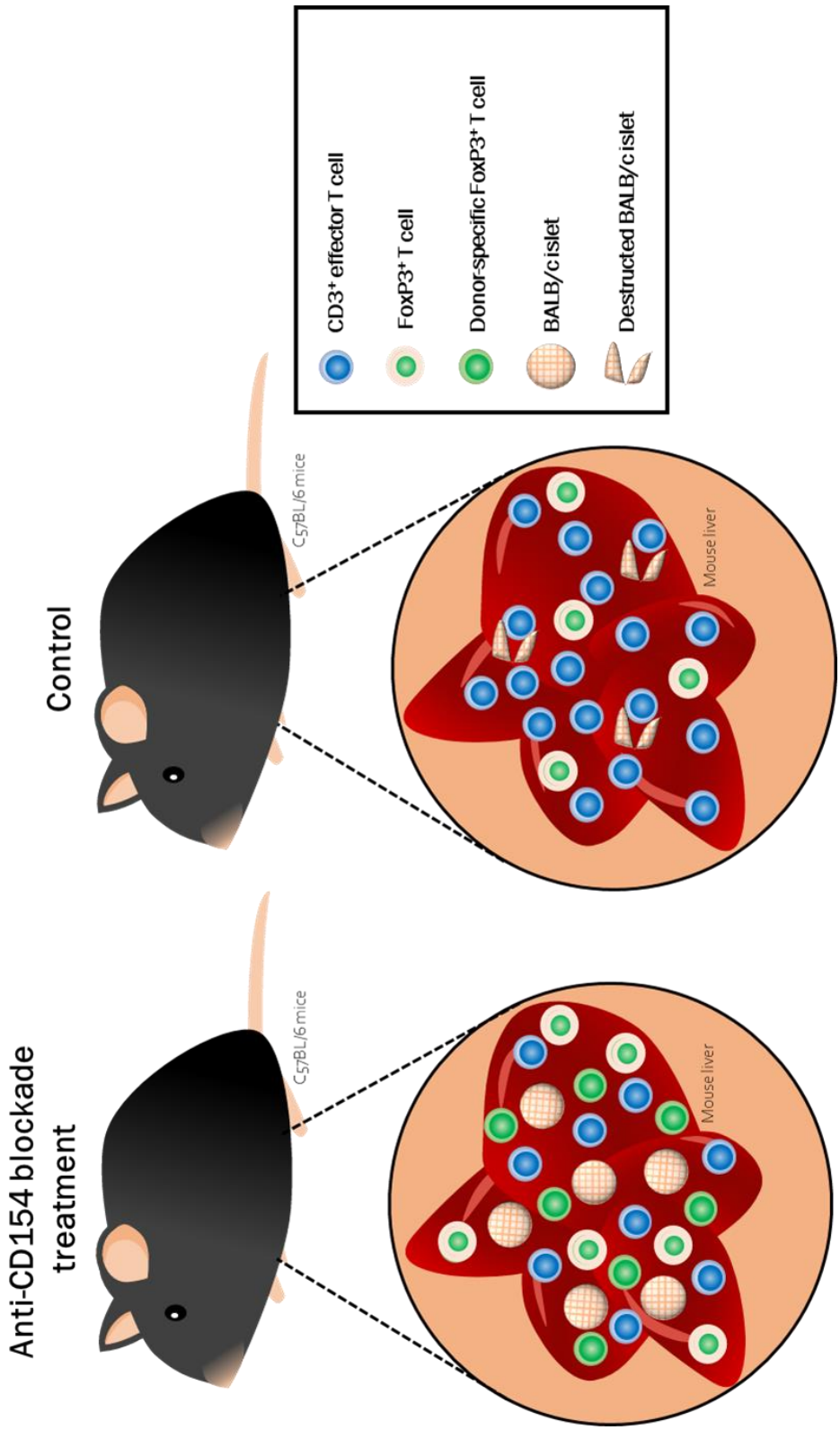

VII. References

1. Kerner W, Bruckel J, German Diabetes A. Definition, classification and diagnosis of diabetes mellitus. Exp Clin Endocrinol Diabetes. 2014;122(7):384-386.
2. von Herrath M. Immunology: insulin trigger for diabetes. Nature. 2005;435(7039):151-152.
3. Pugliese A. Autoreactive T cells in type 1 diabetes. J Clin Invest. 2017;127(8):2881-2891.
4. McCrimmon RJ, Sherwin RS. Hypoglycemia in type 1 diabetes. Diabetes. 2010;59(10):2333-2339.
5. Hering BJ, Clarke WR, Bridges ND, Eggerman TL, Alejandro R, Bellin MD, Chaloner K, Czarniecki CW, Goldstein JS, Hunsicker LG and others. Phase 3 Trial of Transplantation of Human Islets in Type 1 Diabetes Complicated by Severe Hypoglycemia. Diabetes Care. 2016;39(7):1230-1240.
6. Bottino R, Knoll MF, Knoll CA, Bertera S, Trucco MM. The Future of Islet Transplantation Is Now. Front Med (Lausanne). 2018;5:202.
7. Anazawa T, Okajima H, Masui T, Uemoto S. Current state and future evolution of pancreatic islet transplantation. Ann Gastroenterol Surg. 2019;3(1):34-42.
8. Shapiro AM, Pokrywczynska M, Ricordi C. Clinical pancreatic islet transplantation. Nat Rev Endocrinol. 2017;13(5):268-277.
9. Rother KI, Harlan DM. Challenges facing islet transplantation for the treatment of type 1 diabetes mellitus. J Clin Invest. 2004;114(7):877-883.
10. Naesens M, Kuypers DR, Sarwal M. Calcineurin inhibitor nephrotoxicity.

Clin J Am Soc Nephrol. 2009;4(2):481-508.

11. Lim MA, Kohli J, Bloom RD. Immunosuppression for kidney transplantation: Where are we now and where are we going? Transplant Rev (Orlando). 2017;31(1):10-17.

12. Steiner RW, Awdishu L. Steroids in kidney transplant patients. Semin Immunopathol. 2011;33(2):157-167.

13. Zhang G, Zhang L, Duff GW. A negative regulatory region containing a glucocorticosteroid response element (nGRE) in the human interleukin-1beta gene. DNA Cell Biol. 1997;16(2):145-152.

14. Scheinman RI, Cogswell PC, Lofquist AK, Baldwin AS, Jr. Role of transcriptional activation of I kappa B alpha in mediation of immunosuppression by glucocorticoids. Science. 1995;270(5234):283-286.

15. Auphan N, DiDonato JA, Rosette C, Helmberg A, Karin M. Immunosuppression by glucocorticoids: inhibition of NF-kappa B activity through induction of I kappa B synthesis. Science. 1995;270(5234):286-290.

16. Gottlicher M, Heck S, Herrlich P. Transcriptional cross-talk, the second mode of steroid hormone receptor action. J Mol Med (Berl). 1998;76(7):480-489.

17. Rhen T, Cidlowski JA. Antiinflammatory action of glucocorticoids--new mechanisms for old drugs. N Engl J Med. 2005;353(16):1711-1723.

18. Rojas J, Chavez-Castillo M, Chavez-Castillo M, Cabrera M, Cabrera M, Bermudez V, Bermudez V. Glucococorticoid-induced death of pancreatic Beta cells: an organized chaos. JOP. 2015;16(1):11-19.

19. Shapiro AM, Lakey JR, Ryan EA, Korbutt GS, Toth E, Warnock GL, Kneteman NM, Rajotte RV. Islet transplantation in seven patients with type

1 diabetes mellitus using a glucocorticoid-free immunosuppressive regimen. N Engl J Med. 2000;343(4):230-238.

20. Stritesky GL, Jameson SC, Hogquist KA. Selection of self-reactive T cells in the thymus. Annu Rev Immunol. 2012;30:95-114.

21. Nemazee D. Receptor editing in lymphocyte development and central tolerance. Nat Rev Immunol. 2006;6(10):728-740.

22. Mueller DL. Mechanisms maintaining peripheral tolerance. Nat Immunol. 2010;11(1):21-27.

23. Bluestone JA. Mechanisms of tolerance. Immunol Rev. 2011;241(1):5-19.

24. Bhatt S, Fung JJ, Lu L, Qian S. Tolerance-inducing strategies in islet transplantation. Int J Endocrinol. 2012;2012:396524.

25. Alpdogan O, van den Brink MR. Immune tolerance and transplantation. Semin Oncol. 2012;39(6):629-642.

26. Hyvarinen K, Holopainen M, Skirdenko V, Ruhanen H, Lehenkari P, Korhonen M, Kakela R, Laitinen S, Kerkela E. Mesenchymal Stromal Cells and Their Extracellular Vesicles Enhance the Anti-Inflammatory Phenotype of Regulatory Macrophages by Downregulating the Production of Interleukin (IL)-23 and IL-22. Front Immunol. 2018;9:771.

27. Galipeau J, Sensebe L. Mesenchymal Stromal Cells: Clinical Challenges and Therapeutic Opportunities. Cell Stem Cell. 2018;22(6):824-833.

28. Kingsley CI, Nadig SN, Wood KJ. Transplantation tolerance: lessons from experimental rodent models. Transpl Int. 2007;20(10):828-841.

29. Chong AS, Alegre ML, Miller ML, Fairchild RL. Lessons and limits of mouse models. Cold Spring Harb Perspect Med. 2013;3(12):a015495.

30. Lin CH, Wang YL, Anggelia MR, Chuang WY, Cheng HY, Mao Q, Zelken

JA, Lin CH, Zheng XX, Lee WP and others. Combined Anti-CD154/CTLA4Ig Costimulation Blockade-Based Therapy Induces Donor-Specific Tolerance to Vascularized Osteomyocutaneous Allografts. Am J Transplant. 2016;16(7):2030-2041.

31. Oluwole SF, Oluwole OO, Adeyeri AO, DePaz HA. New strategies in immune tolerance induction. Cell Biochem Biophys. 2004;40(3 Suppl):27-48.

32. Fehr T, Sykes M. Tolerance induction in clinical transplantation. Transpl Immunol. 2004;13(2):117-130.

33. Tzakis AG, Reyes J, Zeevi A, Ramos H, Nour B, Reinsmoen N, Todo S, Starzl TE. Early tolerance in pediatric liver allograft recipients. J Pediatr Surg. 1994;29(6):754-756.

34. Mazariegos GV, Sindhi R, Thomson AW, Marcos A. Clinical tolerance following liver transplantation: long term results and future prospects. Transpl Immunol. 2007;17(2):114-119.

35. Orlando G, Soker S, Wood K. Operational tolerance after liver transplantation. J Hepatol. 2009;50(6):1247-1257.

36. Ravindra KV, Wu S, Bozulic L, Xu H, Breidenbach WC, Ildstad ST. Composite tissue transplantation: a rapidly advancing field. Transplant Proc. 2008;40(5):1237-1248.

37. Shin JS, Kim JM, Kim JS, Min BH, Kim YH, Kim HJ, Jang JY, Yoon IH, Kang HJ, Kim J and others. Long-term control of diabetes in immunosuppressed nonhuman primates (NHP) by the transplantation of adult porcine islets. Am J Transplant. 2015;15(11):2837-2850.

38. van Kooten C, Banchereau J. CD40-CD40 ligand. J Leukoc Biol.

2000;67(1):2-17.

39. Mackey MF, Barth RJ, Jr., Noelle RJ. The role of CD40/CD154 interactions in the priming, differentiation, and effector function of helper and cytotoxic T cells. J Leukoc Biol. 1998;63(4):418-428.

40. Ford ML. T cell cosignaling molecules in transplantation. Immunity. 2016;44(5):1020-1033.

41. Hancock WW, Sayegh MH, Zheng XG, Peach R, Linsley PS, Turka LA. Costimulatory function and expression of CD40 ligand, CD80, and CD86 in vascularized murine cardiac allograft rejection. Proc Natl Acad Sci U S A. 1996;93(24):13967-13972.

42. Iwakoshi NN, Mordes JP, Markees TG, Phillips NE, Rossini AA, Greiner DL. Treatment of allograft recipients with donor-specific transfusion and anti-CD154 antibody leads to deletion of alloreactive CD8+ T cells and prolonged graft survival in a CTLA4-dependent manner. J Immunol. 2000;164(1):512-521.

43. Gilson CR, Milas Z, Gangappa S, Hollenbaugh D, Pearson TC, Ford ML, Larsen CP. Anti-CD40 monoclonal antibody synergizes with CTLA4-Ig in promoting long-term graft survival in murine models of transplantation. J Immunol. 2009;183(3):1625-1635.

44. Cardona K, Korbutt GS, Milas Z, Lyon J, Cano J, Jiang W, Bello-Laborn H, Hacquoil B, Strobert E, Gangappa S. Long-term survival of neonatal porcine islets in nonhuman primates by targeting costimulation pathways. Nature Medicine. 2006;12(3):304-306.

45. Hering BJ, Wijkstrom M, Graham ML, Hårdstedt M, Aasheim TC, Jie T, Ansite JD, Nakano M, Cheng J, Li W. Prolonged diabetes reversal after

intraportal xenotransplantation of wild-type porcine islets in immunosuppressed nonhuman primates. Nature Medicine. 2006;12(3):301-303.

46. Cardona K, Milas Z, Strobert E, Cano J, Jiang W, Safley S, Gangappa S, Hering B, Weber C, Pearson T. Engraftment of adult porcine islet xenografts in diabetic nonhuman primates through targeting of costimulation pathways. American Journal of Transplantation. 2007;7(10):2260-2268.

47. Van Der Windt D, Bottino R, Casu A, Campanile N, Smetanka C, He J, Murase N, Hara H, Ball S, Loveland B. Long-term controlled normoglycemia in diabetic non-human primates after transplantation with hCD46 transgenic porcine islets. American Journal of Transplantation. 2009;9(12):2716-2726.

48. Jung KC, Park C-G, Jeon YK, Park HJ, Ban YL, Min HS, Kim EJ, Kim JH, Kang BH, Park SP. In situ induction of dendritic cell–based T cell tolerance in humanized mice and nonhuman primates. The Journal of experimental medicine. 2011;208(12):2477-2488.

49. Monk NJ, Hargreaves RE, Marsh JE, Farrar CA, Sacks SH, Millrain M, Simpson E, Dyson J, Jurcevic S. Fc-dependent depletion of activated T cells occurs through CD40L-specific antibody rather than costimulation blockade. Nature medicine. 2003;9(10):1275-1280.

50. Ferrer IR, Wagener ME, Song M, Kirk AD, Larsen CP, Ford ML. Antigen-specific induced Foxp3+ regulatory T cells are generated following CD40/CD154 blockade. Proceedings of the National Academy of Sciences. 2011;108(51):20701-20706.

51. Chai JG, Ratnasothy K, Bucy RP, Noelle RJ, Lechler R, Lombardi G.

Allospecific CD4+ T cells retain effector function and are actively regulated by Treg cells in the context of transplantation tolerance. European journal of immunology. 2015;45(7):2017-2027.

52. Ochando JC, Homma C, Yang Y, Hidalgo A, Garin A, Tacke F, Angeli V, Li Y, Boros P, Ding Y and others. Alloantigen-presenting plasmacytoid dendritic cells mediate tolerance to vascularized grafts. Nat Immunol. 2006;7(6):652-662.

53. Chen J, Yin H, Xu J, Wang Q, Edelblum KL, Sciammas R, Chong A. Reversing Endogenous Alloreactive B Cell GC Responses With Anti-CD154 or CTLA-4Ig. American Journal of Transplantation. 2013;13(9):2280-2292.

54. Kim EJ, Kwun J, Gibby AC, Hong JJ, Farris A, Iwakoshi NN, Villinger F, Kirk AD, Knechtle SJ. Costimulation Blockade Alters Germinal Center Responses and Prevents Antibody-Mediated Rejection. American Journal of Transplantation. 2014;14(1):59-69.

55. Kawai T, Andrews D, Colvin RB, Sachs DH, Cosimi AB. Thromboembolic complications after treatment with monoclonal antibody against CD40 ligand. Nat Med. 2000;6(2):114.

56. Knosalla C, Gollackner B, Cooper DK. Anti-CD154 monoclonal antibody and thromboembolism revisted. Transplantation. 2002;74(3):416-417.

57. Morrell CN, Sun H, Swaim AM, Baldwin WM, 3rd. Platelets an inflammatory force in transplantation. Am J Transplant. 2007;7(11):2447-2454.

58. Robles-Carrillo L, Meyer T, Hatfield M, Desai H, Davila M, Langer F, Amaya M, Garber E, Francis JL, Hsu YM and others. Anti-CD40L immune

complexes potently activate platelets in vitro and cause thrombosis in FCGR2A transgenic mice. J Immunol. 2010;185(3):1577-1583.

59. Koyama I, Kawai T, Andrews D, Boskovic S, Nadazdin O, Wee SL, Sogawa H, Wu DL, Smith RN, Colvin RB and others. Thrombophilia associated with anti-CD154 monoclonal antibody treatment and its prophylaxis in nonhuman primates. Transplantation. 2004;77(3):460-462.

60. Xie JH, Yamniuk AP, Borowski V, Kuhn R, Susulic V, Rex-Rabe S, Yang X, Zhou X, Zhang Y, Gillooly K and others. Engineering of a novel anti-CD40L domain antibody for treatment of autoimmune diseases. J Immunol. 2014;192(9):4083-4092.

61. Pinelli DF, Wagener ME, Liu D, Yamniuk A, Tamura J, Grant S, Larsen CP, Suri A, Nadler SG, Ford ML. An anti-CD154 domain antibody prolongs graft survival and induces Foxp3(+) iTreg in the absence and presence of CTLA-4 Ig. Am J Transplant. 2013;13(11):3021-3030.

62. Shock A, Burkly L, Wakefield I, Peters C, Garber E, Ferrant J, Taylor FR, Su L, Hsu YM, Hutto D and others. CDP7657, an anti-CD40L antibody lacking an Fc domain, inhibits CD40L-dependent immune responses without thrombotic complications: an in vivo study. Arthritis Res Ther. 2015;17:234.

63. Nicolls MR, Coulombe M, Beilke J, Gelhaus HC, Gill RG. CD4-dependent generation of dominant transplantation tolerance induced by simultaneous perturbation of CD154 and LFA-1 pathways. J Immunol. 2002;169(9):4831-4839.

64. Mai G, Bucher P, Morel P, Mei J, Bosco D, Andres A, Mathe Z, Wekerle T, Berney T, Buhler LH. Anti-CD154 mAb treatment but not recipient CD154

deficiency leads to long-term survival of xenogeneic islet grafts. Am J Transplant. 2005;5(5):1021-1031.

65. Mai G, del Rio ML, Tian J, Ramirez P, Buhler L, Rodriguez-Barbosa JI. Blockade of the PD-1/PD-1L pathway reverses the protective effect of anti-CD40L therapy in a rat to mouse concordant islet xenotransplantation model. Xenotransplantation. 2007;14(3):243-248.

66. Jung DY, Kim EY, Joo SY, Park JB, Moon C, Kim SH, Sim EY, Joh JW, Kwon CH, Kwon GY and others. Prolonged survival of islet allografts in mice treated with rosmarinic acid and anti-CD154 antibody. Exp Mol Med. 2008;40(1):1-10.

67. Samy KP, Butler JR, Li P, Cooper DKC, Ekser B. The Role of Costimulation Blockade in Solid Organ and Islet Xenotransplantation. J Immunol Res. 2017;2017:8415205.

68. Parker DC, Greiner DL, Phillips NE, Appel MC, Steele AW, Durie FH, Noelle RJ, Mordes JP, Rossini AA. Survival of mouse pancreatic islet allografts in recipients treated with allogeneic small lymphocytes and antibody to CD40 ligand. Proc Natl Acad Sci U S A. 1995;92(21):9560-9564.

69. Rossini AA, Parker DC, Phillips NE, Durie FH, Noelle RJ, Mordes JP, Greiner DL. Induction of immunological tolerance to islet allografts. Cell Transplant. 1996;5(1):49-52.

70. Nanji SA, Hancock WW, Luo B, Schur CD, Pawlick RL, Zhu LF, Anderson CC, Shapiro AM. Costimulation blockade of both inducible costimulator and CD40 ligand induces dominant tolerance to islet allografts and prevents spontaneous autoimmune diabetes in the NOD mouse. Diabetes.

2006;55(1):27-33.

71. Arefanian H, Tredget EB, Rajotte RV, Korbutt GS, Gill RG, Rayat GR. Combination of anti-CD4 with anti-LFA-1 and anti-CD154 monoclonal antibodies promotes long-term survival and function of neonatal porcine islet xenografts in spontaneously diabetic NOD mice. Cell Transplant. 2007;16(8):787-798.

72. Arefanian H, Tredget EB, Rajotte RV, Gill RG, Korbutt GS, Rayat GR. Short-term administrations of a combination of anti-LFA-1 and anti-CD154 monoclonal antibodies induce tolerance to neonatal porcine islet xenografts in mice. Diabetes. 2010;59(4):958-966.

73. Arefanian H, Tredget EB, Mok DC, Ramji Q, Rafati S, Rodriguez-Barbosa J, Korbutt GS, Rajotte RV, Gill RG, Rayat GR. Porcine Islet-Specific Tolerance Induced by the Combination of Anti-LFA-1 and Anti-CD154 mAbs Is Dependent on PD-1. Cell Transplant. 2016;25(2):327-342.

74. Molano RD, Berney T, Li H, Cattan P, Pileggi A, Vizzardelli C, Kenyon NS, Ricordi C, Burkly LC, Inverardi L. Prolonged islet graft survival in NOD mice by blockade of the CD40-CD154 pathway of T-cell costimulation. Diabetes. 2001;50(2):270-276.

75. Kenyon NS, Fernandez LA, Lehmann R, Masetti M, Ranuncoli A, Chatzipetrou M, Iaria G, Han D, Wagner JL, Ruiz P and others. Long-term survival and function of intrahepatic islet allografts in baboons treated with humanized anti-CD154. Diabetes. 1999;48(7):1473-1481.

76. Kenyon NS, Chatzipetrou M, Masetti M, Ranuncoli A, Oliveira M, Wagner JL, Kirk AD, Harlan DM, Burkly LC, Ricordi C. Long-term survival and function of intrahepatic islet allografts in rhesus monkeys treated with

humanized anti-CD154. Proc Natl Acad Sci U S A. 1999;96(14):8132-8137.

77. Hori S, Nomura T, Sakaguchi S. Control of regulatory T cell development by the transcription factor Foxp3. Science. 2003;299(5609):1057-1061.

78. Fontenot JD, Gavin MA, Rudensky AY. Foxp3 programs the development and function of CD4+CD25+ regulatory T cells. Nat Immunol. 2003;4(4):330-336.

79. Khattri R, Cox T, Yasayko SA, Ramsdell F. An essential role for Scurfin in CD4+CD25+ T regulatory cells. Nat Immunol. 2003;4(4):337-342.

80. Walker MR, Kasprowicz DJ, Gersuk VH, Benard A, Van Landeghen M, Buckner JH, Ziegler SF. Induction of FoxP3 and acquisition of T regulatory activity by stimulated human CD4+CD25- T cells. J Clin Invest. 2003;112(9):1437-1443.

81. Nishizuka Y, Sakakura T. Thymus and reproduction: sex-linked dysgenesia of the gonad after neonatal thymectomy in mice. Science. 1969;166(3906):753-755.

82. Sakaguchi S, Takahashi T, Nishizuka Y. Study on cellular events in postthymectomy autoimmune oophoritis in mice. I. Requirement of Lyt-1 effector cells for oocytes damage after adoptive transfer. J Exp Med. 1982;156(6):1565-1576.

83. Sakaguchi S, Fukuma K, Kuribayashi K, Masuda T. Organ-specific autoimmune diseases induced in mice by elimination of T cell subset. I. Evidence for the active participation of T cells in natural self-tolerance; deficit of a T cell subset as a possible cause of autoimmune disease. J Exp Med. 1985;161(1):72-87.

84. Sakaguchi S, Sakaguchi N, Asano M, Itoh M, Toda M. Immunologic self-

tolerance maintained by activated T cells expressing IL-2 receptor alpha-chains (CD25). Breakdown of a single mechanism of self-tolerance causes various autoimmune diseases. J Immunol. 1995;155(3):1151-1164.

85. Lee I, Wang L, Wells AD, Dorf ME, Ozkaynak E, Hancock WW. Recruitment of Foxp3+ T regulatory cells mediating allograft tolerance depends on the CCR4 chemokine receptor. The Journal of experimental medicine. 2005;201(7):1037-1044.

86. Taylor PA, Noelle RJ, Blazar BR. CD4(+)CD25(+) immune regulatory cells are required for induction of tolerance to alloantigen via costimulatory blockade. J Exp Med. 2001;193(11):1311-1318.

87. Ochando JC, Yopp AC, Yang Y, Garin A, Li Y, Boros P, Llodra J, Ding Y, Lira SA, Krieger NR and others. Lymph node occupancy is required for the peripheral development of alloantigen-specific Foxp3+ regulatory T cells. J Immunol. 2005;174(11):6993-7005.

88. Muller YD, Mai G, Morel P, Serre-Beinier V, Gonelle-Gispert C, Yung GP, Ehirchiou D, Wyss JC, Bigenzahn S, Irla M and others. Anti-CD154 mAb and rapamycin induce T regulatory cell mediated tolerance in rat-to-mouse islet transplantation. PLoS One. 2010;5(4):e10352.

89. Ferrer IR, Wagener ME, Song M, Kirk AD, Larsen CP, Ford ML. Antigen-specific induced Foxp3+ regulatory T cells are generated following CD40/CD154 blockade. Proc Natl Acad Sci U S A. 2011;108(51):20701-20706.

90. Graca L, Honey K, Adams E, Cobbold SP, Waldmann H. Cutting edge: anti-CD154 therapeutic antibodies induce infectious transplantation tolerance. J Immunol. 2000;165(9):4783-4786.

91. Kendal AR, Chen Y, Regateiro FS, Ma J, Adams E, Cobbold SP, Hori S, Waldmann H. Sustained suppression by Foxp3+ regulatory T cells is vital for infectious transplantation tolerance. J Exp Med. 2011;208(10):2043-2053.

92. Dodd-o JM, Lendermon EA, Miller HL, Zhong Q, John ER, Jungraithmayr WM, D'Alessio FR, McDyer JF. CD154 blockade abrogates allospecific responses and enhances CD4(+) regulatory T-cells in mouse orthotopic lung transplant. Am J Transplant. 2011;11(9):1815-1824.

93. Tan X, Zeng H, Jie Y, Zhang Y, Xu Q, Pan Z. CD154 blockade modulates the ratio of Treg to Th1 cells and prolongs the survival of allogeneic corneal grafts in mice. Exp Ther Med. 2014;7(4):827-834.

94. Rajab A. Islet transplantation: alternative sites. Curr Diab Rep. 2010;10(5):332-337.

95. Ryan EA, Lakey JR, Paty BW, Imes S, Korbutt GS, Kneteman NM, Bigam D, Rajotte RV, Shapiro AM. Successful islet transplantation: continued insulin reserve provides long-term glycemic control. Diabetes. 2002;51(7):2148-2157.

96. Rafael E, Ryan EA, Paty BW, Oberholzer J, Imes S, Senior P, McDonald C, Lakey JR, Shapiro AM. Changes in liver enzymes after clinical islet transplantation. Transplantation. 2003;76(9):1280-1284.

97. Rafael E, Tibell A, Ryden M, Lundgren T, Savendahl L, Borgstrom B, Arnelo U, Isaksson B, Nilsson B, Korsgren O and others. Intramuscular autotransplantation of pancreatic islets in a 7-year-old child: a 2-year follow-up. Am J Transplant. 2008;8(2):458-462.

98. Wang C, Du X, He S, Yuan Y, Han P, Wang D, Chen Y, Liu J, Tian B, Yang

G and others. A preclinical evaluation of alternative site for islet allotransplantation. PLoS One. 2017;12(3):e0174505.

99. Shapiro AM, Ricordi C, Hering BJ, Auchincloss H, Lindblad R, Robertson RP, Secchi A, Brendel MD, Berney T, Brennan DC and others. International trial of the Edmonton protocol for islet transplantation. N Engl J Med. 2006;355(13):1318-1330.

100. Byun N, Kim HJ, Min BH, Shin JS, Yoon IH, Kim JM, Kim YH, Park CG. A novel method for murine intrahepatic islet transplantation via cecal vein. J Immunol Methods. 2015;427:122-125.

101. Lahl K, Sparwasser T. In vivo depletion of FoxP3+ Tregs using the DEREG mouse model. Methods Mol Biol. 2011;707:157-172.

102. Pan X, Xue W, Li Y, Feng X, Tian X, Ding C. Islet graft survival and function: concomitant culture and transplantation with vascular endothelial cells in diabetic rats. Transplantation. 2011;92(11):1208-1214.

103. Estil Les E, Tellez N, Nacher M, Montanya E. A model for human islet transplantation to immunodeficient streptozotocin-induced diabetic mice. Cell Transplant. 2018:963689718801006.

104. Morini S, Brown ML, Cicalese L, Elias G, Carotti S, Gaudio E, Rastellini C. Revascularization and remodelling of pancreatic islets grafted under the kidney capsule. J Anat. 2007;210(5):565-577.

105. Korsgren O, Lundgren T, Felldin M, Foss A, Isaksson B, Permert J, Persson NH, Rafael E, Ryden M, Salmela K and others. Optimising islet engraftment is critical for successful clinical islet transplantation. Diabetologia. 2008;51(2):227-232.

106. Nakano M, Yasunami Y, Maki T, Kodama S, Ikehara Y, Nakamura T, Tanaka

M, Ikeda S. Hepatocyte growth factor is essential for amelioration of hyperglycemia in streptozotocin-induced diabetic mice receiving a marginal mass of intrahepatic islet grafts. Transplantation. 2000;69(2):214-221.

107. Andersson A, Korsgren O, Jansson L. Intraportally transplanted pancreatic islets revascularized from hepatic arterial system. Diabetes. 1989;38 Suppl 1:192-195.

108. Diab RA, Fares M, Abedi-Valugerdi M, Kumagai-Braesch M, Holgersson J, Hassan M. Immunotoxicological effects of streptozotocin and alloxan: in vitro and in vivo studies. Immunol Lett. 2015;163(2):193-198.

109. Rudensky A. Foxp3 and dominant tolerance. Philos Trans R Soc Lond B Biol Sci. 2005;360(1461):1645-1646.

110. Sakaguchi S, Yamaguchi T, Nomura T, Ono M. Regulatory T cells and immune tolerance. Cell. 2008;133(5):775-787.

111. Leguern C. Regulatory T cells for tolerance therapy: revisiting the concept. Crit Rev Immunol. 2011;31(3):189-207.

112. Zhou J, He W, Luo G, Wu J. Fundamental immunology of skin transplantation and key strategies for tolerance induction. Arch Immunol Ther Exp (Warsz). 2013;61(5):397-405.

113. Rogers NJ, Lechler RI. Allorecognition. Am J Transplant. 2001;1(2):97-102.

114. Larsen CP, Steinman RM, Witmer-Pack M, Hankins DF, Morris PJ, Austyn JM. Migration and maturation of Langerhans cells in skin transplants and explants. J Exp Med. 1990;172(5):1483-1493.

115. Richters CD, van Gelderop E, du Pont JS, Hoekstra MJ, Kreis RW, Kamperdijk EW. Migration of dendritic cells to the draining lymph node after allogeneic or congeneic rat skin transplantation. Transplantation.

1999;67(6):828-832.

116. Benichou G, Yamada Y, Yun SH, Lin C, Fray M, Tocco G. Immune recognition and rejection of allogeneic skin grafts. Immunotherapy. 2011;3(6):757-770.

117. Qian S, Lu L, Li Y, Fu F, Li W, Starzl TE, Thomson AW, Fung JJ. Apoptosis of graft-infiltrating cytotoxic T cells: a mechanism underlying "split tolerance" in mouse liver transplantation. Transplant Proc. 1997;29(1-2):1168-1169.

118. Mathes DW, Randolph MA, Solari MG, Nazzal JA, Nielsen GP, Arn JS, Sachs DH, Lee WP. Split tolerance to a composite tissue allograft in a swine model. Transplantation. 2003;75(1):25-31.

119. Chung Y, Ko SY, Ko HJ, Kang CY. Split peripheral tolerance: CD40 ligation blocks tolerance induction for CD8 T cells but not for CD4 T cells in response to intestinal antigens. Eur J Immunol. 2005;35(5):1381-1390.

120. de Mestre A, Noronha L, Wagner B, Antczak DF. Split immunological tolerance to trophoblast. Int J Dev Biol. 2010;54(2-3):445-455.

121. Luo B, Chan WF, Shapiro AM, Anderson CC. Non-myeloablative mixed chimerism approaches and tolerance, a split decision. Eur J Immunol. 2007;37(5):1233-1242.

122. Chan WF, Razavy H, Luo B, Shapiro AM, Anderson CC. Development of either split tolerance or robust tolerance along with humoral tolerance to donor and third-party alloantigens in nonmyeloablative mixed chimeras. J Immunol. 2008;180(8):5177-5186.

123. Fuchimoto Y, Gleit ZL, Huang CA, Kitamura H, Schwarze ML, Menard MT, Mawulawde K, Madsen JC, Sachs DH. Skin-specific alloantigens in

miniature swine. Transplantation. 2001;72(1):122-126.

124. Lin X, Chen M, Liu Y, Guo Z, He X, Brand D, Zheng SG. Advances in distinguishing natural from induced Foxp3(+) regulatory T cells. Int J Clin Exp Pathol. 2013;6(2):116-123.

125. Saemann MD, Kelemen P, Zeyda M, Bohmig G, Staffler G, Zlabinger GJ. CD40 triggered human monocyte-derived dendritic cells convert to tolerogenic dendritic cells when JAK3 activity is inhibited. Transplant Proc. 2002;34(5):1407-1408.

126. Zhou Y, Leng X, Li H, Yang S, Yang T, Li L, Xiong Y, Zou Q, Liu Y, Wang Y. Tolerogenic dendritic cells induced by BD750 ameliorate proinflammatory T cell responses and experimental autoimmune encephalitis in mice. Mol Med. 2017;23:204-214.

127. Zhang X, Kedl RM, Xiang J. CD40 ligation converts TGF-beta-secreting tolerogenic CD4-8- dendritic cells into IL-12-secreting immunogenic ones. Biochem Biophys Res Commun. 2009;379(4):954-958.

128. Jiang XF, Cui ZM, Zhu L, Guo DW, Sun WY, Lin L, Wang XF, Tang YF, Liang J. CD40-CD40L costimulation blockade induced the tolerogenic dendritic cells in mouse cardiac transplant. Int Surg. 2010;95(2):135-141.

129. Yvon ES, Vigouroux S, Rousseau RF, Biagi E, Amrolia P, Dotti G, Wagner HJ, Brenner MK. Overexpression of the Notch ligand, Jagged-1, induces alloantigen-specific human regulatory T cells. Blood. 2003;102(10):3815-3821.

130. Cahill EF, Tobin LM, Carty F, Mahon BP, English K. Jagged-1 is required for the expansion of CD4+ CD25+ FoxP3+ regulatory T cells and tolerogenic dendritic cells by murine mesenchymal stromal cells. Stem Cell

Res Ther. 2015;6:19.

131. Xu LL, Fu HX, Zhang JM, Feng FE, Wang QM, Zhu XL, Xue J, Wang CC, Chen Q, Liu X and others. Impaired Function of Bone Marrow Mesenchymal Stem Cells from Immune Thrombocytopenia Patients in Inducing Regulatory Dendritic Cell Differentiation Through the Notch-1/Jagged-1 Signaling Pathway. Stem Cells Dev. 2017;26(22):1648-1661.

132. Lin Y, Chen W, Li J, Yan G, Li C, Jin N, Chen J, Gao C, Ma P, Xu S and others. Overexpression of Jagged-1 combined with blockade of CD40 pathway prolongs allograft survival. Immunol Cell Biol. 2015;93(2):213-217.

133. Ferrer IR, Wagener ME, Song M, Ford ML. CD154 blockade alters innate immune cell recruitment and programs alloreactive CD8+ T cells into KLRG-1(high) short-lived effector T cells. PLoS One. 2012;7(7):e40559.

134. Lowe M, Badell IR, Thompson P, Martin B, Leopardi F, Strobert E, Price AA, Abdulkerim HS, Wang R, Iwakoshi NN and others. A novel monoclonal antibody to CD40 prolongs islet allograft survival. Am J Transplant. 2012;12(8):2079-2087.

135. Mohiuddin MM, Singh AK, Corcoran PC, Thomas Iii ML, Clark T, Lewis BG, Hoyt RF, Eckhaus M, Pierson Iii RN, Belli AJ and others. Chimeric 2C10R4 anti-CD40 antibody therapy is critical for long-term survival of GTKO.hCD46.hTBM pig-to-primate cardiac xenograft. Nat Commun. 2016;7:11138.

136. Iwase H, Liu H, Wijkstrom M, Zhou H, Singh J, Hara H, Ezzelarab M, Long C, Klein E, Wagner R and others. Pig kidney graft survival in a baboon for 136 days: longest life-supporting organ graft survival to date.

Xenotransplantation. 2015;22(4):302-309.

137. Shin JS, Kim JM, Min BH, Yoon IH, Kim HJ, Kim JS, Kim YH, Kang SJ, Kim J, Kang HJ and others. Pre-clinical results in pig-to-non-human primate islet xenotransplantation using anti-CD40 antibody (2C10R4)-based immunosuppression. Xenotransplantation. 2018;25(1).

138. Ripoll E, Pluvinet R, Torras J, Olivar R, Vidal A, Franquesa M, Cassis L, Cruzado JM, Bestard O, Grinyo JM and others. In vivo therapeutic efficacy of intra-renal CD40 silencing in a model of humoral acute rejection. Gene Ther. 2011;18(10):945-952.

139. Yin H, Kanasty RL, Eltoukhy AA, Vegas AJ, Dorkin JR, Anderson DG. Non-viral vectors for gene-based therapy. Nat Rev Genet. 2014;15(8):541-555.

140. Perper SJ, Westmoreland SV, Karman J, Twomey R, Seagal J, Wang R, McRae BL, Clarke SH. Treatment with a CD40 Antagonist Antibody Reverses Severe Proteinuria and Loss of Saliva Production and Restores Glomerular Morphology in Murine Systemic Lupus Erythematosus. J Immunol. 2019;203(1):58-75.

국문초록

간 내 동종이형 췌도 이식 생쥐모델에서 단기간 CD40-CD154 상호작용 차단에 의한 공여자 특이 FoxP3$^+$ 조절 T 세포 매개 면역관용

이 석 주

서울대학교 대학원

치의과학과 면역 및 분자미생물학 전공

목적

CD40-CD154 상호작용은 수지상세포와 T 세포 사이에서 여러 신호를 제공하는 공동자극분자중 하나이며 T 세포가 활성화하는데 필수적인 신호이다. CD40-CD154 상호작용를 차단하였을 때 많은 논문에서 면역반응이 조절됨이 보고되었다. 특히, 항 CD154 단클론 항체가 포함된 면역억제요법들은 다양한 장기 이식 모델에서 이식 장기의 생존을 증가시키는데 있어 압도적인 효과를 보인다. 많은 논문에서 항 CD154 단클론 항체가 면역관용을 유도한다고 주장하지만 그 어떤 연구에서도 항 CD154 단클론 항체 단일요법을 처리한 동물모델을 이용하여 해당 약물의 직접적인 기전을 밝히지는 않았기에 실제 항 CD154 단클론 항체가 면역관용을 유도하는지는 알 수 없다.

따라서, 이 연구의 목적은 약물억제제 병용요법을 사용한 이전 이식동물모델과는 달리 간 내 동종이형 췌도이식 생쥐모델에서 1. 항 CD154 단클론 단일요법으로도 간 내 동종이형 췌도의 생존이 증가하는지 확인하고, 2. 성공적으로 생착한 췌도가 면역관용에 의해 생존하는지 규명하며, 마지막으로 3. 항 CD154 단클론 항체에 의해 유도된 면역관용의 기전을 밝히고자 한다.

방법

먼저 동종이형 췌도이식 생쥐모델을 만들기 위해, Streptozotocin을 녹인Citrate 용액(120mg/kg)을 8주령 B6 생쥐에 하루에 한번씩 2일에 걸쳐 총 두 번 복강투여하였다. 최소 3일 연속 16.8mmol/L 이상의 혈당을 보인 생쥐를 당뇨생쥐로 판단하였다. 공여췌도는 BALB/c 생쥐로부터 췌장을 분리한 뒤 Collagenase P를 이용하여 췌장을 소화시키고 Ficoll 분리법을 이용하여 순수 췌도만을 분리하였다. 분리한 공여췌도는 Cecum 정맥으로 주입하여 혈류를 따라 간 내로 이식하였다. 그리고 항 CD154 단클론 항체는 이식을 전후로 -1, 0, 1, 3, 5, 그리고 7일에 마리당 0.5mg씩 복강투여하였다. 그리고 꼬리로부터 채혈을 하여 매일 혈당을 체크하였다. 면역관용이 유도되었는지 확인하기 위해 추가 면역억제제 없이 BALB/c 또는 C3H 생쥐 (제 3자 항원) 로부터 얻은 동종이형 췌도를 간 내 BALB/c 동종이형 췌도를 이식하여 정상혈당을 유지하고 있는 B6 생쥐의 신장피막하로 주입하거나 또는 B6 생쥐의

옆구리에 BALB/c 생쥐로부터 얻은 동종이형 피부를 이식하였다. 신장피막하 췌도의 생존을 보기위하여 신장제거술을 진행하였다. 피부이식편의 생착을 실험군과 대조군에서 매일 관찰하여 그룹 간의 피부이식편의 생존기간을 비교하였다. 면역관용의 기전을 보기 위하여 $CD8^+$ T 세포만을 분리하여 IFN-γ ELISpot 분석을 하거나 또는 DEREG 생쥐를 사용하여 췌도이식모델을 만든 뒤 Diphtheria 독소를 투여하여 조절 T 세포만 제거해보았다. 그리고 동종이형 항원에 대한 조절 T 세포의 억제능을 비교 하기 위해 FoxP3-eGFP B6생쥐를 사용하여 췌도이식모델을 만들었고 200일 이상 정상혈당을 유지하는 생쥐에 한 해 비장세포를 분리하고 이어 $FoxP3^+$ 조절 T 세포만을 분리한 뒤 BALB/c 또는 C3H 생쥐로부터 얻은 조사된 비장세포에 의해 각각 증식하는 B6 생쥐 유래 효과 T 세포에 대한 조절 T 세포의 억제능을 혼합림프구반응 실험을 통해 분석하였다.

결과

당뇨가 유발된 B6 생쥐의 간 내 동종이형 췌도를 이식하고 항 CD154 단클론 항체를 투여하였을 때 항체를 처리하지 않은 대조군에 비해 최대 250일 이상 정당혈당을 유지한 것을 확인하였고 이후 간 조직 절편을 얻은 뒤, 면역조직화학염색을 하여 이식한 췌도가 간 내 정상적으로 생착하였음을 확인하였다. 그리고 면역관용임을 확인하기 위해 100일 이상 정상혈당을 유지하고 있는 생쥐의 신장 피막하에 추가

면역억제제 없이 BALB/c 동종이형 췌도와 C3H 동종이형 췌도 (제 3자 항원)를 이식한 결과, BALB/c 동종이형 췌도만이 선택적으로 생존함을 확인하였다. BALB/c 동종이형 피부를 이식한 결과, 간 내 BALB/c 동종이형 췌도가 생착된 생쥐에서 피부이식편의 거부반응이 대조군에 비해 늦춰지는것을 확인하였다. DEREG 생쥐를 이용하여 조절 T 세포가 동종이형 췌도 보호에 중요한 역할을 하는것을 밝혔고 혼합림프구반응 실험을 통해 면역관용을 획득한 B6 생쥐의 조절 T 세포가 BALB/c 생쥐 유래 공여항원에 대해 특이적 억제능을 보임을 확인하였다.

결론

간 내 동종이형 췌도이식 생쥐모델에서 항 CD154 단클론 항체을 투여하여 단기간 CD40-CD40L 상호작용을 차단하였을 때, 공여항원에 대해 특이적인 $FoxP3^+$ 조절 T 세포를 유도함으로서 면역관용을 획득함을 처음으로 확인하였고 in vivo에서 항 CD154 단클론 항체에 의해 공여자 특이 $FoxP3^+$ 조절 T 세포가 유도되는 분자기전을 밝힐 수 있는 첫 동물모델을 확립하였다.

주요어: 항 CD154 단클론 항체 (MR1). 면역관용, 조절 T 세포, 췌도이식, 간

학번: 2014-22041